# SYSTEMS APPROACH OF AGRICULTURAL RESIDUE UTILIZATION FOR VALUE-ADDED CHEMICAL PRODUCTION

By

Zhiguo Liu

A DISSERTATION

Submitted to
Michigan State University
in partial fulfillment of the requirements
for the degree of

Biosystems Engineering – Doctor of Philosophy

2016

## ABSTRACT

SYSTEMS APPROACH OF AGRICULTURAL RESIDUE UTILIZATION FOR VALUE-ADDED CHEMICAL PRODUCTION

By

Zhiguo Liu

More than 120 dry million tons of nutrient-rich animal wastes is annually produced in the U.S., which causes a series of negative environmental consequences such as odor problem, greenhouse gas emission and ground water/surface water contamination. Anaerobic digestion (AD) is one of the widely accepted animal manure management technologies that can not only control odor but also generate renewable energy biogas. Anaerobic digestion technology has advantages of robustness, feedstock flexibility, relatively simple implementation, and low capital investment in treating high-strength organic wastes. However, it is also challenged by: 1) liquid digestate has relatively high levels of chemical oxygen demand and nutrients (phosphorus and nitrogen); 2) more than 50% of carbon is still remained in the solid digestate; 3) biogas has high contents of impurities such as $H_2S$, which requires a complicated purification prior to further uses for energy production; and 4) a relatively large quantity of $CO_2$ in the biogas reduce the energy value of biogas and decrease the efficiency of biogas energy production.

Therefore, in order to advance the application of anaerobic digestion, the goal of this study is to apply systems approaches to develop an integrated process to address the aforementioned challenges and explore alternative value-added outputs from AD. The integrated process includes anaerobic digestion of animal wastes, electrocoagulation, algal cultivation, and fungal culture for fine chemical production and $CO_2$ utilization.

Anaerobic digestion first utilizes some nutrients in animal waste to produce methane. The liquid digestate from anaerobic digestion was then treated by electrocoagulation to reclaim water. Biogas was also incorporated into the electrocoagulation to facilitate water reclamation, removal of impurities (e.g. $H_2S$) from biogas and to improve energy efficiency. Algal cultivation was applied on the reclaimed EC water to further remove nitrogen, fix $CO_2$, and accumulate lipid-rich algal biomass. A fungal fermentation was applied on solid digestate using the EC treated liquid digestate as the processing water to produce a value-added biopolymer – Chitin. In addition, this study also conducted an in-depth investigation on using $CO_2$ derived formate as both carbon and energy sources to simultaneously sequester $CO_2$ and enhance fungal lipid accumulation. With successful completion of the study, an environmental friendly and economically feasible animal waste utilization concept has been elucidated. Consequently, implementing such system could make a major contribution to realizing sustainable animal agriculture in the near future.

To my parents, especially my mother Sizhen Bi for her unconditional support and understanding. To my better half, Muyang Li, for her great patience and strong belief in me. To my beloved son, Arnold L. Liu.

## ACKNOWLEDGEMENTS

I would like to express my enormous appreciations to Dr. Yan (Susie) Liu, my academic advisor and mentor, for her great guidance, help and patience during my Ph.D. program. She is an enthusiastic researcher, who is always available for immediate help and guidance in both academic and everyday life. My thanks go to Dr. Dawn Reinhold for serving as my committee member and providing valuable suggestions on my academic course selections and research advices. I would like to thank Dr. David Hodge for being on my committee board and inputting valuable advices for my research progress. My thanks also go to Dr. Ilsoon Lee for serving on my committee board and for his great guidance and collaborations on several published research projects.

Special thanks to Dr. Wei Liao for his professional guidance and help on research strategies and technical writing skills development. Thanks to Dr. Yinjie Tang's research team in University of Washington for great help and valuable guidance. Thanks to Dr. Bradley Marks and Dr. Renfu Lu for their valuable suggestions on my research topic modifications.

Thanks to my research colleagues in the lab: Dr. Zhenhua Ruan and Dr. Xiaoqing Wang, Patrick Sheridan and Yuan Zhong for their friendship and wonderful time working together in the lab; Marc Vandeberg, Garrett James Knowlton, Charlie Sanders, David Stromberg, Christine Isaguirre, Anna Hermanns, Yingkui Zhong for their great help. Special thanks to Dr. Oishi Sanyal for the pleasant collaboration on multiple projects.

Thanks to Dr. Scott Smith, Dr. Tony Schilmiller and Dr. Dan Jones in Mass Spectrometry Center for their great guidance and help in multiple detection methods development.

## TABLE OF CONTENTS

## LIST OF TABLES

## LIST OF FIGURES

## KEY TO ABBREVIATIONS

| | |
|---|---|
| AD | Anaerobic digestion |
| EC | Electrocoagulation |
| $CO_2$ | Carbon dioxide |
| $CH_4$ | Methane |
| $H_2S$ | Hydrogen sulfide |
| CE | Carbon equivalents |
| COD | Chemical oxygen demand |
| TN | Total nitrigen |
| TP | Total phosphorous |
| TS | Total solid |
| TDS | Total dissolved solid |
| TSS | Total suspended solid |
| VS | Volatile solid |
| TC | Total carbon |
| TOC | Total organic carbon |
| IC | Total inorganic carbon |
| CD | Current density |
| BP | Biogas pumping |
| NBP | No biogas pumping |
| CRD | Complete random design |
| RT | Retention time |

| | |
|---|---|
| SA | Surface area of electrodes |
| GC/MS | Gas chromatography mass spectrometry |
| HPLC | High pressure liquid chromatography |
| GLM | General linear model |
| ANOVA | Analysis of varience |
| NTU | Nephelometric Turbidity Units |
| CSTR | Complete stirred tank reactor |
| HRT | Hydraulic retention time |
| *C. vulgaris* | *Chlorella vulgaris* |
| *M. Isabellina* | *Mortierella Isabellina* |
| *U. Isabellina* | *Umbelopsis isabellina* |
| *R. Oryzae* | *Rhizopus Oryzae* |
| NADH | Nicotinamide adenine dinucleotide |
| NADPH | Nicotinamide adenine dinucleotide phosphate |
| ATP | Adenosine triphosphate |
| PDB | Potato dextrose broth |
| PDA | Potato dextrose agar |
| Y.E | Yeast extract |
| FFA | Free fatty acid |
| F.A.M.E | Fatty acid methyl ester |

# CHAPTER 1 INTRODUCTION

## 1.1 Introduction

Although anaerobic digestion is an effective biological process to treat organic wastes and convert them into biogas for energy production, its further development and application is hurdled by the resulting waste streams: nutrients abundant liquid effluent, fiber rich solid residues and impurities in raw biogas. Ignorance and mishandling of these waste streams not only jeopardize the applicability of AD technology, but also raise potential environmental concerns. Current post-treatments usually involve chemical addition and focus on individual issues separately, overlooking the intrinsic connections between treatments of different waste streams. This 'formulated' strategy potentially brings secondary contamination as well as reduces post-treatment efficiency. This study applied a system approach to develop an integrated system on animal wastes, which synergistically reclaims the water, cleans up the methane gas, and utilizes the solid residues. The integrated system demonstrated an alternative solution to turn animal wastes from an environmental liability into usable resources.

## 1.2 Anaerobic digestion and its challenges

Animal manure is of particular environmental concern due to greenhouse gas emissions, odor, and potential water and soil contamination. The U.S. EPA reported that agriculture contributed about 10% of the U.S. greenhouse gas emissions (in carbon equivalents, CE), primarily as methane and nitrous oxide [1]. About 65% of the methane from agriculture is attributable to animal farms [2]. In addition to greenhouse gas emissions, the dilute nature of manure nutrients such as phosphorus and nitrogen are an environmental challenge for animal farms as well. Nitrogen in the form of ammonia is volatized to the

atmosphere to cause air pollution, and phosphorus can runoff to the surrounding watershed to impact surface and ground water. On the other hand, animal manure with high nutrient content can be used as potential sources for energy and value-added biochemical production. Finding sustainable solutions for such reutilizations would significantly contribute to the development of rural economy.

A recent trend in animal manure management is the renewed interest in using anaerobic digester (AD) technology for energy production and odor control. Anaerobic digestion (AD) is a microbial process to treat organic wastes, which has been historically applied to reduce the odor and pathogen number in animal wastes, and generate methane gas as a renewable energy source [3]. A typical AD process consists of four sequential stages: hydrolysis, acidogenesis, acetogenesis and methanogenesis. As shown in Figure 1.1, organic matters (carbohydrates, fats and proteins) in wastes are first hydrolyzed into monomers (sugar, amino acids) during microbial hydrolysis, and the following acidogenesis and acetogenesis further convert these monomers into carbon dioxide, acetic acid and other organic acids, which are eventually degraded into methane and carbon dioxide by methanogens [4].

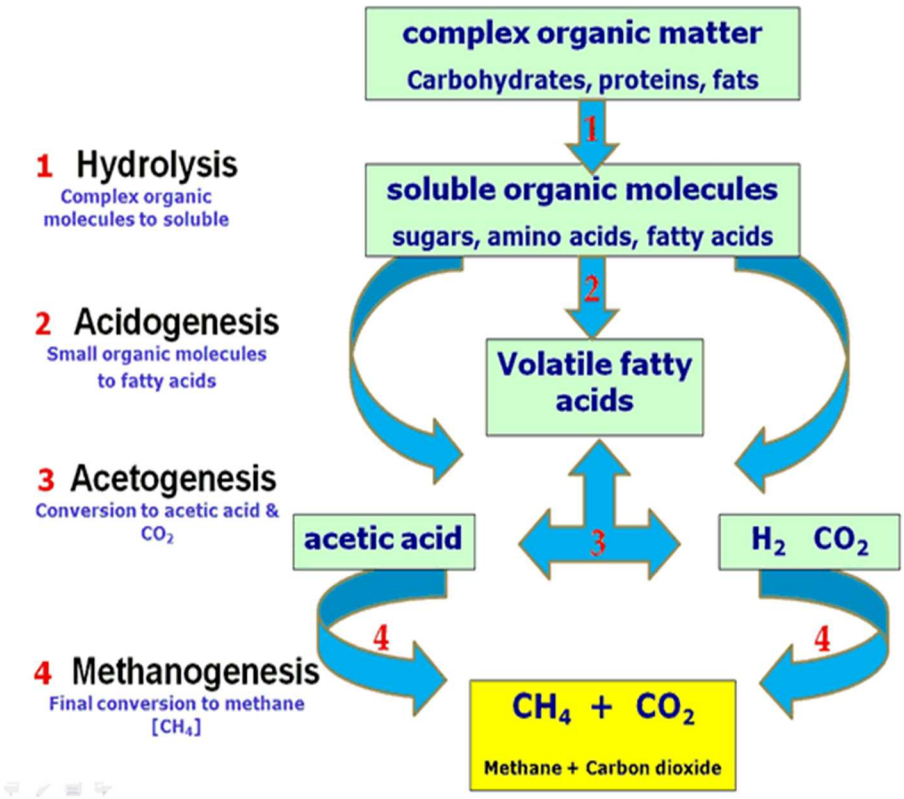


Figure 1.1 Flow diagram of anaerobic digestion process

(Source: http://readigesters.com/digesterbasics.php)

It was reported that over 120 million tons of dairy manure are produced in the U.S. annually [5]. If all of the dairy manure is treated by anaerobic digestion, it could generate the amount of energy that is enough to power 3.5 million American houses and also reduce carbon dioxide equivalent emission of up to 11 million vehicles [6]. Despite its advantages of versatility and efficiency in treating organic wastes as well as its wide installation, the AD process is hampered for further development by its shortcomings of relative high nutrients level of liquid effluent (liquid digestate), low utilization of the fiber-rich solid residues (solid digestate), and high contents of carbon dioxide ($CO_2$), hydrogen sulfur ($H_2S$) and other impurities in biogas, which are briefly summarized as follows:

1. Liquid digestate has relatively high levels of chemical oxygen demand (COD), and nutrients (nitrogen and phosphorus), which could lead to serious environmental consequence if not properly treated. It has been reported that liquid digestate has 8000 – 10,000 mg $L^{-1}$ of chemical oxygen demand (COD), 1000 – 1500 mg $L^{-1}$ of total phosphorous (TP), and 3000 – 5000 mg $L^{-1}$ of total nitrogen (TN) [7].
2. Fiber-rich solid digestate is mainly used for low-end applications: soil amendment, animal bedding and incineration for energy production. Finding high-value applications of solid digestate will significantly improve the economic performance of AD technologies.
3. A large amount of $CO_2$ in biogas decreases the overall carbon utilization efficiency and corresponding energy production. Relatively high contents of $H_2S$ and other impurities could damage the engines and other biogas handling equipment. Removing $H_2S$ and other impurities is critical to ensure biogas utilization for energy production. Developing a method to further sequester $CO_2$ from anaerobic digestion operation can significantly improve overall carbon utilization efficiency and correspondingly reduce the carbon footprint of anaerobic digestion.

Successful addressing the aforementioned challenges will greatly improve the sustainability of anaerobic digestion technology and enable extensive commercial applications in the near future.

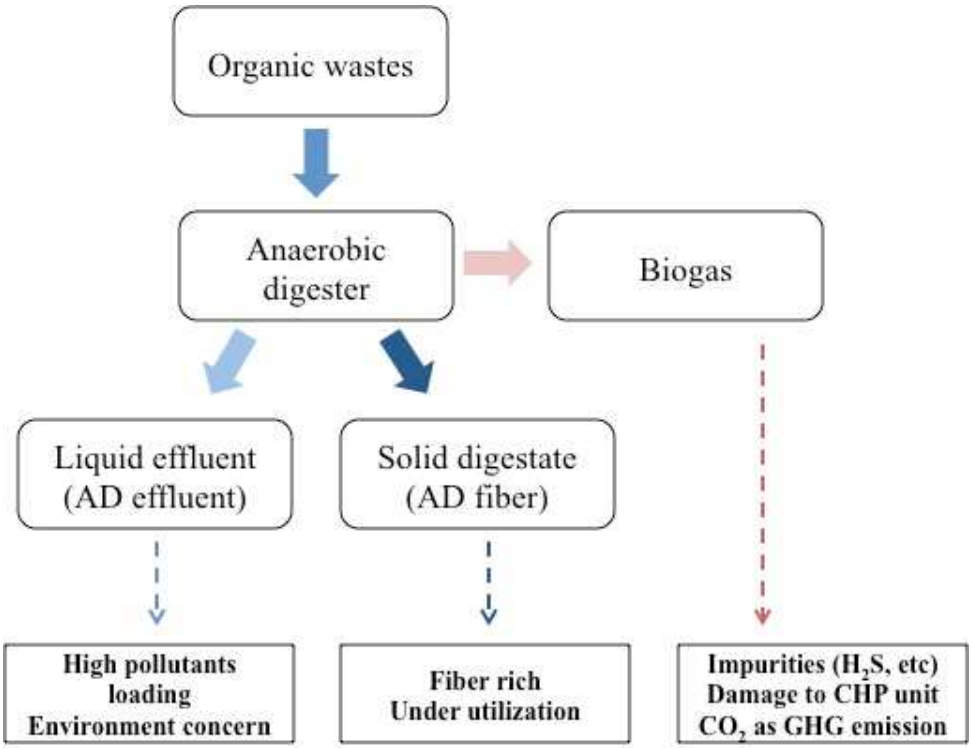


Figure 1.2 Challenges of AD process

### 1.3 Post-treatment of liquid digestate

Various treatment methods from the municipal wastewater treatment plant have been evaluated and studied with respect to the treatment of AD effluent, such as active carbon adsorption [8, 9], coagulation [10], dissolved air flotation (DAF) [11, 12], UV photocatalytic treatment [13], and ozone treatment [14]. However, high energy demand and chemical loadings make these methods less economically and environmentally feasible for liquid digestate treatment, and may also introduce a secondary contamination of chemical accumulation such as heavy metal [15].

Meanwhile, electrocoagulation (EC) has recently been studied to treat high-strength wastewater (high solids and chemical oxygen demand). Due to its high removal efficiency and chemical-free nature, EC requires shorter retention time and avoids a secondary pollution [15]. Different from conventional coagulation process, it utilizes

metal ions (iron, aluminum, etc.) generated in situ, and follows a stepwise mechanism [15, 16]: 1). 'The pledge' - Generation of 'coagulants' from electrolysis of the 'sacrificial electrode', known as metal hydroxo cationic complex, to trigger coagulation process; 2). 'The turn' - Destabilization of colloidal suspensions and emulsions of particles; 3). 'The prestige' - Flocs formation and aggregation for massive precipitation of particles. The Derjaguin-Landau-Verwey-Overbeek (DLVO) coagulation model could describe detailed mechanism of the destabilization step: a). Compression of the double diffuse layer of suspending charged particles; b). Neutralization of surface charges of suspending particles to minimize electronic repulsion force; c). Bridging and blanketing effect of formed flocs to entrap colloidal particles.

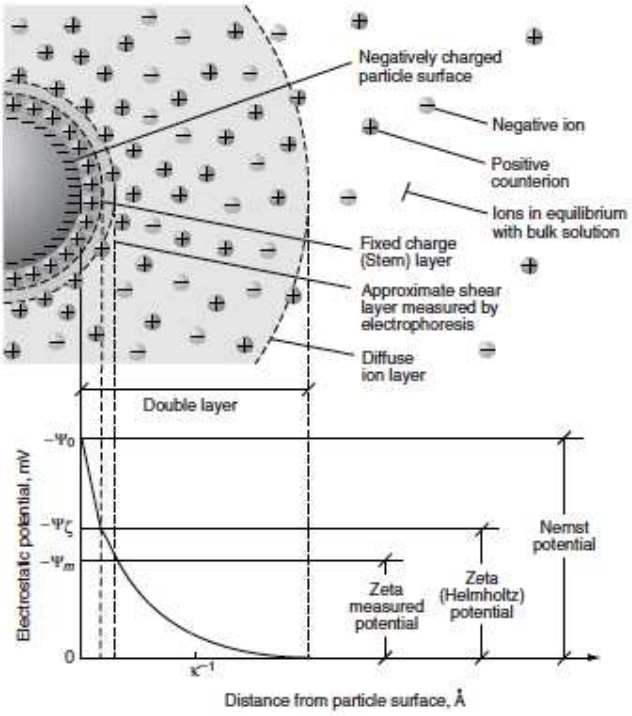


(a)

Figure 1.3 Schematic diagram of electric double layer (a) and the DLVO model describing repulsion and attraction forces (b).

Source: [17]

Figure 1.3 (cont'd)

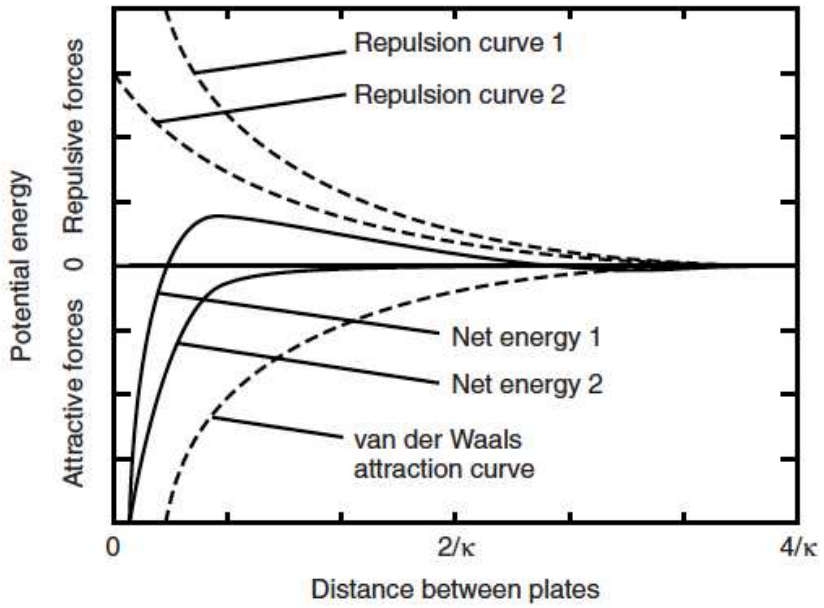


(b)

The stability of particles suspending in solution derives from the balance of two counter-forces: repulsive force from the same electrostatic charges, and attractive force known as the Van de Waals force. Fig. 1.3 (a) shows the electric double layer (EDL) formed on the negative charged surface of particle: the fixed layer where counter ions are tightly adsorbed to the negative charged surface, and the diffusing layer where both negative and positive ions are loosely surrounding the fixed layer. Due to the existence of EDL, the functioning distance of electrostatic repulsive force is longer than that of attraction force; therefore colliding particles would have to overcome a repulsion hurdle before the attracting Van de Waals force is able to bring two particles together, shown as the repulsion curve 1 and net energy curve 1 in Fig. 1.3 (b). If the EDL is invalidated or destabilized, the repulsion force would be greatly reduced (Repulsion curve 2 in Fig. 1.3 (b)), and the repulsion barrier could thus be completely eliminated (Net energy curve 2 in

Fig. 1.3 (b)), leading to a readily collision driven by the Van de Waals attracting force [17].

EC is frequently implemented in wastewater treatment for paper industry [18], mining and metal industry [19], food manufacturing [9], and oil industry [19]. The EC technology has also shown great nutrients removal performances in various agricultural wastewater treatments. Sengil and Ozacar reported 98% and 99% removal efficiency of COD and oil-grease from dairy wastewater [20]. Lei et al. reported a comprehensive study of different parameters' influence on electrochemical treatment of anaerobic digestion effluent from swine manure digester, using Ti/Pt–$IrO_2$ electrode as an anode, and a significant removal efficiency of total organic carbon (TOC) and inorganic carbon (IC) was observed [21]. Kaan Yetilmezsoy, et al. reported that 90% of COD and 92% of color reduction could be achieved by EC post-treatment of poultry manure wastewater [22].

EC treatment is an excellent method to remove COD, TS and TP that are associated with suspended particles, however, it is relative less efficient on compounds with high water solubility, such as ammonia nitrogen. Numerous studies have been conducted to remove ammonia nitrogen from liquid digestate. Jiang et al developed a system to recover ammonia from dairy manure digester as nitrogen fertilizer using air stripping technology [23]. Algal cultivation is also considered as an effective way to remove ammonia nitrogen from liquid digestate. Mulder reported several sustainable nitrogen removal technologies and concluded that algal cultivation is one of the good technologies that can remove 23-78% of total nitrogen in the effluent [24]. Li et al., reported an 83-99% of total nitrogen removal by culturing freshwater microalgae *Scenedesmus* sp. under an

optimal N/P ratio [25]. Wang et al. reported a 100% of ammonia nitrogen removal and 82.5% of total nitrogen removal through culturing oil-rich green microalgae *Chlorella* sp. on liquid digestate [25], indicating that lipid-based biofuel can be produced along with nutrients removal by algae cultivation. In addition, EC water (supernatant after the EC treatment of liquid digestate), even with relative high level of nitrogen, provides a water stream that could potentially serve as processing water for the applications with large water demand and low water quality requirement.

### 1.4 Utilization of solid digestate

Solid digestate was generally considered as a 'recalcitrant' material since accessible organic compounds in organic wastes have been degraded and utilized during anaerobic digestion, and relative large portions of recalcitrant organic fractions such as lignin were often observed [26]. Applications of solid digestate are thus mainly limited to animal bedding [27], soil amendments [26, 28], and plant growth medium [29]. Biochar production from various anaerobically digested biomasses is another potential application of AD solid residues [30-32].

Recent studies have suggested that despite the relative high 'recalcitrance', the solid digestate demonstrated a similar overall glucose conversion ratio compared to regular energy crops [33], and it could be used as a potential feedstock for fuel and chemical production [34].

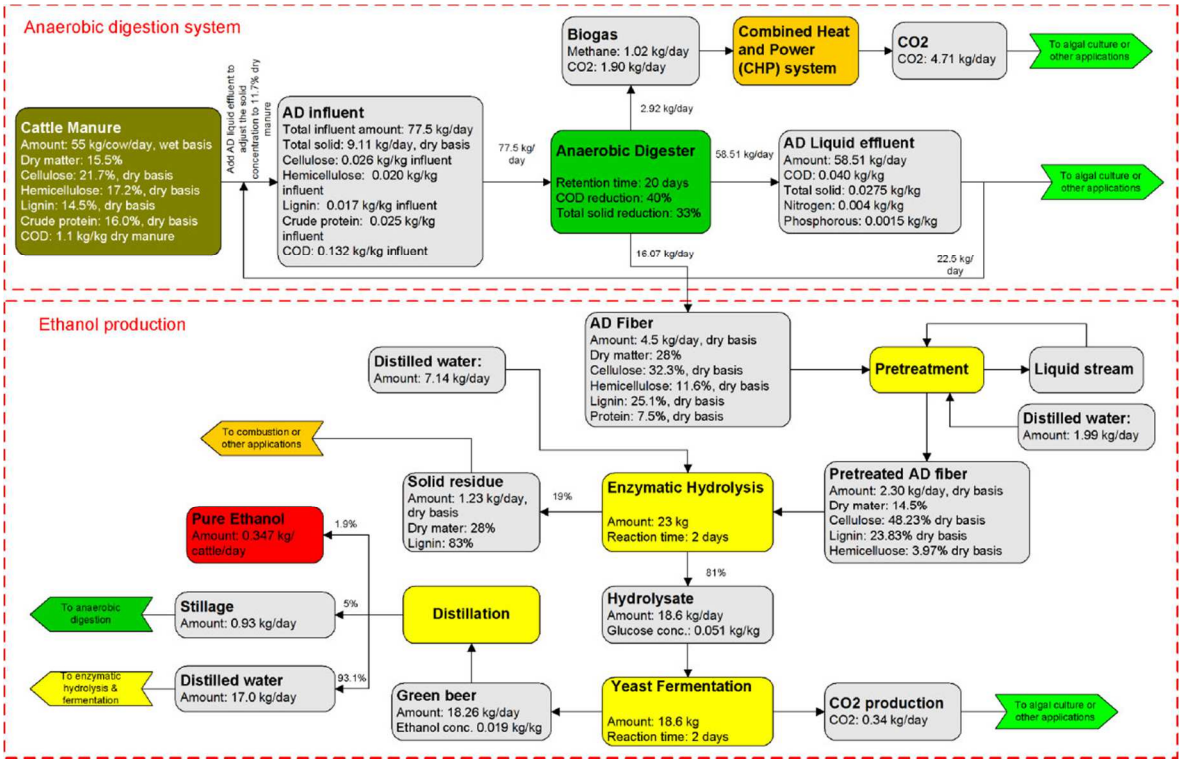


Figure 1.4 Mass balance of integrated anaerobic digestion and biorefinery of ethanol production per dairy cow.

Source: [35]

Yue *et al.* reported an integrated system of anaerobic digestion and ethanol production (Figure 1.4). 32.3% of cellulose, 11.6% of hemicellulose and 25.1% of lignin in solid digestate were obtained after anaerobic digestion, which led to a final ethanol production of 0.347 kg/cattle/day. Based on the integrated process, 1.67 billion gallons of ethanol production could be achieved from 120 million tons of cattle manure generated annually in the United States [35]. Bramono *et al.* also reported production of butanol by mesophilic clostridium species from sugar derived from anaerobic digested fiber with yield of 0.235g/g glucose and 0.247g/g xylose [36]. Yuan et al. expanded utilization of solid digestate to advanced biodiesel's production by combining anaerobic digestion with aerobic fungal fermentation process to produce biodiesel, and achieved a positive net energy output of 57 MJ/L biodiesel [37].

Although these studies revealed promising pathways to utilize solid digestate for bioalcohol and biodiesel production, these pathways are still hurdled by: 1) High processing cost and investment input; 2) Low revenue in return; and 3) Limitations of available technologies for competitive industrial scale application [38, 39]. Thus, developing biorefinery systems to target on fine chemicals [38] [39] is urgently needed to enable value-added utilization of solid digestate. It has been reported that lignocellulosic biomass could be used to produce a variety of block chemicals, such as succinic acid [40], itaconic acid [41], lactic acid [42], acrylic acid [43], and ethylene [44]. High value biopolymers such as natural amino polysaccharide – chitin and its N-deacetylated derivative – chitosan are also produced using fungal cultivation [45]. Fungal chitin/chitosan production has advantages of lower level of inorganic materials, no geographic or seasonal limitations [46, 47], better effectiveness in inducing the plant immune response (as a fertilizer) [48]. Therefore, producing chitin/chitosan from solid digestate could be a technically and economically feasible solution for both animal agriculture and chitin/chitosan industry.

### 1.5 Upgrade of raw biogas and utilization of $CO_2$

Depending on feeds and operational conditions of anaerobic digestion, biogas mainly consists of methane ($CH_4$, 40-75%) and carbon dioxide ($CO_2$, 15-60%). Other impurities such as hydrogen sulfide ($H_2S$, 0.005-2%), water ($H_2O$, 5-10%), and ammonia ($NH_3$, <1%) are also detected in the biogas [49]. The efficiency of energy conversion from methane to electricity and heat is often adversely influenced by these impurities [7]. Since $H_2S$ can be converted to $SO_2$ and $H_2SO_4$ during biogas processing that are detrimental to engine and other accessary equipment [50], $H_2S$ and other sulfur

containing compounds in the biogas are considered highly toxic to anaerobic digestion system, particularly on biogas utilization for energy production. Removal of $H_2S$ is therefore necessary prior to biogas utilization of energy generation. Several technologies have been developed and applied, such as adsorption by Ethylenediaminetetraacetic acid (EDTA) coupled $Fe^{3+}$ solution [51] and active carbon [52], bioadsorption [53], and metal ion precipitation [54]. However, similar to the treatment of liquid digestate, these methods require not only additional chemical and energy but also expensive gas clean-up equipment, which make biogas energy production less economically viable, particularly for small-scale digestion systems [7]. Therefore, simple yet effective methods to remove $H_2S$ with minimal chemical and energy input are in great need.

$CO_2$ is a major component in the biogas besides methane. It is not toxic to biogas utilization, however, its presence does reduce the energy efficiency of biogas, and makes biogas upgrading difficult due to its adverse effect on interchangeability of biogas (Figure 1.5) [49]. Several $CO_2$ removal techniques have been developed and applied in biogas upgrading process, including high pressure water adsorption [55], chemical scrubbing [56], and membrane separation [57-59]. All of these $CO_2$ removal technologies focus on improving methane fuel quality, and thus have little to do with $CO_2$ sequestration. Therefore, in order to further reduce carbon footprint of anaerobic digestion, new $CO_2$ sequestration technologies need to be considered and studied.

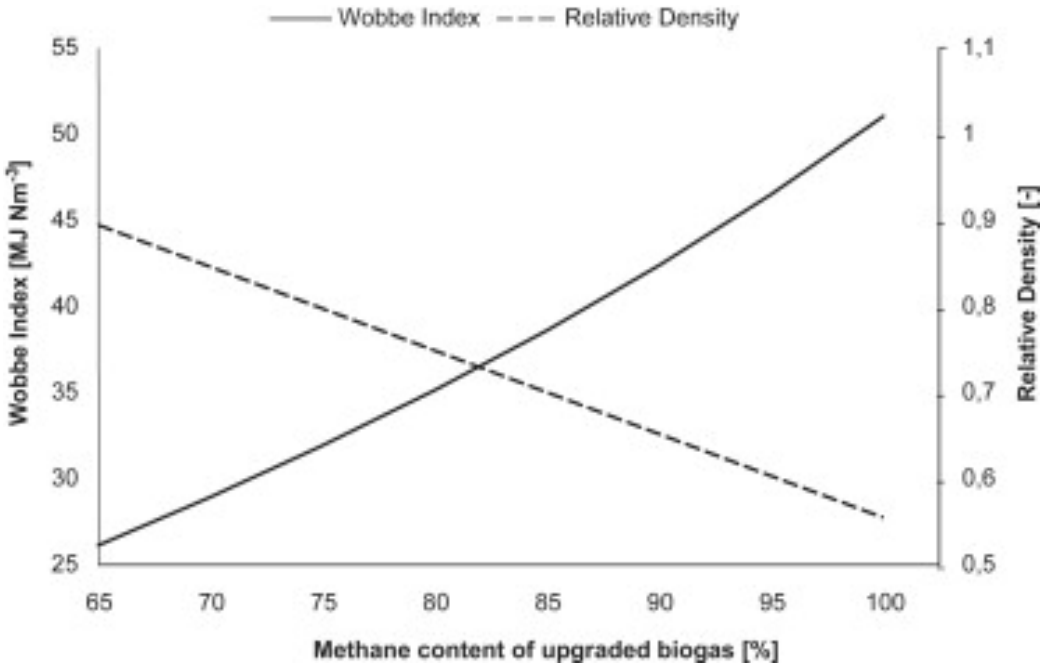


Figure 1.5 Wobbe index and relative density as function of methane content of the upgraded gas*

Source: [49]

* Wobbe Index or Wobbe number is an indicator of the interchangeability of fuel gases such as natural gas, liquefied petroleum gas, biogas, etc.

Algal cultivation is an effective and environmental friendly technology for $CO_2$ fixation due to its photosynthetic nature and relatively simple nutrients demand [60]. Considering good tolerance to concentrated nutrients (nitrogen and phosphorous) and fast growth rate (compared to crops), algae culture has been used to remove excessive nutrients from wastewater streams and to produce biofuels and other value-added chemicals [61] at the same time. Chen, *et al* reported a fresh water algal assemblage that could tolerant 200 g $m^{-3}$ nitrogen level and reached 6.83 g $m^{-2}d^{-1}$ of biomass productivity in a semi-continuous raceway pond [62]. Tang, *et al.* investigated the response of two algae species to different $CO_2$ feeding concentrations, and found that higher $CO_2$ levels were beneficial to algal lipid synthesis [63].

Electrochemical reduction of $CO_2$ is considered as another promising technology that could potentially complete the anthropogenic carbon cycle by recycling $CO_2$ into various compounds with different electrodes and electrolysis conditions [64]. Three groups of electrodes could be categorized (Figure 1.6), depending on whether the electrode could bind the reduction intermediate or not and if carbon monoxide (CO) could be further reduced [64].

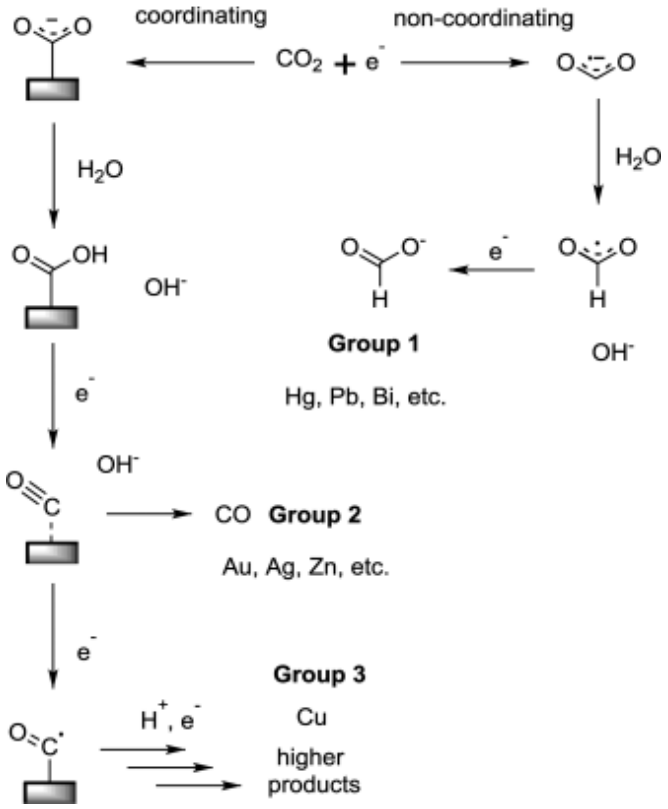


Figure 1.6 Mechanism for electrochemical CO2 reduction on metal surfaces in water.

Source: [64]

Metals in Group 1 can be used in electrochemical reduction of $CO_2$ since they do not bind the highly reactive intermediates that react with water to form formic acid as final product. Formic acid has been the primary product from $CO_2$ reduction on metals with very high hydrogen evolution reaction (HER) overpotentials, which is essential to avoid

the easier reaction of electrolysis of water to generate hydrogen instead of $CO_2$ reduction [65]. Over 97% of faradaic efficiency has been reported to reduce $CO_2$ for formate production [66, 67]. In addition to chemical conversion, biological conversion from $CO_2$ to formate was also reported [68, 69]. Schuchmann and Muller reported a hydrogen-dependent carbon dioxide reductase from *Acetobacterium woodii*, which was 2000-time more effective than the fastest chemical catalysis of $CO_2$ to formate conversion [68]. Torsten Reda, et al. also discovered that a tungsten-containing formate dehydrogenase enzyme (FDH1) could efficiently help the electrochemical fixation of $CO_2$ with much-reduced over-potential requirement and great selectivity to the sole end product of formate [69].

Formate is a simple one-carbon organic compound widely involved in different biochemical reactions [70, 71], making formate a great intermediate to extend biological utilization of $CO_2$ beyond photosynthesis. Li, *et al.* reported an integrated electro-microbial system to convert $CO_2$ to higher alcohols with formate as the intermediate energy carrier as shown in Figure 1.7. $CO_2$ was converted into formic acid through electrochemical reduction, and the genetic modified strain *R. eutropha LH74D* was cultured in the same reactor to produce isobutanol and 3-methyl-1-butanol (3MB) from formate [72]. This inspiring study demonstrates a direct utilization of $CO_2$ converted formate as carbon source for production of biofuels, which represents a novel path in $CO_2$ reutilization.

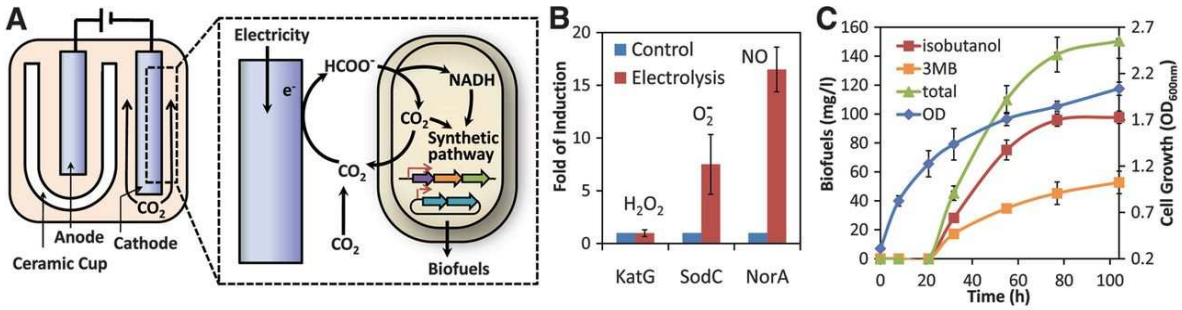


Figure 1.7 An integrated electromicrobial process to convert $CO_2$ to higher alcohols.

(A) Electricity powered the electrochemical $CO_2$ reduction on the cathode to produce formate, which is converted to isobutanol and 3MB by the engineered *R. eutropha*. (B) *R. eutropha* strains harboring a reporter gene driven by promoters that respond to reactive oxygen and nitrogen species showed increased reporter activity upon electrolytic exposure. (C) Engineered strain *R. eutropha* LH74D showed healthy growth and produced over 140 mg/l biofuels in the integrated electromicrobial reactor with electricity and $CO_2$ as the sole energy and carbon sources, respectively.

Source: [72]

It has also been reported that supplementation of formate could facilitate *Penicillium chrysogenum* cultivation and Penicillin G production in fungal fermentation [73]. The co-consumption of formate and glucose shed lights into the potential metabolic advantage of adding formate in fungal fermentation from perspective of extra energy source [73]. Similar enhancement in oleaginous fungus fermentation of *Mortierella Isabellina* for lipid production by formate was also reported [74], however, the underlying mechanism was unclear.

In summary, raw biogas from AD process needs to go through purification and upgrade process to remove detrimental impurities ($H_2S$) and increase the purity of methane. $CO_2$ from raw biogas and end product of methane processing needs further sequestration to pursue a carbon neutral system. Conversion $CO_2$ to formic acid is a promising pathway since formate provides versatile functions during fungal fermentation such as direct contribution to biofuels (isobutanol), and indirect enhancing certain metabolic pathways

to accumulate the targeted products such as lipid from oleaginous fungus. In order to maximize the advantage of formate addition, it is important to understand the underlying mechanism of formate metabolism in fungus.

### 1.6 Objectives

As shown in Figure 1.8, the goal of this study is to develop a sustainable biorefinery concept to address the challenges of organic waste treatment and utilziation: treatment of nutrient-rich liquid digestate using EC technology, utilization of solid digestate using fungal fermentation, and removal impurities in raw biogas and recycle $CO_2$ to facilitate fungal metabolism. To achieve this, the following objectives are set:

1. To design and optimize a novel EC process (EC system integrated with biogas pumping, EC reactor design and scale-up),
2. To investigate integration of EC treatment and algal cultivation for further purification of AD liquid effluent and $CO_2$ fixation,
3. To investigate integration of EC treatment and fungal fermentation to utilize solid digestate for production of value-added chemicals,
4. To investigate formate metabolism in fungus fermentation.

The proposed integrated system is expected to provide a synergistic solution to realize value-added utilization of biogas, liquid digestate and solid digestate.

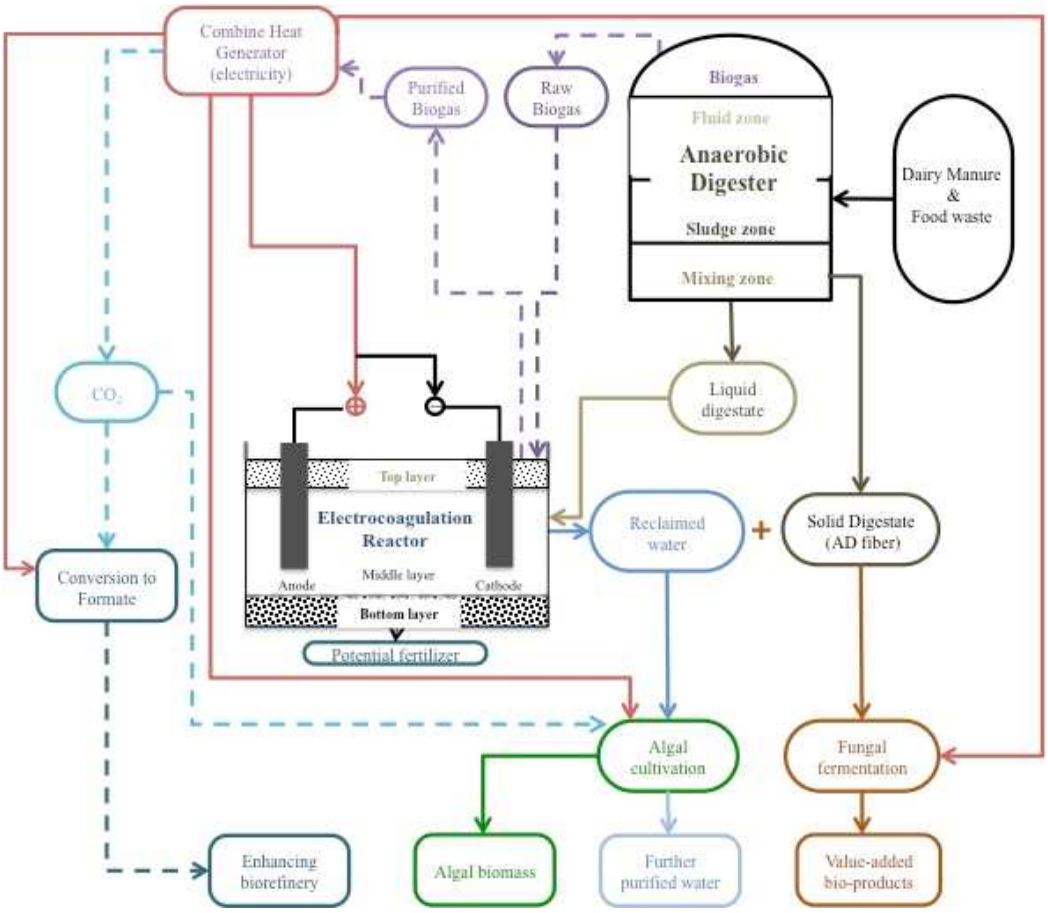


Figure 1.8 Integrated system to address challenges of AD process *

*Red: energy flow; purple: biogas flow; light brown: untreated liquid digestate; light blue: treated liquid digestate; green: algal cultivation; dark brown: fermentation on AD fiber; bright blue: $CO_2$ fixation

# CHAPTER 2 A NEW MULTIPLE-STAGE ELECTROCOAGULATION PROCESS ON ANAEROBIC DIGESTION EFFLUENT TO SIMULTANEOUSLY RECLAIM WATER AND CLEAN UP BIOGAS

## 2.1 Abstract

A new multiple-stage treatment process was developed via integrating electrocoagulation with biogas pumping to simultaneously reclaim anaerobic digestion effluent and clean up biogas. The 1st stage of electrocoagulation treatment under the preferred reaction condition led to removal efficiencies of 30%, 81%, 37% and 100% for total solids, chemical oxygen demand, total nitrogen and total phosphorus, respectively. Raw biogas was then used as a reactant and pumped into the effluent to simultaneously neutralize pH of the effluent and remove $H_2S$ in the biogas. The 2nd stage of electrocoagulation treatment on the neutralized effluent showed that under the selected reaction condition, additional 60% and 10% of turbidity and chemical oxygen demand were further removed. The study concluded a dual-purpose approach for the first time to synergistically combine biogas purification and water reclamation for anaerobic digestion system, which well addresses the downstream challenges of anaerobic digestion technology.

**Key words**: Electrocoagulation, anaerobic digestion, biogas purification, nutrient removal, water reclamation

## 2.2 Introduction

Anaerobic Digestion (AD) has been proved as a practical and efficient technology to treat organic wastes (i.e., animal manure, municipal sludge, and food wastes), and produce renewable energy [75] and other value-added products [2]. However, liquid effluent from AD (Liquid AD effluent) still has relative high levels of biological oxygen demand

(BOD), chemical oxygen demand (COD), and nutrients (nitrogen and phosphorus). Appropriate treatments of liquid AD effluent are needed to further reclaim water. Physical and chemical methods such as sedimentation, flocculation, coagulation, ozone, and activated carbon, followed by reverse osmosis (RO) are often used to reclaim water from the effluent [10, 76]. Chemical uses and relatively low efficiency of these methods prevent their wide adoption by waste management. Compared to those conventional physical and chemical treatment methods, electrocoagulation (EC) technology, with advantages of shorter retention time, better removal of smaller particles, without the addition of coagulation-inducing reagents, and minimum secondary chemical contamination [77], represents a superior process to reclaim water from various organic waste streams. EC technology applies direct current electrolytic process and the flocculent separation to coagulate, precipitate, and float solids and pollutants. Metal electrodes in EC unit are made of iron or aluminum or other metals [78]. During the electrocoagulation reaction, current destabilizes electrostatically suspended solids that further react with cationic species from the anode metal to form precipitated or floated metal oxides and hydroxides [78]. EC technology has been used to treat AD effluent and other wastewater. It has been reported that EC process has very high efficiency to remove total solids, turbidity, and COD [79]. Bellebia et al demonstrated that EC can remove up to 75% and 99% of COD and turbidity, respectively, from paper mill effluent [18]. Mollah et al presented a 80% removal of total solids from slaughterhouse wastewater using EC [80]. Factors such as current density, retention time, initial pH, electrode distance, salt concentration, and electrode type have significant influences on EC performance. Among them, pH is the most important one [16, 81, 82]. pH during the EC

process is gradually increased due to the increase of hydroxyl ions from cathodes. It has been reported that high pH is disadvantageous in solids and nutrients removal during EC [20, 83]. Controlling pH during EC process could be a simple and effective way to enhance the separation performance and improve energy efficiency. On the other hand, biogas from AD contains several by-products such as $H_2S$ and $CO_2$ besides the main compound of methane [84]. The existence of these by-products adversely influences biogas utilization for electricity generation since some of they are corrosive to engines and combustors. $H_2S$ is one of the most corrosive compounds in the biogas, which is converted into $SO_2$ and $H_2SO_4$ damaging gas-handling equipment during the biogas combustion. Many efforts have been made to remove $H_2S$ and other by-products from biogas. Ethylenediaminetetraacetic acid (EDTA) coupled $Fe^{3+}$ solution has been used to adsorb $H_2S$ in biogas [85]. Metal ions such as $Cu^{2+}$, $Zn^{2+}$ and $Fe^{3+}$ were applied to precipitate sulfate-based compounds [54]. Activated carbon was studied to absorb $H_2S$ in biogas [52, 86, 87]. Other chemical abatement and biological absorption have also been reported as effective methods to remove $H_2S$ [88-91]. However, most of these approaches either require additional chemicals or need complicated systems to support, which make it economically and environmentally difficult to implement them.

Considering both facts of biogas with relatively high $H_2S$ content and EC treated AD effluent with high pH and metal ion level, mixing these two streams could facilitate EC treatment of AD effluent and simultaneously clean up biogas. Therefore, the objective of this study is to develop a novel combined water reclamation and biogas clean-up process using a multiple-stage and biogas facilitated electrocoagulation on AD effluent, which synergistically improves the efficiencies of AD effluent treatment and biogas utilization,

and provides a new route to address the downstream challenges of anaerobic digestion technology.

## 2.3 Material and Methods

### 2.3.1 Preparation of the liquid AD effluent

AD effluent was obtained from a 1000 $m^3$ plug flow anaerobic digester in the Anaerobic Digestion Research and Education Center (ADREC) at Michigan State University (MSU). The feeds for the plug flow digester were dairy manure (60%) and food waste (40%). Thirty-three cubic meter of the feed with a total solids content of 10% was fed daily to the digester. The digester was operated at 40°C and 30 days hydraulic retention time. The dairy manure was from the MSU Dairy Teaching and Research Center, and the food wastes were from MSU cafeterias. The AD effluent was first filtered with a 200-mesh sieve to remove large-sized chunks. The filtrate was collected and then diluted with water to an initial total solid (TS) of approximately 1% (w/w). The diluted filtrate as the liquid AD effluent for this study was collected and stored at 4 °C. The characteristics of the liquid AD effluent were listed in Table 2.1.

| Parameters | Value |
|---|---|
| pH | 7.5-8.0 |
| TS (w/w %) | 0.90±0.03[a] |
| TSS (mg $L^{-1}$) | 4125[b] |
| TDS (mg $L^{-1}$) | 2035[b] |
| TOC (mg $L^{-1}$) | 2332[b] |
| Color absorbance (527.5 nm) | 0.718[b] |
| Conductivity (μs $cm^{-1}$) | 4740.7[b] |
| COD (mg $L^{-1}$) | 9140±140[a] |
| TP (mg $L^{-1}$) | 340±17.3[a] |
| TN (mg $L^{-1}$) | 1233±101[a] |

Table 2.1 Characteristics of AD liquid effluent

a: Data represent the average of three replicates with standard deviation.

b: Data represent the average of two replicates.

### 2.3.2 Experimental setup

A combined EC and biogas pumping unit was established to carry out the study. The liquid AD effluent was first treated by an EC, the liquid portion from the 1st EC treatment was separated and bubbled by raw biogas, and then a 2nd EC was applied on the biogas treated liquid to reclaim the water (Fig. 2.1). Another combined EC process without biogas pumping was also conducted as the control.

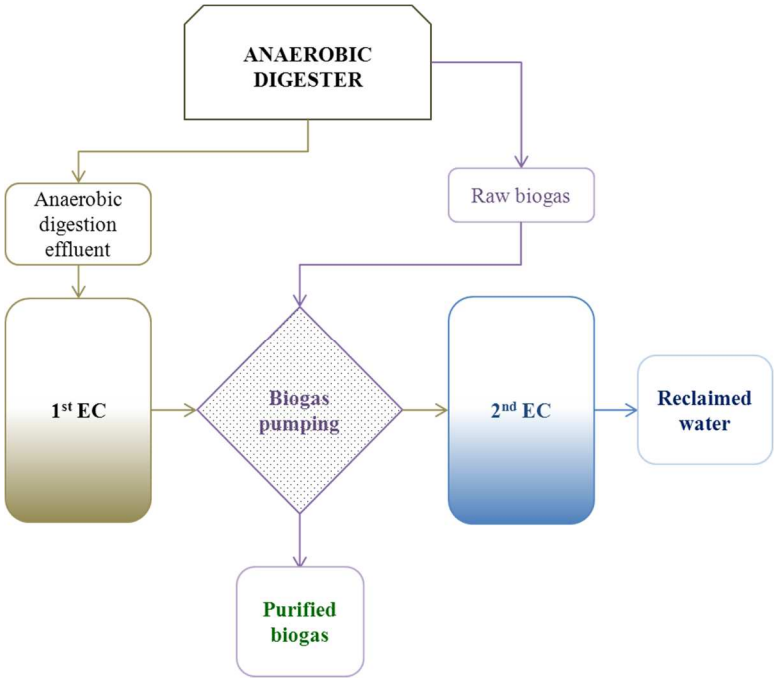


(a)

Figure 2.1 Demonstration of EC treatment and biogas pumping process.

(a) Flowchart of EC and biogas pumping process. (b) Schematic of the EC unit. (c) Schematic of the biogas pumping unit

Figure 2.1 (cont'd)

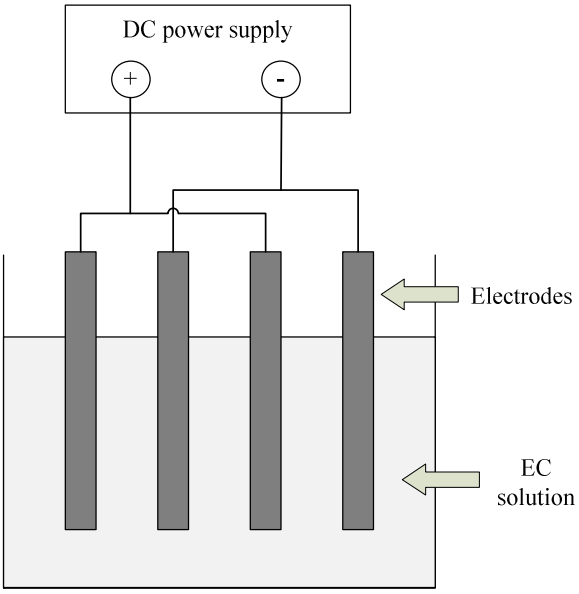


(b)

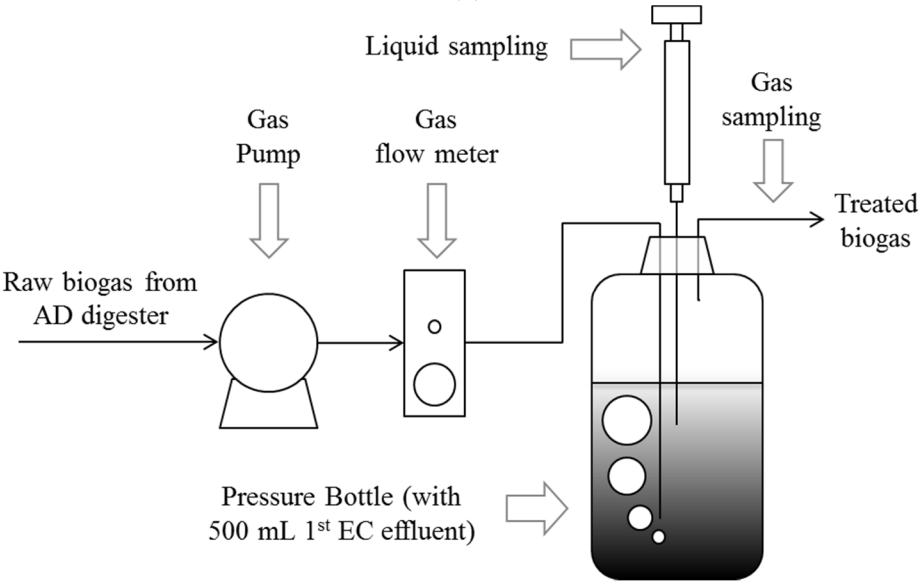


(c)

### 2.3.2.1 EC setup and operation

DC power supply (XPOWER™ 30V 3A) was selected to provide electricity. Two pairs of steel CRS 1018 were used as electrodes for both anodes and cathodes (Fig. 2.1(b)). Three different effective electrode surface areas of 62 $cm^2$, 134 $cm^2$ and 210 $cm^2$ were tested. Rectangular glass containers (effective volume of 500 mL) were adopted as reactors. PVC holders were placed on the top of the beakers to hold electrodes in the

reactors with 1 cm distance between electrodes. The electrodes were connected with power supply and with each other in parallel pattern.

Five hundred milliliter of the liquid AD effluent was used for individual EC runs. Voltage and power consumption were monitored throughout EC operation via a Kill A Watt ™ power monitor. The pH was also measured with Fisher ™ Scientific pH meter. The EC treated liquid was separated into three phases of top foaming layer, middle supernatant, and bottom solid layer. Post-EC treatments described as follow were conducted differently for 1st EC and 2nd EC.

Post 1st EC treatment: Three layers were clearly separated after the 1st EC treatment. The middle part was siphoned out and stored at 4 °C.

Post 2nd EC treatment: Since the middle supernatant was overlapped with the thicker top foaming layer and bottom solid layer, a mixing and settling process was applied after the 2nd EC. After 30 min settlement, the clear supernatant was collected for nutrient analysis and removal efficiency evaluation.

#### 2.3.2.2 Biogas pumping setup and operation

500 ml of collected supernatant (middle part) from the 1st EC was used as the solution. Raw biogas was bubbled into the solution via a pump (Gast™), and the flow rate was controlled at 1 vvm (volume gas/volume treated liquid/minutes, the corresponding flow is 0.5 L/min) by an air flow meter from VWR ™. The gas flow correction factor of the air flow meter to measure biogas flow is 1.0067, which is calculated based on the specific biogas gravity (1.011) at the operational conditions of 35°C and 5 inches water pressure. A gas outlet on the top of the bottle and a luer-lock 12'' gauge 20 needle submerged in the solution were installed for releasing biogas and taking biogas and liquid samples,

respectively (Fig. 2.1(c)). Bubble size was around 1 mm of diameter (based on the observation from pumping the biogas into the tap water). Liquid samples were taken every 10 min for pH measurement. Airbags were used to take gas samples. $H_2S$ concentrations in the original biogas and treated biogas were monitored during the pumping process.

### 2.3.3 Experimental design

A complete random design (CRD) was applied to optimize the 1st EC treatment. Three factors of current strength (I), retention time (RT), and electrode surface area (SA) were studied to conclude removal efficiencies of TS, COD and turbidity. Three levels of individual factors were tested: 0.5A, 1A, and 2A for I; 20, 40, and 60 min for RT; and 62, 134, and 210 $cm^2$ (A, B, C) for SA.

For the 2nd EC treatment, a CRD was again used to study the effects of the experimental conditions on water reclamation. Three levels of I (0.5A, 1A, and 2A) and two levels of RT (20 and 40 minutes) with a fixed SR of 62 $cm^2$ were tested; TS, COD, TP, and TN were measured to evaluate the performance of the 2nd EC.

### 2.3.4 Mass balance analysis

In order to evaluate the performance of the studied EC processes, mass balance on total iron, total nitrogen, total phosphorus, sulfur, and water was conducted on the preferred conditions of the EC processes with biogas pumping (BP) and no biogas pumping (NBP). Since water reclamation is a target of this study, liquid recovery was used to present how much water can be reclaimed by the preferred processes. The liquid recovery is defined as: liquid recovery (%) = volume of the reclaimed water after the treatment (ml) / volume of the original solution before the treatment (ml) x 100%.

### 2.3.5 Analytical methods

TS content was measured according to the dry weight method. COD, total phosphorus (TP) and total nitrogen (TN) were analyzed via HACH ™ standard methods [92]. Turbidity was measured by the EPA standard method [93]. The total iron concentration was analyzed by HACH™ standard metal prep set TNT™ 890. The sulfide ion concentration in the solution was tested by USEPA 4500-S2-D Methylyne Blue Method using a standard kit from HACH™. Ionic conductivities of liquid samples were measured using conductivity probe (Vernier Software & Technology, US). Total carbon (TC) and inorganic carbon (IC) were measured by a Shimadzu TOC-VCPN Total Organic Carbon Analyzer (Columbia, MD, USA). Total organic carbon (TOC) was calculated using TC to subtract IC. Total suspended solid (TSS) and total dissolved solid (TDS) were analyzed based on the following procedure: The solution was naturally settled for 30 min; Specific volume for different solution (25 mL for EC treated effluent and 10 mL for AD effluent) was filtered through a glass fiber filter with pore size of 0.7 μm and diameter of 25 mm (EMD Millipore, Germany); Filtrate and retained solid on the filter were then dried at 105°C overnight to obtain TSS and TDS, respectively. The color of lipid samples (AD effluent and EC treated water) was measured at the wavelength of 527.5 nm that was the representative visible wavelength for the effluents obtained from a light absorbance profiling test on Shimadzu UV-1800 spectrophotometer (Fig. S5).

Methane ($CH_4$), carbon dioxide ($CO_2$), and hydrogen sulfide ($H_2S$) contents in the biogas samples were measured using an SRI 8610C gas chromatography system. Hydrogen ($H_2$) and Helium ($H_e$) were used as a carrier gas with pressure set at 21 psi. The system was equipped with a thermal conductivity detector and kept at a constant temperature of

150 °C. The injection volume was 5 mL with 100 µL used for analysis. Ammonia ($NH_3$) and other trace gas components were identified using Agilent 6890/5973 GC/MS and CTC Combi PAL at the Michigan State University Mass Spectrometry and Metabolomics Core Facility. 100 µL gas sample with split ratio of 100:1 was injected into Agilent GS-GasPro® column (30 m, 0.32 mm, 7 inch cage). The separation of gas compounds was achieved using the temperature profile: 40°C for 2.8 min, 40°C $min^{-1}$ to 260°C, and 260°C for 5 min. Gas compounds were identified by comparing their m/z values with the ChemStation database.

### 2.3.6 Statistical analysis

General linear model (GLM) analysis using the Statistical Analysis System program 9.3 (SAS Institute, Inc. Cary, NC) was conducted to investigate the effect of reaction conditions on EC. I, RT, and SA were taken as parameters. Analysis of variance (ANOVA) and pair-wise comparisons were used to interpret the data and draw conclusions.

## 2.4 Results and Discussion

### 2.4.1 The 1st EC treatment

TS and COD removal effects were demonstrated in Figure 2.2. According to the GLM analysis (Fig. 2.2 and Table A1(a)), the experimental runs with the current of 2A had a significantly ($p<0.05$) better COD removal (62.9%) than other current levels. The higher currents of 1A and 2A also had better TS removal than the lower current of 0.5 A (Fig. 2.2 and Table A1(b)). Under the current of 2A, longer RT and smaller SA were beneficial for both COD and TS removal. The results indicate that current density (current strength on unit surface area of electrodes) was critical to improve the electrocoagulation

performance on AD liquid effluent, which is consistent with other studies on various waste streams [22, 94]. It was reported that high current density leads to generation of a large amount of cations and gas bubbles, cations act as coagulants to agglomerate small particles to form flocs in the solution, the gas bubbles then float the flocs to the surface, and the water is reclaimed [95, 96]. With more particles being removed by flocculation and flotation, the electrical conductivity of the EC solution was correspondingly decreased. Thus, the electrical conductivity could serve as an indirect indicator of EC performance of particle removal. As shown in Figures 2.2 and Figure A2, a big drop of electrical conductivity was observed with the runs under 2A that had better TS and COD removal than other current levels.

Considering TS and COD removal, the EC conditions of 2A, 60 min with electrode surface area of 62 $cm^2$ were selected to carry on the 1$^{st}$ stage EC treatment of AD effluent. Dynamic change of COD, TP and TN during the selected EC treatment was further investigated (Fig. 2.3(a)). TP was dropped from 340 mg/L to 0 mg/L within 60 min of HR, and a COD removal of 86% was achieved during 60 min of EC. However, TN content was barely impacted by the EC treatment, maintaining a relative high level of 1000 mg/L. It is because over 80% of total nitrogen in the liquid AD effluent was in the form of ammonia. Ammonia is highly soluble in water and thus difficult to be removed by EC. Both pH and power consumption kept increasing during the 1$^{st}$ EC (Fig. 2.3(b)). At the end of the 1$^{st}$ EC, the pH and power consumption reached 11.5 and 0.12 kWh/L respectively.

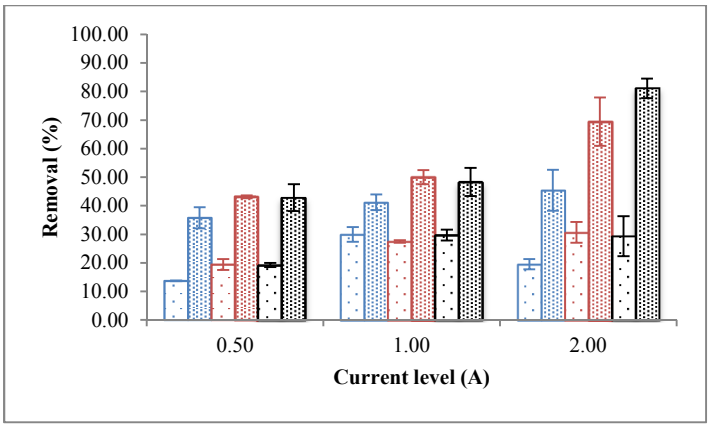


(a)

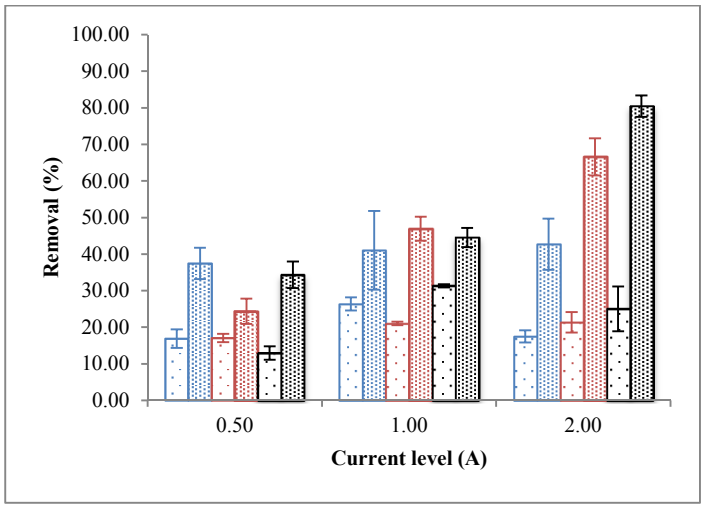


(b)

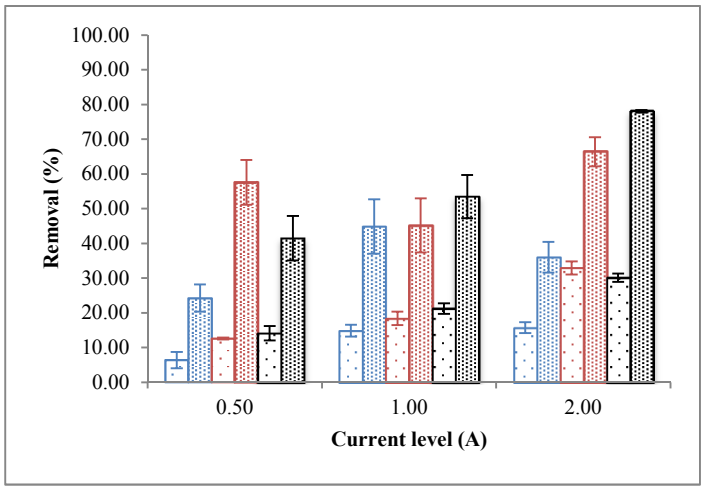


(c)

Figure 2.2 TS and COD removal of 1st stage EC *

*Columns with sparse dots stand for TS removal, and columns with dense dots stand for COD removal. Blue (left), red (middle) and black (right) stand for the retention times of 20, 40 and 60 min respectively. (a) TS and COD removal efficiency with electrode

surface area of 62 $cm^2$. (b) TS and COD removal efficiency with electrode surface area of 134 $cm^2$. (c) TS and COD removal efficiency with electrode surface area of 210 $cm^2$. * Data represent the average of three replicates with standard deviation

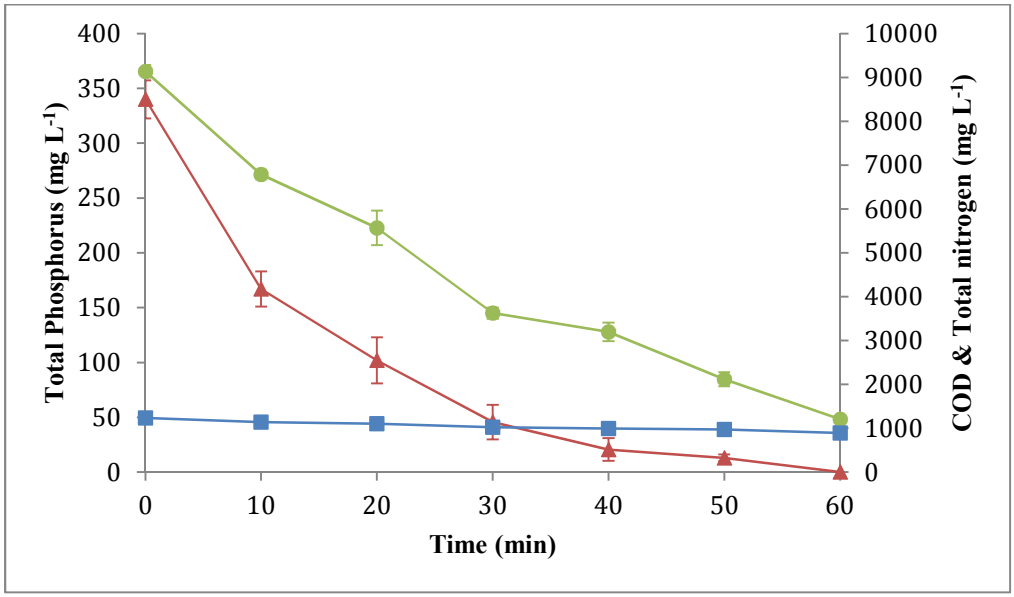


(a)

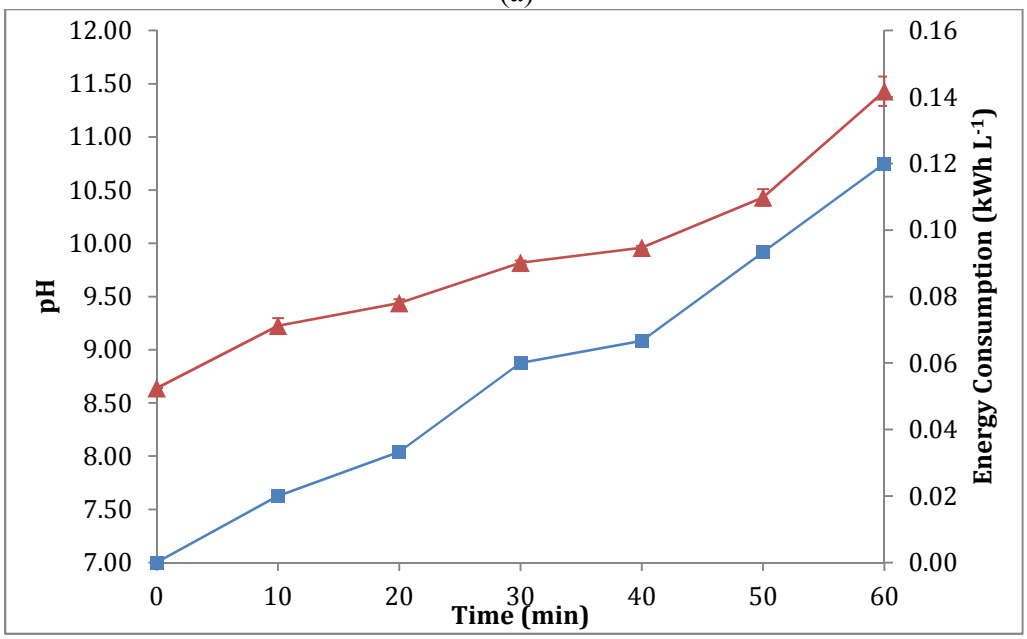


(b)

Figure 2.3 Dynamic change of nutrients, pH and power consumption of 1st EC under the selected conditions*

(a) Dynamic change of TP, COD and TN of AD effluent. Red triangle stands for TP, green circle stands for COD, and square blue stands for TN. (b) Dynamic change of pH and power consumption of AD effluent. Red triangle stands for pH change, and blue square stands for energy consumption.
*Data of power consumption, TP and COD are the average of three replicates

### 2.4.2 Biogas cleanup and pH adjustment of the EC effluent

Although significant improvement of TS, COD, and TP removal were obtained from the 1st EC, COD was still at a level over 1000 mg/L, which means that both organic and inorganic pollutants were still abundant in the EC effluent [81]. In order to achieve water reclamation from AD liquid effluent, an additional EC is needed. However, as shown in Figure 2.3(b), pH of the solution was very high at the end of the 1st EC due to the production of hydroxide ion ($OH^-$) during the EC. It has been reported that a high initial pH would negatively influence the EC performance [22, 97-99]. Under high pH level, removal efficiency of COD, TS and other nutrients during EC treatment is largely reduced, and energy demand is dramatically increased, which make EC process energy intensive and less efficient. It has also been reported that pH range of 4.0 – 8.0 is preferred as initial pH for EC to have a good nutrients removal performance with relatively less energy demand [100, 101]. A pH adjustment was thereby necessary in EC treatment to maintain a good efficiency. On the other hand, the byproducts of $CO_2$ and $H_2S$ in biogas are acidic, and using them to neutralize the pH of EC solution can address both issues of biogas cleanup and EC performance efficiency. A biogas pumping step was thus introduced to mix raw biogas and the 1st EC effluent.

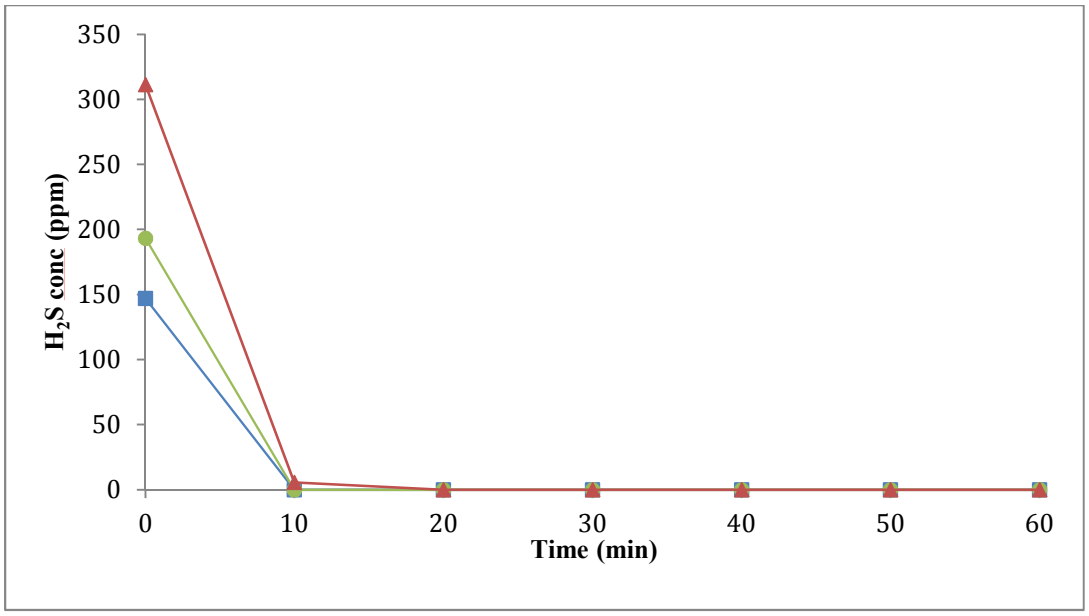


(a)

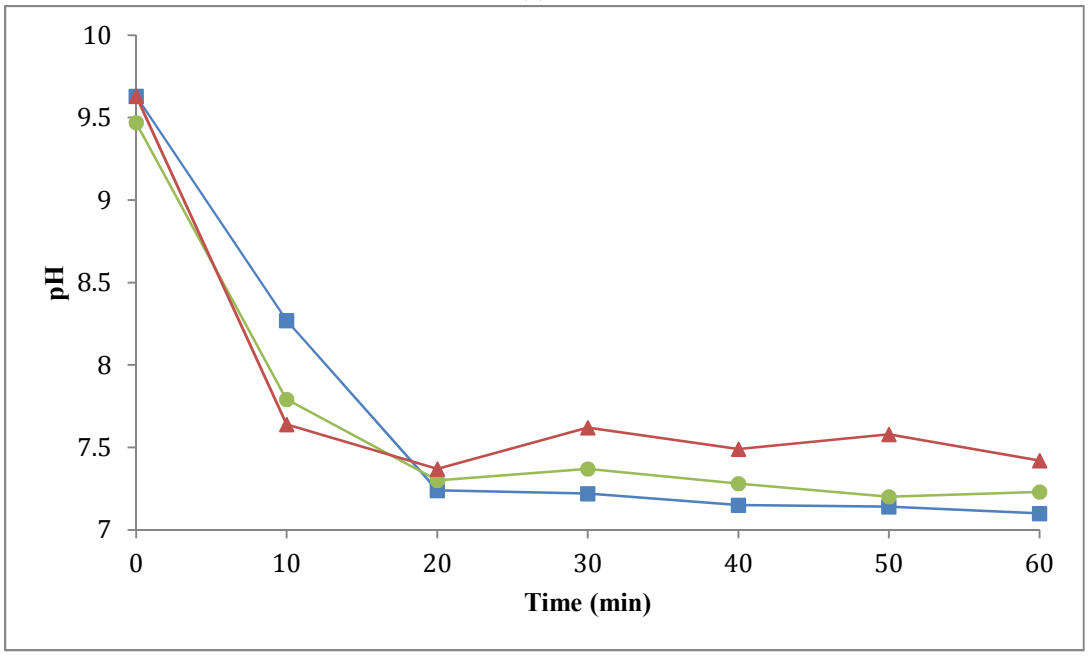


(b)

Figure 2.4 $H_2S$ and pH change of 1st EC effluent during biogas pumping

Blue square stands for batch 1, green circle stands for batch 2, red triangle stands for batch 3. (a) Dynamic change of $H_2S$ concentration. (b) Dynamic change of pH

As shown in Figure 2.4(a), $H_2S$ concentration dramatically dropped from 300 ppm to 0 ppm in the first 20 min of biogas pumping, and maintained no detectable for the rest of the testing period (60 minutes). However, once the $H_2S$ concentration in the biogas

exceeded 300pm, there was small amount of $H_2S$ (35 ppm) detected in the treated biogas at the end of the testing period (Table A1). These results indicated that the conditions of 60 minutes and 1 vvm are good for the biogas containing 300 ppm or less $H_2S$, but may not be suitable for the biogas with high $H_2S$ content. In-depth studies are needed to further understand the effects of EC solution and biogas pumping on $H_2S$ removal. Gas analysis also demonstrated that $CH_4$ content stayed stable during the biogas pumping. $CO_2$ was declined slightly at the beginning of the biogas pumping, and backed up to the content similar with the raw biogas (Table A1). There was no significant amount of $NH_3$ detected in the raw biogas, as well as in the treated biogas (Figure A3). Meanwhile, the pH level of the liquid effluent had a substantial reduction, and a pH of 7.25 was obtained at the end of the biogas pumping (Fig. 2.4(b)). The results elucidated that the combined operation not only efficiently removed $H_2S$ from biogas as a key step for biogas purification, but also acidified the solution to facilitate the following EC process. The $H_2S$ removal of biogas pumping could be theoretically explained based on the following reactions [102]:

$$H_2S = HS^- + H^+$$

$$2Fe^{3+} + HS^- = 2Fe^{2+} + S\downarrow + H^+$$

$$Fe^{2+} + H_2S + 2OH^- = FeS\downarrow + 2H_2O$$

At the initial stage of biogas pumping, the abundance of hydroxyl ions ($OH^-$) promoted the dissolving of hydrogen sulfide ($H_2S$) into water and disintegrated into hydrosulfide ions ($HS^-$) and hydrogen ions ($H^+$). The latter two reactions consequently occurred and

functioned in $H_2S$ fixation. The hydrogen ions ($H^+$) also react with $OH^-$, which drives the equilibrium of these reactions towards the right side. With formation of FeS and S, the other characteristics of the BP effluents besides pH were significantly changed as well. BP effluent had 1.87 g/L and 308 NTU of COD and turbidity, correspondingly, which were higher than 1.00 g/L and 277 NTU of NBP effluent (Table 2.2).

| Parameter | NBP effluent | BP effluent |
|---|---|---|
| Total solids (%, w/w) | 0.5±0.1[a] | 0.6±0.1[a] |
| COD ($mgL^{-1}$) | 1000±140[a] | 1873±23[a] |
| TN ($mgL^{-1}$) | 801[b] | 777[b] |
| Turbidity (NTU) | 277.0±54.1[a] | 308.0±14.2[a] |
| Ionic conductivity ($\mu s\ cm^{-1}$) | 2986.5[c] | 4893.2[c] |

Table 2.2 Characteristics of 1st EC effluent

a: Data represent the average of three replicates with standard deviation.
b: TN data represent the average of two replicates. TN tests were measured separately for kinetic change, and may not comply with other data set.
c: Ionic conductivity represent the average of two replicates.

### 2.4.3 The 2nd EC treatment

The 2nd EC carried on the BP effluent from the 1st EC treatment was compared with the control (NBP effluent) to further evaluate the impacts of gas pumping on the performance of the 2nd EC. The effects of I and RT on turbidity, COD removal, pH, and power consumption of the 2nd EC effluent were demonstrated in Figures 2.5 and 2.6. Turbidity removal of the 2nd EC on both BP and NBP effluent were generally enhanced with the increase of RT and I, except for the EC on NBP under 1A where the turbidity removal was decreased with increase of RT (Fig. 2.5(a)). The data also demonstrated that all EC treatments on BP effluent had significantly ($P<0.05$) higher turbidity removal than the EC on NBP effluent. COD removal had a similar trend (Fig. 2.5(b)). Increase of RT and I

improved the COD removal of both NBP and BP effluent. The EC on BP effluent also presented obvious enhancement on COD removal compared to the EC on NBP effluent. Better turbidity and COD removal of the 2nd EC on BP effluent is partially attributed to lower pH of BP effluent (Fig. 2.6(b)) that is in favor of generation of more metal ions and increase of conductivity. The metal ions react with $OH^-$ ions in the solution to form metal hydroxide, which is one of the most important factors in removing COD and suspended solid (turbidity) via EC treatment [81]. The increased conductivity leads to low dynamic voltage (IR) drop of the electrolysis [16], therefore, less energy was needed by the EC on BP effluent. The 2nd EC on BP effluent only consumed 0.08 kWh/L (at 2A and 40 minutes) that was about half power demand of the corresponding 2nd EC on NBP effluent (Fig. 2.6(a)). In addition, total nitrogen (TN) change was also different between NBP and BP effluent. BP effluent had a significantly less TN removal (15.7%) in the 2nd EC treated solution than that of NBP effluent (39.7%). Those differences are also related with the pH difference between BP and NBP effluent. As shown in Figure 2.6(b), pH of the 2nd EC treated solution on NBP effluent remained above 9.5, which was much higher than that of BP effluent (pH around 8). There were over 80% of TN in liquid AD effluent was in the form of ammonia. Since high pH drives the equilibrium of ammonia and ammonium towards ammonia, more ammonia was thus released from the EC of the NBP effluent that led to low TN in the solution.

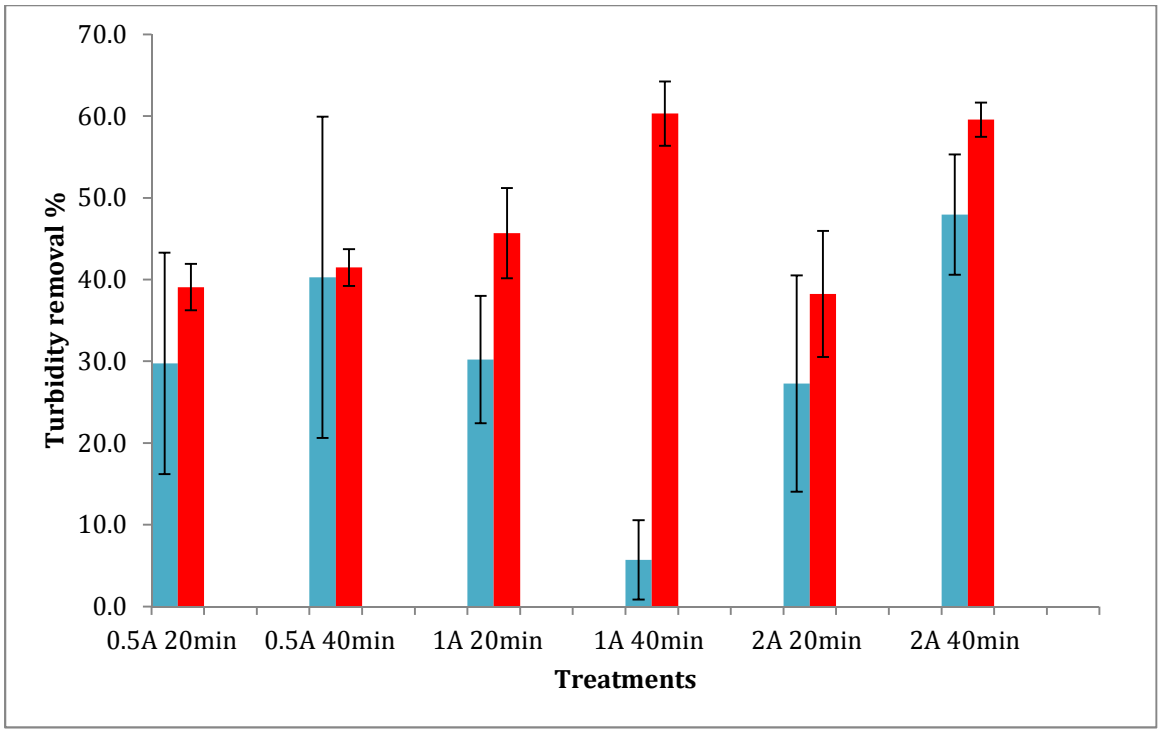


(a)

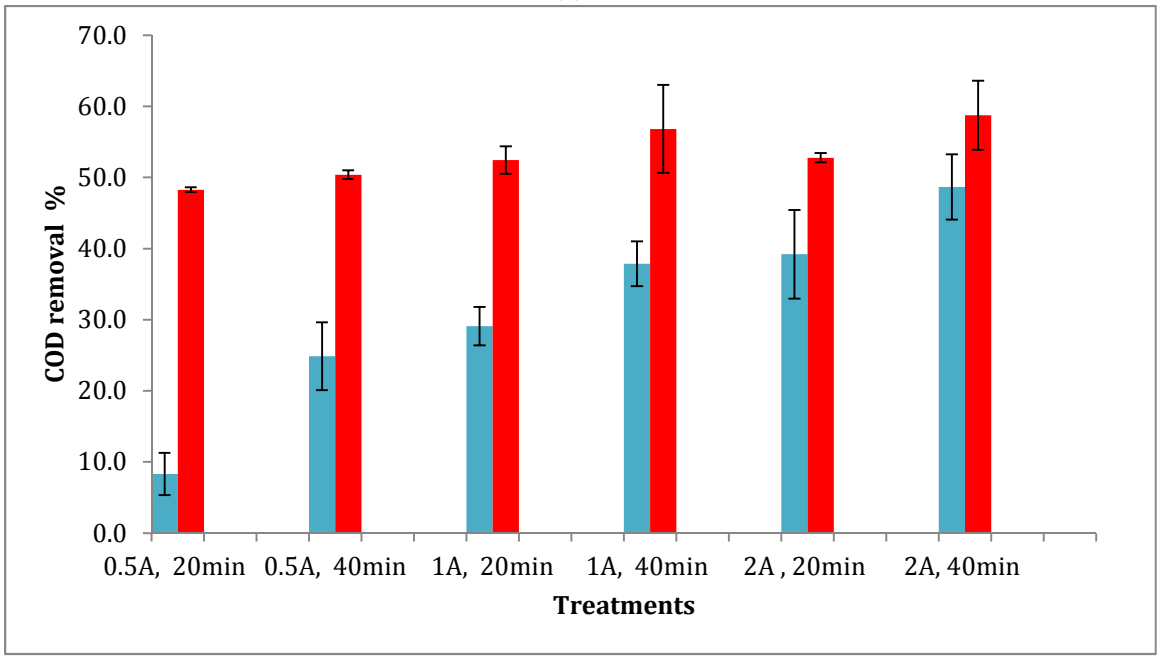


(b)

Figure 2.5 Comparison of COD and turbidity removal between no-biogas-pumped (NBP) and biogas pumped (BP) after 2nd EC *

Light blue square (left) stands for NBP, red square (right) stands for BP. (a) Turbidity (b) COD removal. *Data represent the average of three replicates with standard deviation.

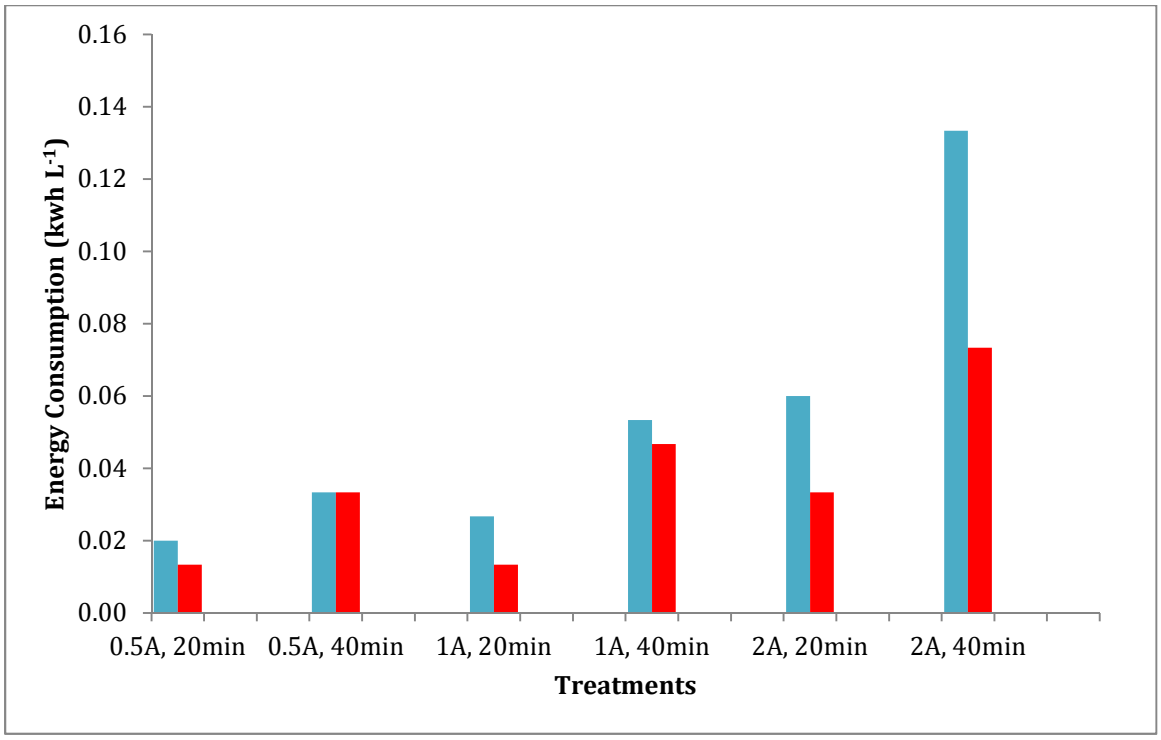


(a)

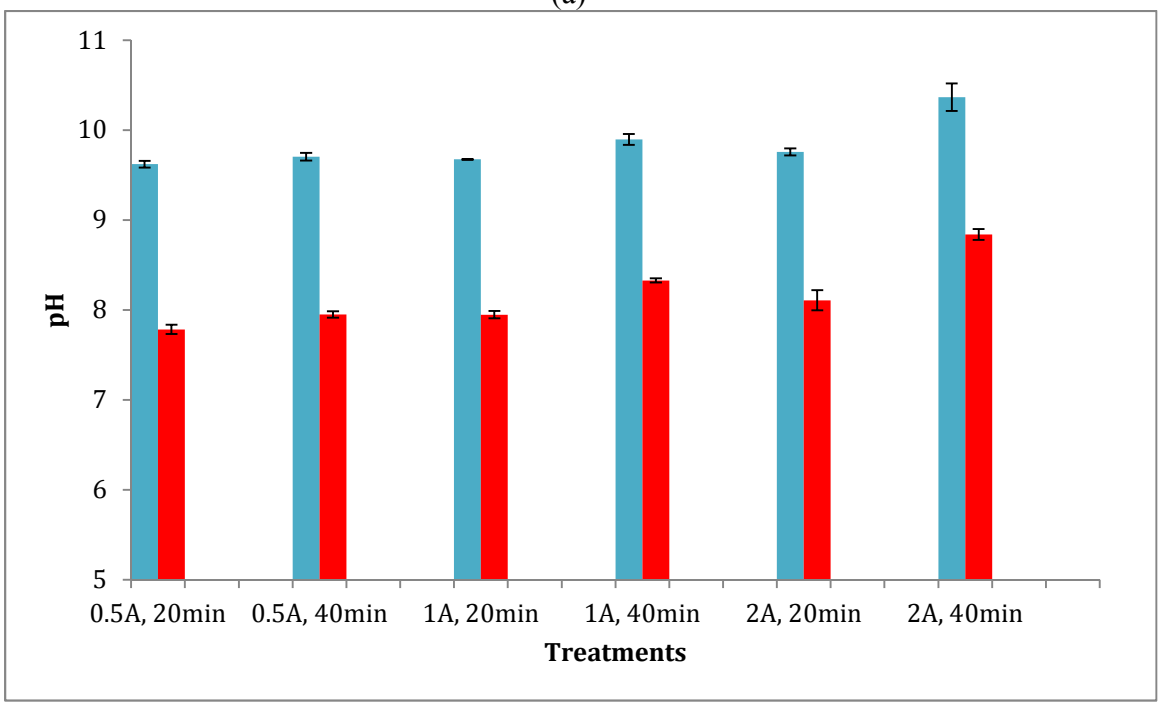


(b)

Figure 2.6 Comparison of power consumption and pH between no-biogas-pumped (NBP) and biogas pumped (BP) after 2nd EC *

Light blue square (left) stands for NBP, red square (right) stands for BP. (a) Power consumption, (b) pH. *Data represent the average of three replicates with standard deviation.

The pair-wise comparison based on both turbidity and COD removal indicated that the preferred EC conditions (I and RT) for BP and NBP effluents were 1A and 40 minutes, and 2A and 40 minutes, respectively. Under the preferred conditions, the 2nd EC had better effects on BP effluent (removed 56% of COD and 60% of turbidity) compared to NBP effluent (49% of COD removal and 48% of turbidity removal) (Fig. 2.5). The solution from the preferred EC with BP had COD, TN and turbidity of 809 mg/L, 655 mg/L, and 114 NTU, respectively, and the solution from the preferred EC with NBP had corresponding numbers of 513 mg/L, 443 mg/L, and 144 NTU (Table 2.3).

| Parameter | Two-stage EC with NBP | Two-stage EC with BP |
|---|---|---|
| TSS (mg $L^{-1}$) | ND | 168 |
| TDS (mg $L^{-1}$) | 2574 | 2106 |
| TOC (mg $L^{-1}$) | 60 | 101 |
| Color absorbance (at 527.5 nm) | 0.085 | 0.082 |
| COD (mg $L^{-1}$) | 513.3±46.0 | 808.7±116.1 |
| TN (mg $L^{-1}$) | 443.3±56.9 | 655.2 ±5.9 [c] |
| Turbidity (NTU) | 144.2±20.4 | 113.6±6.8 |
| Conductivity (µs $cm^{-1}$) | 4778.8 | 3939.9 |

Table 2.3 Characteristics of the treated solutions from two-stage EC with NBP and BP [a, b, c]

a: NBP treatment was carried on at I of 2A and RT of 40 min, and BP treatment was carried on at I of 1A and RT of 40 min.
b: Data represent the average of three replicates with standard deviation.
c: The number was from the run at I of 2A and RT of 40 min.

### 2.4.4 Comparison of two-stage EC processes with NBP and BP

The preferred two-stage EC processes with BP and NBP were compared to evaluate the performance of combined EC and BP approach (Table 2.4). The data presented that there were no significant differences on COD and TP removal between two processes. TN removal of the EC with NBP (65%) is better than the one with BP (47%) due to the effects of high pH on the formation of volatile ammonia nitrogen (released during the EC

treatment). The liquid recovery of the EC with NBP (55%) was also better than that with BP (34%).

| Parameter | Two-stage EC with NBP[c] | Two-stage EC with BP[d] |
|---|---|---|
| COD removal (%)[a] | 94.3±0.5 | 91.0±1.3 |
| TP removal (%)[a] | 100 | 100 |
| TN removal (%)[a] | 64.7±6.3 | 46.9±0.5[c] |
| TSS removal (%)[e] | >99.9 | 95.9 |
| TOC removal (%)[e] | 97.4 | 95.7 |
| Color reduction (%)[e] | 88.2 | 88.6 |
| Liquid recovery (%) [b] | 54.9±1.5 | 34.0±6.5 |
| Overall energy consumption (kwh $L^{-1}$ treated solution) | 0.25 | 0.16 |

Table 2.4 Comparison of the selected multiple-stage EC processes with BP and NBP

a: Removal was calculated based on unit volume of solution. Data represent the average of three replicates with standard deviation.
b: Recovery was calculated based on the volume of the initial solution. Data represent the average of three replicates with standard deviation.
c: This set of data was derived from 2nd EC with I of 2A and RT of 40 min.
d: This set of data was derived from 2nd EC with I of 1A and RT of 40 min.
e: Data represent the average of two replicates.

As shown in Figure 2.7, the turbidity and color of EC solution without BP was gradually improved from 1st EC to 2nd EC. A transparent and light yellow solution was obtained after the 2nd EC (Fig. 2.7(a)). After the biogas pumping, the color of the solution turned into black, and the turbidity was higher than the original AD liquid effluent (Fig. 2.7(b)) that was caused by the generation of ferrous sulfide (FeS) and sulfide (S) from reactions of ferric/ferrous ions and $H_2S$. The dark color and high turbidity of the BP solution had less influence on the transparency of the final treated solution. There was no significant difference on color between NBP and BP treated effluent (Table 2.3). The turbidity of the

BP solution after 2nd EC was lower than the NBP solution (Table 2.3). Furthermore, analyses of TSS and TOC also demonstrated that high removal efficiencies of TSS and TOC were obtained for both NBP and BP treatments (Table 2.4). As for ionic conductivity, the significant reduction during the 1st EC treatment showed a good removal of dissolved solids in the AD effluent (Table 2.2). Biogas pumping greatly increased the ionic conductivity, which indicated that the physiochemical properties of EC solution was changed by biogas pumping, and more conductible ions became available. The fine and relatively coarse particles were observed in the settlement of the EC with BP, which also indicated that $H_2S$ might influence the formation of flocculation and clarity of the treated solution during the 2nd EC as well. An in-depth study is on-going at the authors' research group to understand this change. Moreover, the EC with NBP (0.25 kwh/L) consumed much more energy than the EC with BP (0.16 kwh/L) (Table 2.4, Fig. A4).

(a)

(b)

Figure 2.7 Turbidity and color change of the solution during electrocoagulation processes (a) Left to right: AD effluent, solution after 1st EC, supernatant after 2nd EC. (b) Left to right: AD effluent, solution after 1st EC and biogas pumping, supernatant after 2nd EC

| Mass balance | | | Volume (mL) | TN[a] (mg) | TP[a] (mg) | Fe[b] (mg) | S (mg)[b] |
|---|---|---|---|---|---|---|---|
| 1st EC stage | Input | AD effluent | 500 | 616.7 ± 50.3 | 170 ± 8.7 | 19.4 ± 1.0 | - |
| | | Electrodes loss | - | - | - | 2100 ± 100 | - |
| | Output | 1st EC sludge & other loss | 196.7 ± 5.8 | 344.2 ± 62.4 | 170 ± 8.7 | 2017.8 ± 79.1 | - |
| | | 1st EC solution | 303.3 ± 5.8 | 272.5 ± 48.3 | 0 | 101.6 ± 37.9 | - |
| 2nd EC stage with NBP[c] | Input | 1st EC solution | 500 | 400.5 ± 2.1 | - | 142.8 ± 6.7 | - |
| | | Electrodes loss | - | - | - | 1333.3 ± 57.7 | - |
| | Output | 2nd EC sludge & other loss | 47.8 ± 1.9 | 182.4 ± 14.8 | - | 1473.0 ± 59.1 | - |
| | | 2nd EC solution | 452.2 ± 1.9 | 218.1 ± 48.3 | - | 3.2 ± 0.5 | - |
| 2nd EC stage with BP[c] | Input | 1st EC solution | 500 | 388.5 ± 61.5 | - | 135 ± 11.3 | 3.8 ± 0.1 |
| | | Electrodes loss | - | - | - | 633.3 ± 115.5 | - |
| | Output | 2nd EC sludge & other loss | 68.3 ± 7.1 | 105.7 ± 35.4 | - | 741.6 ± 110.3 | - |
| | | 2nd EC solution | 431.7 ± 7.1 | 282.8 ± 7.1 | - | 26.7 ± 8.1 | 0 |

Table 2.5 Mass balance analysis

a: Data represent the average of three replicates with standard error; TP data are average of two replicates;
b: Data are from EC treatments on a different batch of AD effluent, and represented the average of three replicates with standard error;
c: 2nd EC condition for NBP group was 2A of I and 40 minutes of RT; 2nd EC condition for BP group was 1A of I and 40 minutes of RT.

The mass balance analysis shows that the total iron losses for NBP and BP were 3,433 and 2,733 mg per run, respectively (Table 2.5), and over 95% of the consumed iron precipitated down and mixed into the sludge for EC with either NBP or BP. Nitrogen removal from the AD effluent by EC with NBP and BP were 65% and 54%, respectively (Table 2.5). Evaporated ammonia at high pH during the EC and ammonium/nitrite salts adsorbed by sludge could be the main causes of nitrogen removal during the EC. Since the pH for the 2nd EC after BP was lower than that after NBP, the nitrogen removal of EC with BP was not as efficient as EC with NBP. The sulfur analysis during the EC with BP showed that 1 L of EC solution was capable of adsorbing 7.6 mg sulfur in 60 minutes at a biogas flow rate of 0.5 L/min with a $H_2S$ concentration of 300 ppm, and there were no

sulfide ions detected in the solution after 2nd EC operation. The $H_2S$ absorption data demonstrate that combining EC with BP could have a biogas clean-up capacity of up to 60 L biogas (with a $H_2S$ concentration of 300 ppm) per 1 L EC solution.

**2.5 Conclusions**

This new technology of combining biogas cleanup and AD effluent reclamation not only demonstrates a potential in facilitating EC process by reducing power consumption, but also provides an alternative of $H_2S$ removal for biogas purification. Under the preferred conditions, 90% of COD and 100% TP in AD effluent were removed. Implementation of the biogas pumping operation reduced about 36% of overall power consumption compared with that without biogas pumping. This integration provides a new approach to simultaneously reclaim AD effluent and remove $H_2S$ from biogas, which well addresses the downstream challenges of anaerobic digestion and further advances the adoption of AD technology on waste management.

# CHAPTER 3 SYNERGISTIC INTEGRATION OF ELECTROCOAGULATION AND ALGAL CULTIVATION TO TREAT LIQUID ANAEROBIC DIGESTION EFFLUENT AND ACCUMULATE ALGAL BIOMASS

## 3.1 Abstract

An integrated system of electrocoagulation and algal cultivation was developed to treat a high strength wastewater – anaerobic digestion liquid effluent for reclaimed water and value-added algal biomass production. The integrated system synergistically takes advantages of both electrocoagulation and algal cultivation to enhance the efficiencies of wastewater treatment. The electrocoagulation treated wastewater had low turbidity with better light penetration (108 NTU) to enable algal growth. The algal cultivation had high-efficiency removal of phosphorus (99.4%) and nitrogen (88.2%). The dissolved iron in the electrocoagulation treated wastewater enhanced lipid accumulation of the algae. The results present that total phosphorus and nitrogen in the reclaimed water were 0.78 g $L^{-1}$ and 35.5 mg $L^{-1}$ respectively, and the harvested algal biomass had 35% of lipid, 53% of protein, and 6.4 % of carbohydrate. This study concluded a new route for agricultural wastewater treatment that turns wastewater from an environmental liability into a valuable asset.

**Key words**: Anaerobic digestion liquid effluent, electrocoagulation, *Chlorella vulgaris*, algal biomass, nitrogen, and phosphorus.

## 3.2 Introduction

It has been reported that 335 million dry tons of farm organic wastes and 60 million tons of food wastes are generated annually in the U.S. [103]. Proper handling of these wastes is critical to alleviate their environment impacts such as: greenhouse gas emission,

surface/ground water contamination, and odor problem. Anaerobic digestion (AD) as a natural biological process has been widely used in organic waste management practices, which simultaneously confines the wastes and produces methane for energy generation[4]. However, the main drawback of AD technologies is that they do not possess adequate efficiency to remove nutrients (phosphorus and nitrogen) in the wastes. Therefore, the liquid effluent from anaerobic digestion (liquid digestate) needs to be further treated before discharging.

Various approaches have been developed to treat liquid digestate, such as active carbon adsorption [9], coagulation [10] and ozone treatment [14]. These approaches have demonstrated efficient nutrient removal from the liquid digestate, however, chemical supplement, secondary contamination and low solid content requirement are the main barriers that limit their applications to treating liquid digestate [15]. Electrocoagulation (EC) as an electron driven coagulation method overcomes the disadvantages of the aforementioned chemical and physical approaches. Since it simultaneously coagulates and floats solids in the solution, EC is very good at handling relatively high-strength wastewater, and represents a superior method to treat liquid digestate [16]. As a matter of fact, EC has been widely adopted in industries such as paper and pulp [18], mining and metal [19]. Our previous study has demonstrated that EC has an outstanding performance on removing chemical oxygen demand (COD), phosphorus, and turbidity from liquid digestate [104]. However, the study also shows that EC has limited capability to remove nitrogen. It is mainly due to high solubility of ammonium/ammonia ($NH_4^+/NH_3$) in the liquid digestate (>80% of total nitrogen). Neither electrocoagulation nor electroflotation

(two main processes in EC approach) is able to efficiently remove high soluble substances in the effluent.

Meanwhile, algal culture has been reported as a biological process that is able to efficiently remove nitrogen in a variety of wastewater. *Chlamydomonas reinhardtii* is able to remove 55% of nitrogen from municipal wastewater [105]. *Chlorella vulgaris* efficiently uptakes 88% of nitrogen from the ammonia rich wastewater [106]. Other algal species such as *Scenedesmus obliquus* [107], *Scenedesmus dimorphus* [108], and *Nannochloris sp.* [109] also demonstrate good nitrogen removal capability from wastewater. In addition, algal biomass also serves a biorefining feedstock for biofuel and chemical production. However, directly culturing algae on liquid digestate is impracticable due to the high turbidity and solid content of liquid digestate. A pretreatment step to remove solids and turbidity is necessary to enable algal growth on liquid digestate.

Therefore, in order to effectively treat liquid digestate and utilize nutrients for valuable chemical production, integration of EC and algal cultivation was investigated in this study. EC treatment was first applied to remove turbidity of the liquid digestate, increase light transmission and decrease possible inhibitors for algal growth. Algal cultivation was then used to further remove nutrients, accumulate algal biomass, and reclaim water.

## 3.3 Material and Methods

### 3.3.1 Liquid digestate

The liquid digestate was collected from a 2,500 $m^3$ anaerobic digester in the Anaerobic Digestion Research and Education Center (ADREC) in Michigan State University. The feed of the anaerobic digester was a mixture of 60% of dairy manure and 40% of food

wastes. The dairy manure was from the MSU dairy teaching and research farm. The animal feeds of the dairy farm were alfalfa and corn silage blended based on the Natural Research Council (NRC)'s standard Total Mixed Rations (TMRs) for dairy cattle. [110] The food wastes were from MSU cafeterias. The digester is a completely stirred tank reactor (CSTR) operated at temperature of 35°C and retention time of 25 days. A screw press separator with 2 mm screen was used to separate liquid and solid fractions of the digestate. The liquid fraction was diluted 10 times and then used as the liquid digestate for this study. The liquid digestate had 0.5 (w/w) of total solids, 300 mg $L^{-1}$ of total nitrogen, 140 mg $L^{-1}$ of total phosphorus, and 2,100 mg $L^{-1}$ of COD. The pH of the liquid digestate is 8.0.

### 3.3.2 EC treatment

A 3 L column EC reactor was constructed with anode surface area/volume ratio (S/V) as 0.124 $cm^{-1}$, which was reported as the most effective S/V ratio from a previous study [104]. A steel rod was fixed in the center of column reactor as anode, and a surrounding steel pipe was placed against the inner wall of reactor as cathode. The sketch of the reactor is demonstrated in Figure 3.1. A DC power supply (XPOWER™ 30V 5A) was used to power the EC reactor. The current was maintained at 5 A. The retention time of the EC treatment was determined by nutrients and turbidity that satisfy the requirements of algae cultivation. The EC effluent was centrifuged at 460 g for 10 min, and the supernatant (EC water) was collected for algal cultivation.

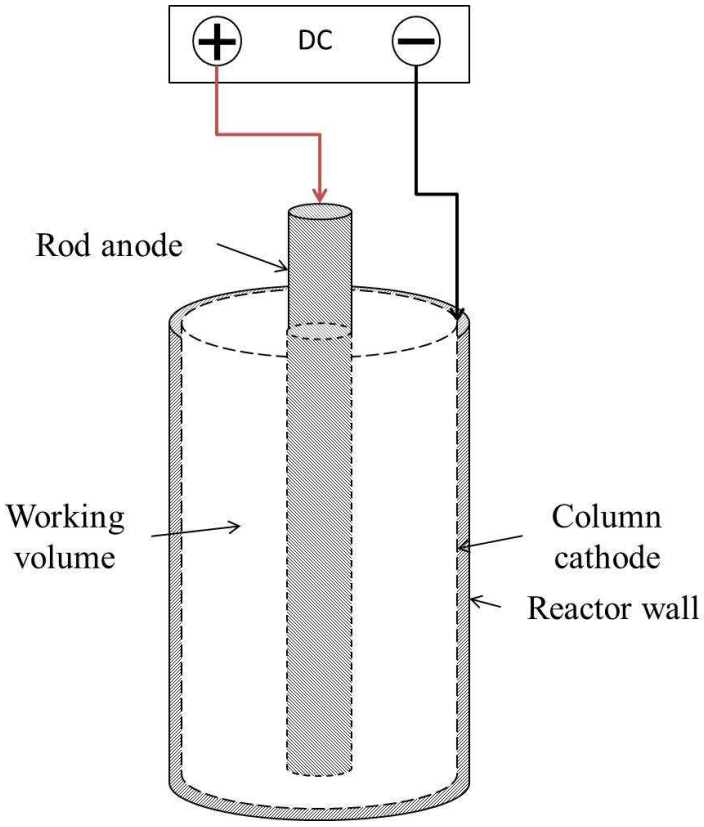


Figure 3.1 Sketch of column EC reactor

### 3.3.3 Selection of algal strain

Three algae strains of *Chlamydomonas reinhardtii 18798*, *Scenedesmus dimorphus 1237* and *Chlorella vulgaris 395* (purchased from UTEX Culture Collection of Algae at the University of Texas at Austin) were selected and cultured on the EC water to evaluate and compare their capacity of nutrient uptake. Tris-Acetate-Phosphate (TAP) medium was prepared for activation of algae strains [111]. 50 ml of sterilized TAP medium was used to culture the seed of each strain in 250 ml flask, and the flask was shaken on a shaker at 180 rpm under continuous light intensity (10 klux) and room temperature. 20 ml of the seed were then inoculated into 300 ml EC water in 500 ml glass bottles for cultivation. The initial dry algal biomass was 0.06 g $L^{-1}$. The EC water was supplemented

by Hutner's trace elements [112]. The pH was maintained approximately 6-7. Samples were taken periodically to monitor cell growth, nutrients utilization and other parameters.

### 3.3.4 Cultivation of selected algae on the EC water

TAP medium was used again to culture the seed of the selected algal strain. The culture conditions were the same with selection of algal strain, except that $CO_2$ was supplied for cultivation of the selected alga. Different $CO_2$ levels were achieved by pumping filtered air and pure $CO_2$ at different flow rates into the culturing bottles. Samples were taken periodically to monitor cell growth, nutrients utilization and other parameters. Parameters such as biomass concentration (g $L^{-1}$), biomass productivity (g $L^{-1}$ $d^{-1}$) and specific growth rate ($d^{-1}$) [63] were adopted to demonstrate the growth condition of *Chlorella vulgaris.*

### 3.3.5 Analysis methods

Total solid (TS) of AD effluent was gravitationally measured after oven-drying overnight. Total nitrogen (TN), total phosphorus (TP), total iron (Fe) and COD were measured according to HACH™ standard methods [113, 114]. Turbidity was measured using MicroTPW Field Portable Turbidimeter (HF Scientific Inc.). Algal cell number was counted using hemacytometer. Algal biomass was collected by centrifuge at 8000 g for 10 min. Dry matter of algal biomass was gravitationally measured after over-drying. Algal carbohydrate content was analyzed according to NREL standard method [115]. Protein content was then measured by BCA standard method (Bio-Rad Laboratories Inc.) after using sonication (Ultrasonic Liquid Processors, Qsonica, LLC, Newtown, CT) to break down algal cell wall. Algal lipids were extracted and measured according to Bligh and Dyer method [116].

### 3.3.6 Statistical analysis

Student t-tests were conducted on TP and TN removal efficiencies at different $CO_2$ levels and analyzed by StatPlus® coupled with Microsoft Excel®. Unequal variances were assumed to get conservative results, and analysis was made with 5% of Type I error. The statistical analysis summary is provided in supplementary Table A2-A6.

## 3.4 Results and discussion

### 3.4.1 EC treatment of the liquid digestate

It has been reported that current density, S/V ratio, and retention time are the key parameters of EC treatment [16], and configuration of EC reactor greatly influences EC performance [117]. They must be optimized according to characteristics of individual wastewater. The comparison of different type of EC reactors indicates that under the same reaction conditions (current, S/V ratio, and retention time), column reactors were generally more energy efficient than conventional rectangular reactors to treat liquid digestate (data not shown), so that a column reactor was adopted as the EC reactor for AD effluent treatment in this study (Figure 3.1).

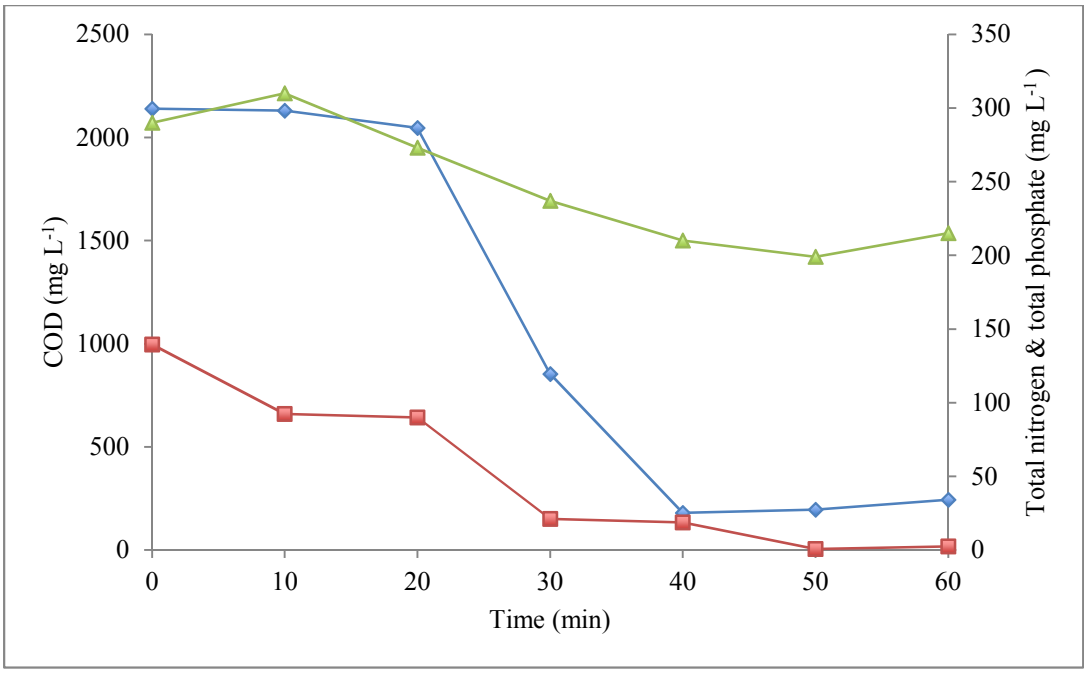


Figure 3.2 Dynamic change of nutrients during EC process in cylindrical reactor

Blue diamond stands for COD, red square stands for total phosphate, and green triangle stands for total nitrogen.
Data are average of two replicates.

The dynamic changes of COD, TN, and TP during the EC treatment are demonstrated in Figure 3.2. COD and TP were significantly removed from the liquid digestate in 40 minutes of the treatment, while TN was only slightly reduced during the entire EC treatment. Removal efficiencies of COD, TP, and TN reached 89%, 98%, and 26% after 60 minutes of the EC treatment. High TP and COD removal are mainly due to that both of them are associated with solids in the liquid digetate. Phosphorus in the liquid digestate is mostly in orthophosphate and attached on the surface of fine particles [16]. COD is mainly from organic matter in the suspended solids. Both of them precipitated along with TS removal during the EC treatment. The results also verified that soluble ammonia/ammonium are difficult to be removed by EC treatment. Therefore, the biological process of algal cultivation was implemented to remove nitrogen and further

reclaim the water. However, due to the nutrients demand of algal growth, certain amount of phosphorus besides nitrogen needs to be provided. The EC treatment has to be adjusted to satisfy both requirements of maximizing COD/TP/TS removal and maintaining the basic nutrient for algal cultivation, so that 40 minutes of the EC treatment was selected to treat the liquid digestate and prepare the EC water for algal cultivation. The TN, TP, Turbidity and COD after 40 minutes of the treatment were 237 mg $L^{-1}$, 18.8 mg $L^{-1}$, 108 NTU and 180 mg $L^{-1}$, respectively.

### 3.4.2 Selection of algae strain

*C. reihardtii, S. dimorphus,* and *C. vulgaris* are widely used to remove nutrients from a variety of wastewater [118, 119]. In order to select the right strain to carry out the nitrogen removal, all three strains were cultured on the EC water. The experimental data show that *C. vulgaris* had much better growth than *C. reihardtii* and *S. dimorphus*. (Fig. 3.3).

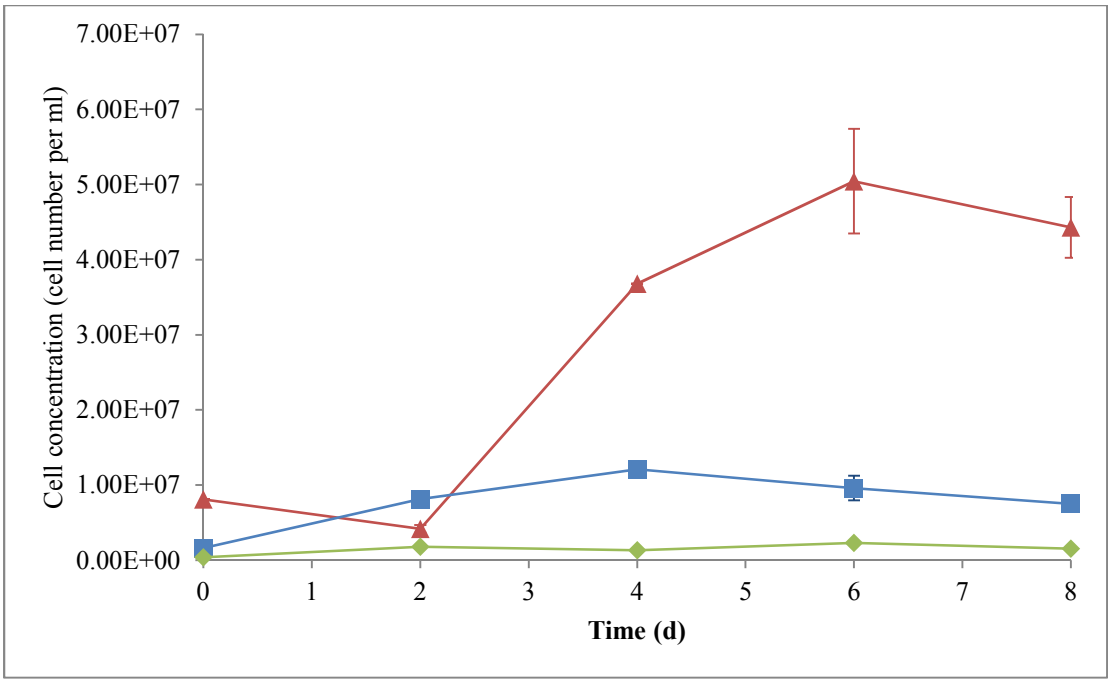


Figure 3.3 Growth of different algae on EC water

Blue square stands for *Scenedesmus dimorphus*, red triangle stands for *Chlorella vulgaris*, green diamond stands for *Chlamydomonas reihardtii*.
Data are average of two replicates.

The cell number of *C. vulgaris* reached 5.1 x $10^7$ $ml^{-1}$ during 6 days cultivation, while *C. reihardtii* and *S. dimorphus* only had 9.6 x $10^6$ $ml^{-1}$ and 2.3 x $10^6$ $ml^{-1}$ respectively. Tan et al. has reported that the ammonia concentrations in the range of 20 – 250 mg $L^{-1}$ have no significant influence on *C. vulgaris* growth [120], which further indicates that *C. vulgaris* was capable of tolerating relatively high nitrogen concentration as such in the EC treated AD wastewater. *C. vulgaris* was thus selected as the algal strain to carry out the treatment of the EC water.

### 3.4.3 Cultivation of *C. vulgaris* on the EC water

#### 3.4.3.1 Effect of carbon dioxide ($CO_2$) level on algal growth and nutrients removal

It has been reported that $CO_2$ level has great impacts on algae, and high $CO_2$ concentration are detrimental to algal growth [121]. Therefore, three $CO_2$ levels (0.04%,

5% and 10%) were adopted by this study to delineate their impacts on both *C. vulgaris* growth and nutrient removal on the EC water.

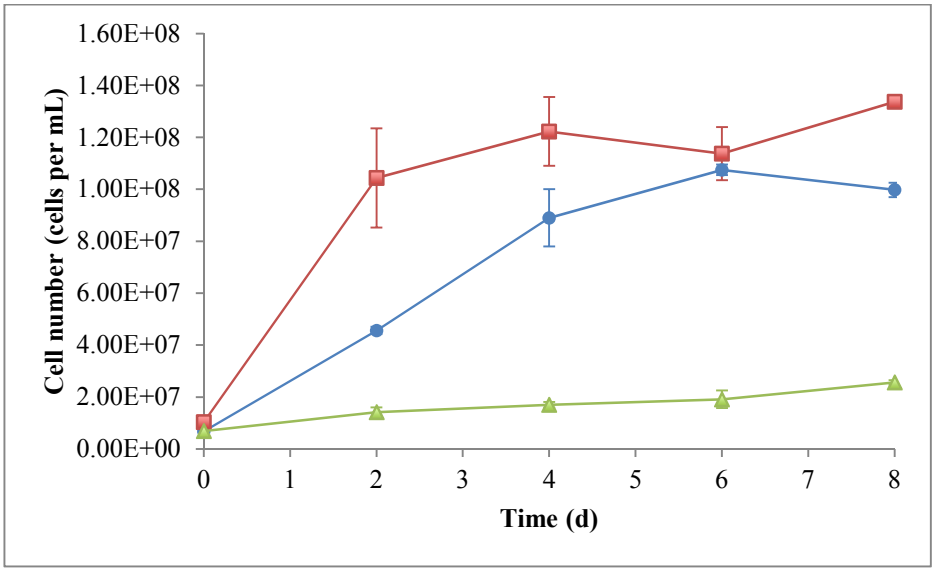


(a)

Figure 3.4 Algal growth with different $CO_2$ feeding levels (a) Cell number (b) Biomass (c) Total nitrogen removal (d) Total phosphorus removal

Red square stands for algal cultivation with 5% $CO_2$, blue diamond stands for algal cultivation with 10% $CO_2$, and green triangle stands for algal cultivation with 0.04% $CO_2$

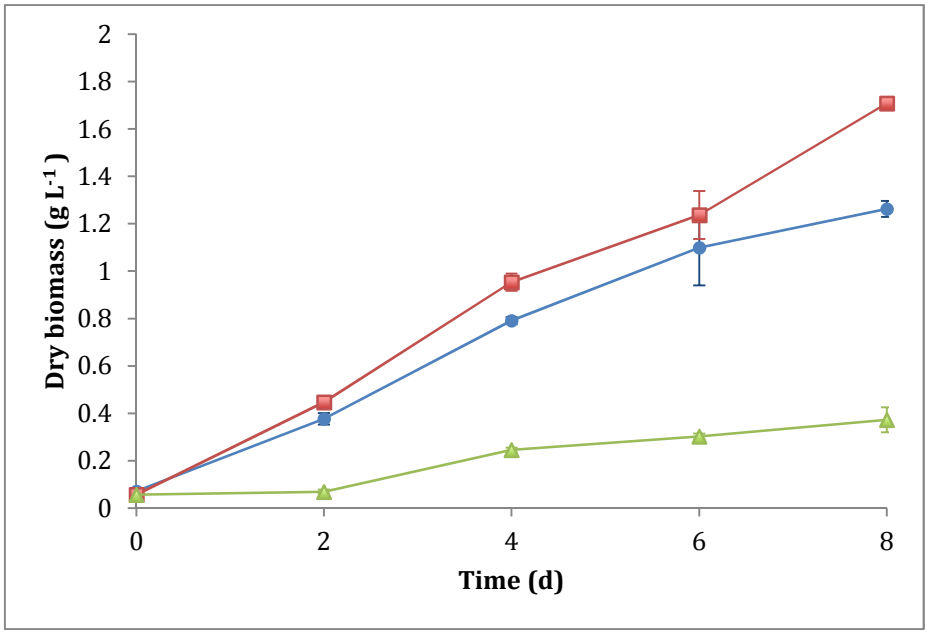


Figure 3.4 (b)

Figure 3.4 (cont'd)

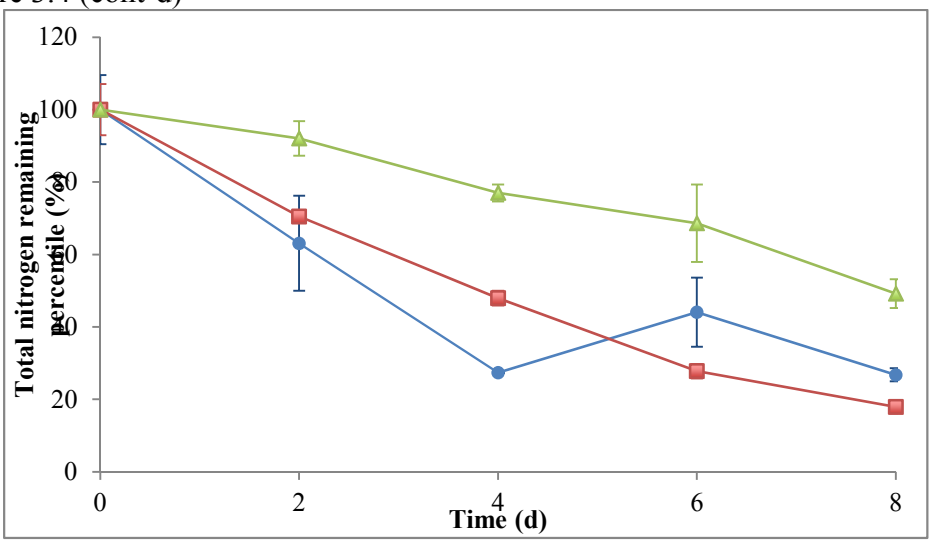


(c)

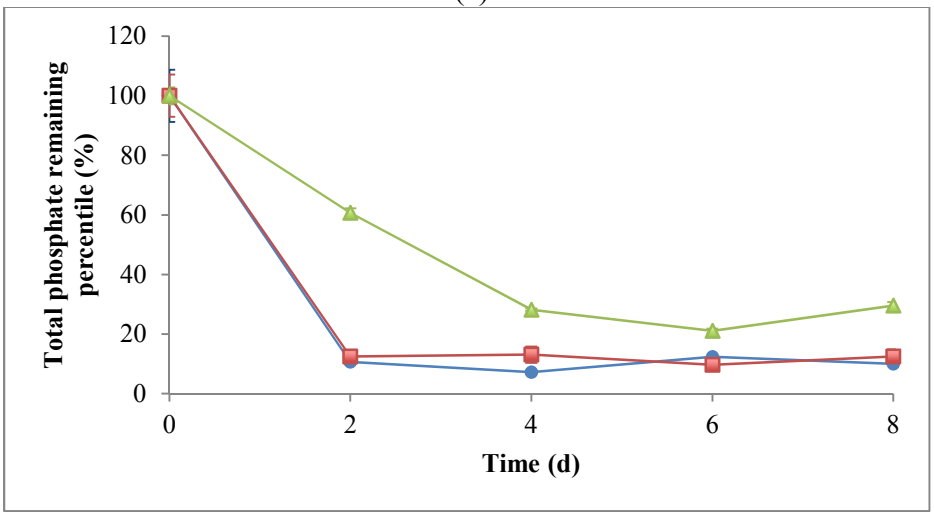


(d)

The experimental data demonstrate that 5% $CO_2$ led to significant better algal growth than 10% and 0.04% $CO_2$ (Fig. 3.4 (b)). The culture at 5% $CO_2$ had the biomass concentration, biomass productivity, and specific growth rate of 1.71 g $L^{-1}$, 0.22 g $L^{-1}$ $d^{-1}$, and 1.03 $d^{-1}$, respectively, which were much higher than them from the corresponding cultures at 0.04% and 10% $CO_2$ (Table 3.1). The results of biomass accumulation were consistent with previous reports [63, 121]. However, changes of cell number and biomass amount during the culture were slightly different (Fig. 3.4(a) & (b)). The algal biomass amount increased consistently throughout cultivation, while the cell number leveled off

after 2-4 days of the cultivation (depending on different $CO_2$ levels). It has been reported that light shading effect plays a key role on this phenomenon [122]. Low light intensity alters cell division and algal cells intend to grow bigger [123], which could be the reason for different patterns between cell number and biomass amount.

| $CO_2$ level (%) | $B_{max}$ | $P_{max}$(g $L^{-1}$ $d^{-1}$) | $\mu_h$ ($d^{-1}$) |
|---|---|---|---|
| 0.04 | 0.37 | 0.05 | 0.36 |
| 5 | 1.71 | 0.22 | 1.03 |
| 10 | 1.26 | 0.18 | 0.83 |

Table 3.1 Maximum biomass concentration ($B_{max}$), maximal biomass productivity ($P_{max}$) and highest specific growth rate ($\mu_h$) of C. vulgaris under different $CO_2$ levels

Data are average of two replicates.

As aforementioned, using algal culture to remove nitrogen was the main purpose of combining EC and algal culture to treat the liquid AD digestate. The experimental results show that algal culture is very efficient to remove the nitrogen and phosphorus in the EC water. TN removal of the cultures at 0.04%, 5%, and 10% $CO_2$ reached 50.8%, 82.1%, and 73.2%, respectively, during 6 days culture (Table 3.2). It is apparent that the culture at 5% $CO_2$ had the TN removal (82.1%) significantly better than other two cultures at 0.04% and 10% $CO_2$. TP removal has similar pattern with nitrogen removal. 70.5%, 87.5% and 90.0% of TP were removed from the EC water at 0.04%, 5% and 10% $CO_2$, respectively. Different from TN removal, at the end of the 6 days culture, there was no significant difference on TP removal between 5% and 10% $CO_2$. For the culture at 5% $CO_2$, the TN and TP contents was reduced to 35.5 and 0.78 mg/L, respectively.

| $CO_2$ level (%) | TN removal % | TP removal % | Final TN (mg $L^{-1}$) | Final TP (mg $L^{-1}$) |
|---|---|---|---|---|
| 0.04 | 50.8 | 70.5 | 62 | 1.67 |
| 5 | 82.1 | 87.5 | 35.5 | 0.78 |
| 10 | 73.2 | 90 | 45 | 0.52 |

Table 3.2 Total nitrogen (TN) and total phosphorous (TP) removal under different $CO_2$ levels

Data are average of two replicates.

The experimental data demonstrate that dynamic changes of TN and TP removal at different $CO_2$ levels were closely related with the algal growth; however, the patterns between TN and TP were slightly different. Algal cell number was quickly increased in the initial stage of the culture with rapid consumption of TP, and then stopped once TP content was leveled off at a relatively low level (Figs. 3.4 (a) & (d)). Meanwhile, algal cell mass kept increasing with continuous consumption of nitrogen (Figs. 3.4 (b) & (c)). Phosphorus limited condition has been reported to play a critical role in plant cell division because phosphorus is an essential component in nucleic acids [124], so that the phosphorus deficiency inhibited cell division [125]. Even though cell division was impeded by low phosphorus, consumption of TN was not interrupted since synthesis of non-phosphorus compounds was not directly linked to phosphorus content, and cell mass was correspondingly increased [125].

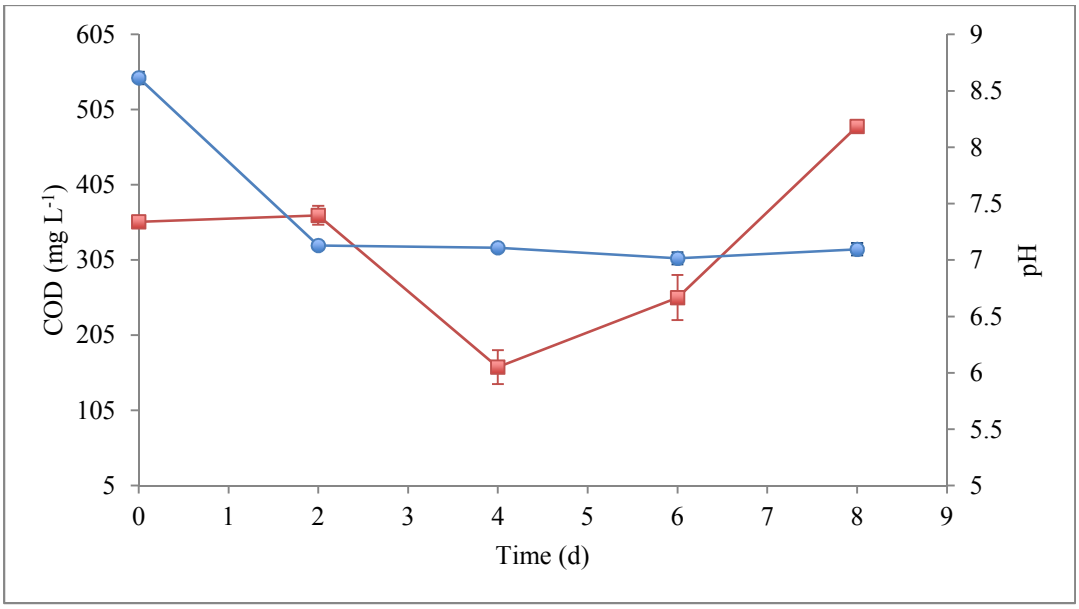


Figure 3.5 Change of pH and COD level during algae cultivation with 5% $CO_2$

Red square stands for COD and blue circle stands for pH.
Data are average of two replicates.

Soluble COD content and pH level during algal cultivation were also monitored as shown in Figure. 3.5. pH level dropped to 7.13 as 5% $CO_2$ was provided and stayed stable throughout cultivation. A rough "V" shaped curve was obtained for COD change, with COD level climbed back up to almost 500 mg $L^{-1}$ after a major decrease at four days. This phenomenon was possibly caused by the secretion of extracellular polymeric substances (EPS) during algal cultivation. Figure. 3.4 (a) shows that stationary phase of algal culture started from four days, and the phosphorus availability also became notably limited. It was reported that environmental changes (nutrients availability, light intensity, etc) play important roles in the secretion of EPS by algae cells [126], which could potentially contribute to the COD level. Wang M, et al. also reported that under nitrogen rich medium, algae cells tend to secret more EPS, such as extracellular proteins and polysaccharides [127], than relative low nitrogen level. Therefore, it is reasonable to assume that the in the exponential growth phase, the living environment for algal cells is not limited and the significant growth of algae results in the decrease of COD. However, as phosphorus kept being utilized to become scarce after four days, algal biomass entered the stationary phase, and nitrogen level was still relative high, living condition for algae was no longer favorable, which triggered a major secretion of EPS to cause the increase of COD level. Further investigations would be implemented to get more information.

#### 3.4.3.2 Algal biomass composition analysis

*C. vulgaris* biomass from the culture at 5% $CO_2$ had 52.9% of protein, 6.4% of carbohydrate and 35% of lipid (Table 3.3). Compared to literature reports [128], the algal biomass obtained from the present study had significantly higher lipid content and lower carbohydrate content, which was not expected considering the facts that EC water has

high nitrogen concentration. A previous study has reported that the algal biomass culturing on nitrogen rich wastewater (AD effluent) had lipid content of approximately 10% dry matter, and protein content of more than 20% dry matter [62]. The lipid content from the current study was 3.5 times higher than the previous report using the similar medium.

| | Content % |
|---|---|
| Protein | 52.9 ± 3.96 |
| Carbohydrate | 6.4 ± 1.50 |
| Lipid | 35.0 ± 2.56 |

Table 3.3 Composition of algal biomass

Data are average of three replicates

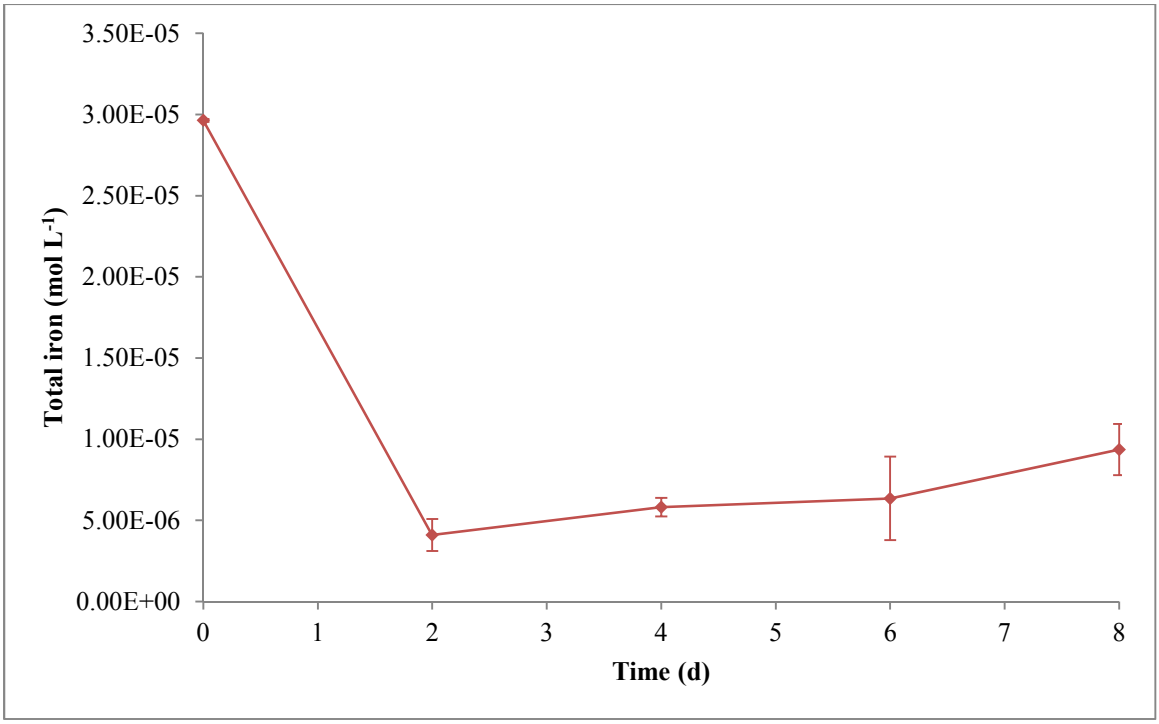


Figure 3.6 Change of dissolved total iron during algae cultivation with 5% $CO_2$

Data are average of two replicates.

It has been reported that $Fe^{3+}$ ion supplement can significantly improve lipid synthesis of *C. vulgaris* [129]. High iron content in EC treated AD liquid effluent may have facilitated the algal lipid accumulation. The change of dissolved iron was thus monitored for 5%

$CO_2$ (Fig. 3.6). The dramatic decrease on the ion centration in the solution indicates the assimilation of dissolved iron by algal biomass, which is consistent with the previous report [129]. Therefore, besides nutrient removal and algal biomass accumulation, combining EC and algal cultivation overcomes the disadvantage of less algal lipid accumulation on the nitrogen rich medium, and improves the quality of algal biomass for lipid-based biofuel and chemical production.

### 3.5 Conclusion

The EC – Algal process joint presented in this study not only generate cleaner water, but also provides an alternative upgrade in agricultural wastewater treatment by accumulating value-added algal biomass. Overall TP, TN and COD removal of 99.4%, 88.2% and 77.4% were achieved respectively, and the algal growth rate reached 1.03 $d^{-1}$ under favorable $CO_2$ condition. 35% of lipid content in algal biomass under nitrogen rich condition was also obtained, benefiting from the dissolved iron in the EC water. This study concluded a new pathway to utilize agricultural wastewater, and serves as a good example of integrating chemical and biological treatments to attain better environmental and economic viability.

# CHAPTER 4 A SUSTAINABLE BIOREFINERY DESIGN TO CONVERT AGRICULTURAL RESIDUES INTO VALUE-ADDED CHEMICALS

## 4.1 Abstract

A sustainable biorefinery concept integrating anaerobic digestion (AD), electrocoagulation (EC) and fungal fermentation was studied to convert an agricultural residue – animal manure into a high-value chemical – chitin. Animal manure was first treated by an AD to produce methane gas for energy generation to power following the biorefinery. The resulting liquid digestate was treated by EC to reclaim water. Enzymatic hydrolysis and fungal fermentation were then applied on the cellulose-rich solid digestate using the EC reclaimed water as the processing water to produce chitin. The studied biorefinery concept converts 1 kg dry animal manure into 17 g fungal biomass containing 12% of chitin (10% of glucosamine), and generate 1.7 MJ renewable energy and 8.5 kg irrigation water. Therefore, an energy positive and fresh-water free value-added chemical production was achieved.

Key words: Anaerobic digestion, Electrocoagulation, AD fiber, biorefinery, chitin, water saving

## 4.2 Introduction

There are 450,000 animal feeding operations (AFOs) in the U.S., which produces approximately 1.3 billion wet tons (335 million dry tons) of animal waste per year [130] [103]. Animal wastes are of particular environmental concern due to greenhouse gases emission, odor problem, and potential surface and ground water contamination. A recent trend in animal manure management is the renewed interest in using anaerobic digester (AD) technology for energy production and carbon sequestration [4, 131]. Even though

AD is an effective method for producing methane for energy production and reducing volatile organics in manure, it is incompetent to sequester all carbons and remove nutrients in animal wastes. Solid digestate still has a high carbon content [34, 132], and liquid digestate contains significant amounts of nitrogen, phosphorus, and total solids [133, 134].

Many studies have been carried out to treat liquid digestate such as active carbon adsorption [8], chemical coagulation and flocculation [10], UV treatment [13] and ozone treatment [14]. Regardless good treatment performance of these methods, high-energy input and additional chemical usage make them less attractive to be implemented in real applications. Meanwhile, electrocoagulation (EC) has recently been studied to treat high-strength wastewater (high solids and chemical oxygen demand). Due to its high removal efficiency and chemical-free nature, EC technology requires shorter retention time and avoids a secondary pollution [15]. Our previous studies have successfully established an EC treatment process that was capable of simultaneously treating AD liquid effluent and cleaning up raw biogas [104], and developed a tandem membrane filtration process to purify the EC treated water [135]. The relatively clean EC treated water can then be used as the processing water for cellulosic biorefinery.

As for solid digestate, treatments such as composting and incineration have been widely applied. Besides these traditional methods, Sun *et al* applied pyrolysis to convert solid digestate into biochars as absorbing materials [32]. Biological conversion processes have also been developed to use solid digestate as a viable cellulosic feedstock for bioethanol production [34, 75, 136]. These studies indicate that solid digestate has much better commercial uses as cellulosic biorefining feedstock rather than soil amendments or

combustion fuels. Compared to bioethanol that is relatively low price, other value-added chemicals should be taken into account to make the solid digestate utilization more economically feasible.

Chitin is a natural amino polysaccharide widely distributed in the animal and plant kingdom. The structure of chitin is a linear polysaccharide made up of unbranched β-(1,4)-2-acetamido-2-deoxy-D-glucopyranosyl residues which is also called N-acetyl- D-glucosamine. The structural characteristics make chitin a very constructive biopolymer that can be used as coagulating agents in wastewater treatments, plant seed coating agents in agricultural industry, and biomaterials (e.g. absorbable sutures) in biomedical industry [137] [138]. Traditionally, chitin and chitosan are extracted from crustacean insects and shellfishes. Compared to the chitin from shellfishes, fungal chitin has advantages of lower level of inorganic materials, no geographic or seasonal limitations [46, 47], better effectiveness in inducing the plant immune response while utilized as a fertilizer [48].

Therefore, in order to convert animal manure into a high-value chemical – chitin, this paper developed a sustainable biorefinery concept integrating AD, EC and fungal fermentation (Fig. 4.1). Animal manure was first treated by an AD to produce methane gas for energy generation to power the entire biorefinery. The resulting liquid digestate was treated by EC to reclaim water. Enzymatic hydrolysis and fungal fermentation were then applied on the cellulose-rich solid digestate using the EC reclaimed water as the processing water to produce chitin. The self-sustaining biorefinery not only converts AD solid residues into high value-added products, but also eliminates fresh water use and external power supply, which represents a promising utilization alternative of agricultural waste management.

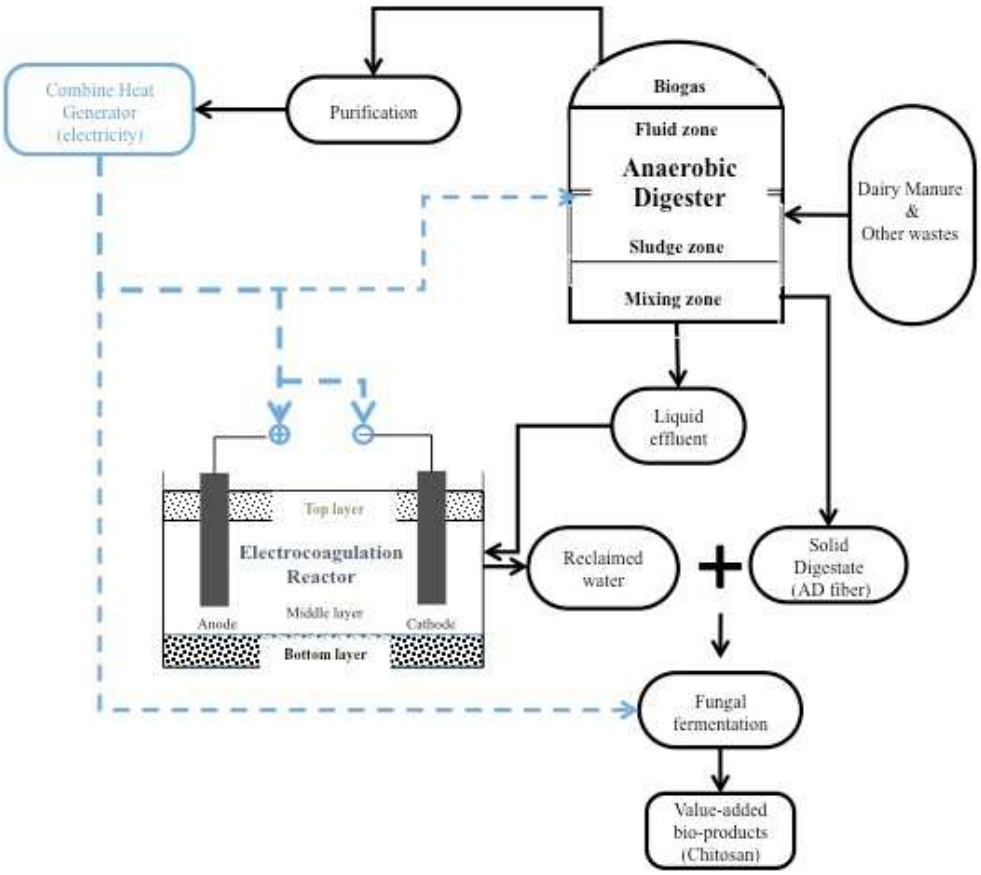


Figure 4.1 Overview of self-sustaining bio-refinery design *

*Black lines are for mass flow; blue lines are for energy flow.

## 4.3 Methods and Material

### 4.3.1 Anaerobic digestion

Anaerobic digestion of animal manure was carried out on a commercial anaerobic digester located at a private dairy farm (3,000 cows) in Michigan (*42N 46′ 29.51″, 85W 19′ 10.14″*). The animal feeds of the dairy farm were alfalfa and corn silage blended based on the Natural Research Council (NRC)'s standard Total Mixed Rations (TMRs) for dairy cattle [139]. The farm uses corn straw as the bedding materials, and adopted scrap system to collect animal feces. The digester is a completely stirred tank reactor (CSTR) operated at temperature of 40ºC and retention time of 22 days. The effective

volume of the digester is 10,000 $m^3$. The biogas is combusted by two 400 kW caterpillar® generators to produce electricity. Two 5.5 kW FAN® screw press separators with 2 mm screen are implemented to separate liquid and solid digestate of AD effluent. The liquid and solid digestates were used to carry out the following EC treatment and fungal fermentation, respectively

### 4.3.2 Electrocoagulation treatment

EC was conducted in a column EC reactor described in previous study [140] with minor modifications. Current level, retention time and working volume were set as 10A, 150 minutes and 3.5 L, respectively. Initial total solid (TS) level of AD effluent was diluted to 2.7% from original effluent. Voltage was monitored during treatment at time interval of 10 minutes. The EC effluent was collected and centrifuged at 230x *g* for 10 minutes to prepare the EC water for following experiments.

### 4.3.3 Fungal fermentation of solid digestate

#### 4.3.3.1 Pretreatment and enzymatic hydrolysis of solid digestate

The EC water was used as the processing water to carry out pretreatment and enzymatic hydrolysis of solid digestate. The pretreatment was carried out under the optimal conditions of 10% of total solid loading, 2% of NaOH, 121°C of reaction temperature, and 2 hours of reaction time (the optimization data not shown). The pH of the treated slurry was adjusted to 5.5 by adding 76% sulfuric acid. C-TEC3 enzyme cocktail with H-TEC (sponsored by Novozyme North America, Franklinton, NC) was then added into the slurry to carry out enzymatic hydrolysis of mono-sugar release for 63 hours under 50°C and a shaking speed of 150 rpm. The enzyme cocktail was prepared as: 9.10 mg cellulose (CTEC3, protein content of 218 mg $ml^{-1}$) and 1.43 mg xylanase (HTEC3, protein content

of 171 mg $ml^{-1}$) per gram of dry matter of the initial solid digestate. The hydrolysate was centrifuged at 7,025x *g* for 10 minutes, and the supernatant was further detoxified by $Ca(OH)_2$ prior to the fermentation. The pH of the supernatant was adjusted to 10 with addition of $Ca(OH)_2$ and the solution was maintained at 50°C for 5 hours with a shaking speed of 150 rpm. The $Ca(OH)_2$ treated supernatant was centrifuged at 7,025x *g* for 10 minutes again. The detoxified supernatant was collected. The pH was adjusted to 6.0 before the supernatant was stocked at -20°C for further uses. All non-specified reagents were purchased from Sigma-Aldrich®.

#### 4.3.3.2 Fungal strain and fermentation process

*Rhizopus oryzae* ATCC 20344 (purchased from ATCC) was the strain used for chitin/chitosan accumulation. Spores of *R. oryzae* ATCC 20344 were collected from the culture on the potato dextrose agar (PDA) medium (Sigma-Aldrich®). The spore concentration of the collected spore solution was approximately $10^7$ spores/ml. 0.5 ml of spore solution were inoculated to 100 ml of sterilized potato dextrose broth (PDB) medium (Sigma-Aldrich®) with 8 g $L^{-1}$ yeast extract (Acumedia®), and cultivated at 30 °C, 180 rpm for 36 hours to prepare the seed. The detoxified solution from section 2.3 was mixed with 3 g $L^{-1}$ of $CaCO_3$ and trace elements reported previously [141], and sterilized under 121 °C for 15 minutes as fermentation medium preparation. 5 ml of the seed was inoculated to 45 ml of the fermentation medium. The fermentation was carried out at 30 °C and 180 rpm with three replicates for 120 hours. Samples were taken during the process to monitor kinetics of substrate consumption, growth, and product production.

### 4.3.4 Analytical methods

Chemical oxygen demand (COD), total phosphate (TP) and total nitrogen (TN) of animal wastes, liquid digestate, and EC treated water was measured using analytical kits purchased from HACH company [104]. Total solid (TS), volatile solid (VS), cellulose, hemicellulose, and lignin of animal wastes and solid digestate were analyzed using the methods developed by National Renewable Energy Laboratory (NREL) [142]. A High-performance Liquid Chromatography (HPLC) equipped with Aminex 87H column, micro de-ashing guard column and a refractive index detector was used to analyze sugars and organic acids. The HPLC method was adopted from a previous study [141]. Cellulose conversion was calculated as reported [34]. Xylan conversion was calculated as ((Volume of enzymatic hydrolysate) (L) * (Xylose concentration) (g $L^{-1}$)) / ((Weight of solid digestate used for pretreatment) (g) * (Total solid content) (% w/w) * (Xylan content) (% w/w) * 1.136) * 100. Chitin/chitosan was extracted from the collected fungal biomass [143, 144], and glucosamine content was also measured [145].

## 4.4 Results and Discussion

### 4.4.1 Anaerobic Digestion

The characteristics of animal wastes (AD feedstock) were analyzed and summarized in Table 4.1. High concentrations of COD, TN and TP in the animal wastes provide good nutritious sources to support growth of anaerobic microbes. 454 metric tons of the wet animal wastes are fed daily into the digester. Under 22 days of hydraulic retention time (HRT) and 40°C of culture temperature, the AD generates 8,495 $m^3$ biogas per day with a methane content of 60% (v/v), and produces 40 metric tons per day of wet solid digestate

and 397 metric tons per day of liquid digestate. The energy demand to maintain the temperature of the AD and power accessory equipment is 5,760 MJ/day.

As aforementioned, AD is a natural and biological process that is good at confining organic wastes and producing renewable energy, though, it has limitations on completely degrading fiber and removing nutrients in agricultural wastes [132, 146]. A large portion of cellulose, hemicellulose and lignin still remained in the solid digestate (Table 4.3), and nutrients (P and N) in inorganic forms exist in both liquid and solid digestate (Table 4.2). In order to improve the efficiency of animal wastes utilization, new approaches to convert these remaining compounds into value-added chemicals needs to be developed. EC and fungal fermentation were adopted by this study to produce chitin/chitosan from the digestate.

| **Characteristics of animal wastes (AD feedstock)** | **Value*** |
|---|---|
| Total solids (%,TS) | 7.97 ± 0.45 |
| Volatile solids (%, VS) | 78.61 ± 1.31 |
| COD (mg $L^{-1}$) | 93,450 ± 2,474 |
| TP (mg $L^{-1}$) | 2,423 ± 49.33 |
| TN (mg $L^{-1}$) | 3,673 ± 110.2 |
| **Digester performance** | **Value** |
| Operating temperature (°C) | 40 |
| HRT (days) | 22 |
| Biogas production ($m^3$ $day^{-1}$) | 8,495 |
| Methane composition (%) | 60 |
| Animal wastes feeding the AD (wet tons $day^{-1}$) | 454 |
| Solid digestate generated (wet tons $day^{-1}$) | 40 |
| Liquid digestate generated (tons $day^{-1}$) | 397 |
| Average energy demand for the AD operation (MJ $day^{-1}$) | 5,760 |

Table 4.1 Characteristics of animal wastes and performance of the commercial CSTR digester

*: Data are average of three replicates with standard deviation.

### 4.4.2 Electrocoagulation of the liquid digestate

It has been tested that the liquid digestate with a high COD concentration is not amendable for fungal fermentation of chitin accumulation (data not shown). The liquid digestate must be treated prior to use as the processing water for the fermentation. EC as a non-membrane technology has advantages of high TS/COD removal efficiency and dual-function of biogas clean-up and water reclamation [104], so that EC was carried out to treat the liquid digestate in this study. Table 4.2 shows the characteristics of liquid digestate and EC water as well as the performance efficiency of the EC treatment. Removal of TS, COD, TP, and TN during the EC were 70.5%, 82%, 92.3% and 33.3%, respectively. Compared to the removal of TS, COD, and TP, EC has lower efficiency on TN removal. It has been reported that EC is highly efficient in removing solid-dependent nutrients - TS, TP and COD [15], while it is incompetent in removing highly soluble compounds from solution such as ammonium ion (the main form of nitrogen in the liquid digestate) [140][104]. Nevertheless, high level of nitrogen is favorable for fungal biomass growth and chitin/chitosan synthesis, while limits production of other metabolites such as lactic acid and fumaric acid [42, 147, 148]. Therefore, using EC water with high nitrogen content could be beneficial for *R.oryzae* culture to limit lactic acid production and accumulate more chitin/chitosan.

Energy consumption is the main concern for the EC process. Electricity use during the EC process was monitored. The voltage was kept stable at 16 ± 4 V in the first 120 minutes, and increased to 30 V in the last 30 minutes of the process when the EC water turned into a relatively clear solution (Fig. A6). According to the principle of electrocoagulation, colloidal condition formed by charged (mostly negatively) particles

has to be primarily broken to trigger massive precipitation [15, 16]. Such solid precipitation leads to increase of electronic resistance, and subsequently results in the rapid climbing of voltage. The total energy consumption of the EC was 446 KJ $L^{-1}$ liquid digestate.

| | Characteristics | Value |
|---|---|---|
| Liquid digestate | Total solids (%, TS) | 2.64 ± 0.03 |
| | COD (mg $L^{-1}$) | 9,490 ± 14.1 |
| | TP (mg $L^{-1}$) | 120 ± 0.0 |
| | TN (mg $L^{-1}$) | 1495 ± 43.84 |
| EC water | Total solids (%, TS) | 0.78 ± 0.11 |
| | COD (mg $L^{-1}$) | 1706.2 ± 19.4 |
| | TP (mg $L^{-1}$) | 9.25 ± 0.35 |
| | TN (mg $L^{-1}$) | 997.5 ± 31.82 |
| Removal Efficiency | TS removal (%) | 70.5 |
| | COD removal (%) | 82.0 |
| | TP removal (%) | 92.3 |
| | TN removal (%) | 33.3 |

Table 4.2 Characteristics of liquid digestate and EC water and performance of EC treatment

### 4.4.3 Fungal conversion of solid digestate into chitin/chitosan using the EC water as the processing water

#### 4.4.3.1 Pretreatment and enzymatic hydrolysis of solid digestate using the EC water as the processing water

The solid digestate has relatively high contents of cellulose (21% TS) and xylan (12% TS), which provides a good carbohydrate source. A three-step process of pretreatment, enzymatic hydrolysis and detoxification was applied on the solid digestate to convert cellulose and hemicellulose into amendable culture solution for *R. oryzae* fermentation. The EC water was used as the processing water. The hydrolysate after the three-step process contains 16 g $L^{-1}$ glucose, 11 g $L^{-1}$ xylose, and 2 g $L^{-1}$ acetate. The cellulose and

xylan conversion of the three-step process were 64% and 78%, respectively, which is well aligned with a previous study [34]. The results also demonstrate that the EC water has no negative impact on pretreatment, enzymatic hydrolysis and detoxification of the solid digestate.

| Characteristics of solid digestate | Value [a] |
|---|---|
| Total solids (%, TS) | 26.27 ± 1.11 |
| Volatile solids (% VS) | 87.70 ± 0.44 |
| Cellulose (% TS) | 20.56 ± 0.21 |
| Xylan (% TS) | 11.77 ± 0.39 |
| Lignin (% TS) | 33.05 ± 0.23 |
| **Sugar and acid concentrations of hydrolysate [b]** | **Value [a]** |
| Glucose (g $L^{-1}$) | 15.78±0.36 |
| Xylose (g $L^{-1}$) | 11.49±0.15 |
| Acetate (g $L^{-1}$) | 2.23±0.10 |
| **Cellulose and xylan conversion** | **Value [a]** |
| Cellulose conversion (%) | 64.34 ± 2.28 |
| Xylan conversion (%) | 78.18 ± 2.77 |

Table 4.3 Characteristics of solid digestate and hydrolysate as well as cellulose and xylan conversion during the pretreatment and enzymatic hydrolysis

a. Data are average of three replicates with standard deviation.
b. The concentrations were for the hydrolysate after pretreatment, enzymatic hydrolysis and detoxification.

#### 4.4.3.2 Fungal fermentation on the hydrolysate to produce chitosan

Fungal fermentation was carried out using the hydrolysate as the medium. The kinetic data demonstrate that *R. oryzae* can utilize glucose and xylose in the hydrolysate to accumulate biomass and produce chitin/chitosan (Fig. 4.2). However, consumption of glucose and xylose was observed in a tandem pattern where xylose utilization was after glucose was mostly consumed. In addition, glucose was consumed much faster than xylose, which indicates that *R. oryzae* prefers glucose to xylose as a carbon source, which is consistent to previous report [149]. Acetate was not significantly consumed during the

fermentation, indicating that acetate is not a carbon source for *R. oryzae*. It is also interesting to observe that there was minimum lactate accumulation during the fermentation on the hydrolysate. It has been reported that lactate metabolism of *R. oryzae* is significantly influenced by nitrogen content in the medium [42]. High level of nitrogen tends to be more favorable for cell growth and chitin synthesis than lactate accumulation. The EC water as the processing water contains 998 mg $L^{-1}$ of total nitrogen, which most likely influenced the fermentation for biomass accumulation and no lactate production. At the end of exponential phase (96 hours), the biomass reached the maximum concentration of 6.17 g $L^{-1}$. The corresponding biomass yield was 33% based on the amount of consumed glucose and xylose. However, even though xylose has been consumed by *R. oryzae*, there was still 5.81 g $L^{-1}$ of xylose left in the broth at the end of the exponential growth stage. The xylose utilization efficiency was only 44%. Improving *R. oryzae* of xylose utilization is currently under investigation.

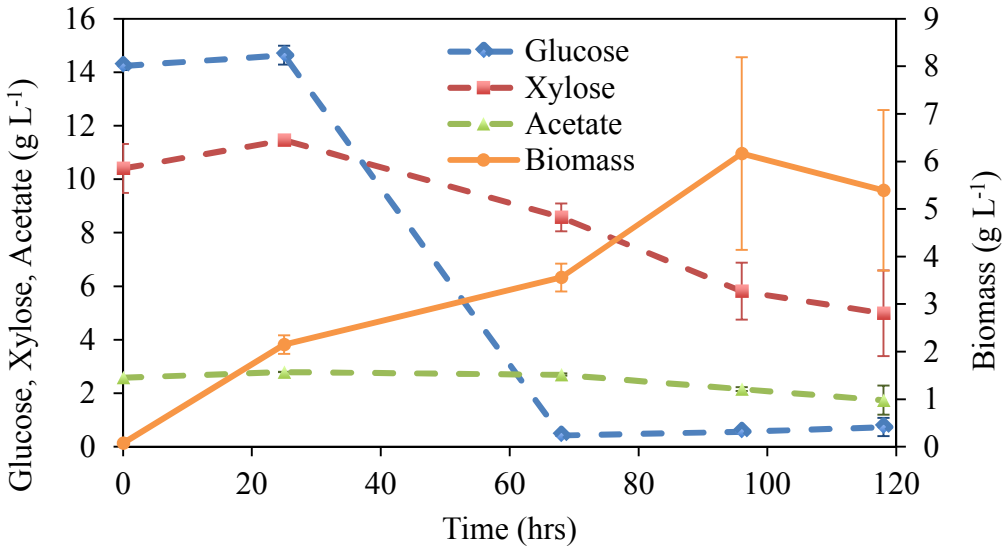


Figure 4.2 Cell growth and sugar utilization kinetic

Correspondingly, relationship between chitin/chitosan, glucosamine and biomass during the fermentation was also delineated (Fig. 4.3). Similar to the growth kinetics, chitin/chitosan and glucosamine all peaked at 96 hours, which is consistent with the reported observation that extractable chitosan content maximized at the end of exponential phase [47]. The maximum concentrations of chitin/chitosan and glucosamine were 0.75, and 0.50 g $L^{-1}$, respectively. The yields of chitin/chitosan and glucosamine were 4.10% and 2.73% based on the amount of consumed glucose and xylose.

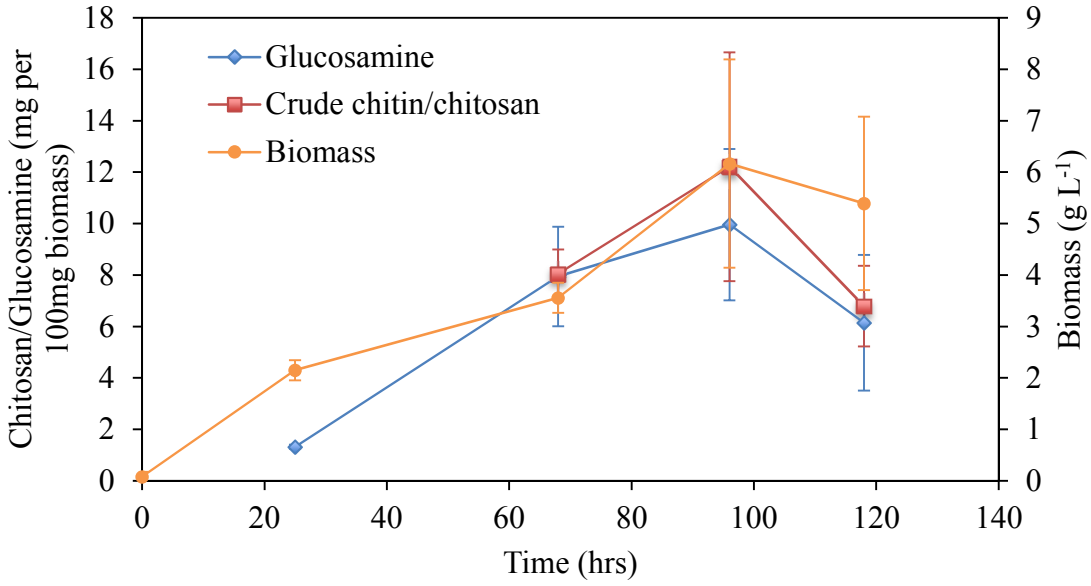


Figure 4.3 Chitosan accumulation kinetic

Several fungal strains such as *Aspergillus niger*, *Mucor rouxii*, and *Candida albicans* have been studied to produce chitin/chitosan on different feedstock (Table 4.4). Among them, *R. oryzae* is the one that demonstrates better performance on chitin/chitosan accumulation. Higher chitin/chitosan contents and yields were observed in previous studies (Table 4.4), however, most of them used pure sugar or starch as the feedstock. There were only a few studies partially using agricultural residues as feedstock for

chitin/chitosan production [42, 147, 150]. This study is the first report that uses animal wastes as the sole carbon source to culture *R. oryzae* and accumulate chitin/chitosan.

| Origin strain | Feedstock | Fermentation time (days) | Chitin/chitosan content | Reference |
|---|---|---|---|---|
| *Rhizopus oryzae ATCC 20344* | 100% AD fiber with treated AD effluent | 3 | 12.2 | This study |
| *Aspergillus niger* | Yeast, peptone and dextrose broth | 15 | 11.1[a] | [47] |
| *Mucor rouxii* | Yeast, peptone and dextrose broth | 21 | 20.13[a] | [47] |
| *Rhizopus oryzae MTCC 262* | Deproteinized whey | 3 | 11.9 | [150] |
| *Rhizopus oryzae NRRL 395* | Steamed rice | 3 | 20[b] | [151] |
| *Rhizopus oryzae 0602* | Glucose, peptone, yeast extract, etc. | 4 | 4.91 | [152] |
| *Rhizopus oryzae 0263* | Glucose, peptone, yeast extract, etc. | 4 | 4.43 | [152] |
| *Cunninghamella echinulata* | Glucose, peptone, yeast extract, etc. | 4 | 7.14 | [152] |
| *Aspergillus niger TISTR3245* | PDB | 16 | 11 | [153] |
| *Rhizopus oryzae TISTR3189* | PDB | 6 | 14 | [153] |
| *Zygosaccharomyces rouxii TISTR5058* | PDB | 2 | 3.6 | [153] |
| *Candida albicans TISTR5239* | PDB | 2 | 4.4 | [153] |
| *Rhizopus oryzae YPF-61A* | Glucose | 6 | 7.5 | [154] |
| *Rhzious oryzae NRRL 395* | 100% potato hydrolysate | 3 | 25 | [42] |
| *Rhizopus oryzae ATCC 20344* | 50% manure liquid with 20g/L glucose | 2 | 21 | [147] |

Table 4.4 Partial fungal chitin/chitosan production summary

[a] Data shown are glucosamine content
[b] Data shown is chitin/chitosan content only in mycellia

### 4.4.4 Mass and energy balance analysis

A mass and energy balance was conducted to evaluate the system performance (Table 4.5). The AD generated 162 g methane per kg dry animal wastes of methane, 290 g per kg dry animal wastes of solid digestate, and 11,234 g per kg dry animal wastes of liquid

digestate. A portion of the liquid digestate (2,063 g per kg dry animal wastes) mixed with 1,323 g per kg dry manure of fermentation effluent was treated by EC to prepare the EC water for fermentation use. The EC sludge (1,573 g per kg dry animal wastes) rich in phosphorus can be used as a fertilizer. The fungal fermentation on the hydrolysate of the solid digestate generated 17 g per kg dry animal wastes of fungal biomass that has 12% of chitin/chitosan and 10% of glucosamine. The water was completely self-sustained, and the fresh water was not needed. In addition, the EC water can completely cover the processing water for the fungal fermentation. A large demand of fresh water is one of the major challenges for fermentation processes of value-added chemical production [155-158]. Applying wastewater as processing water is becoming favorable to make the bioprocesses more sustainable [159, 160]. The results in this study demonstrate that combining AD and EC can generate the processing water to satisfy the demand of the fungal fermentation of value-added chitin/chitosan production. Besides the EC water used as the processing water, there is an extra amount of liquid digestate (9,171 g per kg dry animal wastes) rich in nitrogen and phosphorus, which can be used as liquid fertilizer. Energy balance also demonstrates that integrating AD with EC and fungal fermentation lead to an energy positive biorefining process (Table 4.5). AD as a powerhouse in the system generated 6.95 MJ per kg animal wastes of energy. EC and fungal fermentation (with pretreatment and hydrolysis) consumed 1.47 and 3.63 MJ per kg animal wastes, respectively, to satisfy the demands of water treatment and fermentation process to convert 290 g of solid digestate into 17 g of chitin/chitosan. A positive net energy output of 1.69 MJ per kg animal wastes was achieved by the studied biorefining concept.

| Mass Balance [b] | | AD | EC process [c] | Fungal fermentation |
|---|---|---|---|---|
| Solid | Mass input (g/kg dry feedstock) | -1,000.0 | -89 | -290.0 |
| | Mass input (iron from EC) (g $kg^{-1}$ dry feedstock) | - | -13.5 | - |
| | Mass output (solid in the solid digestate, EC sludge, and fermentation slurry) (g $kg^{-1}$ dry feedstock) | 290.0 | 88.5 | 16.6[d] |
| | Mass output (solid in the liquid digestate and EC water) (g $kg^{-1}$ dry feedstock) | 483.0 | 14.0 | - |
| | Mass output (Methane) (g $kg^{-1}$ dry feedstock) | 162.0 | - | - |
| Water | Water input (g $kg^{-1}$ dry feedstock) | -11,547.0 [e] | -1,974 [f] | -796.0 [g] |
| | Supplemental water input (g $kg^{-1}$ dry feedstock) | - | -1,323 [h] | -1,814.0 [i] |
| | Water output in the solid and sludge (g $kg^{-1}$ dry feedstock) | 796.0 | 1,484.0 | - |
| | Water output in the effluent (g $kg^{-1}$ dry feedstock) | 10,494.0 [j] | 1,814.0 [k] | 2,444 [l] |
| **Energy balance** | | | | |
| Energy input (MJ $kg^{-1}$ dry feedstock) | | -0.16 [m] | -1.47 [n] | -3.63 [o] |
| Energy output (MJ $kg^{-1}$ dry feedstock) | | 6.95 [p] | - | - |
| Net energy (MJ $kg^{-1}$ dry feedstock) | | 6.79 | -1.47 | -3.63 |
| Overall net energy (MJ $kg^{-1}$ dry feedstock) | | | 1.69 | |

Table 4.5 Mass balance analysis for AD-biorefinergy process to produce chitininous fungal biomass [a]

a. All inputs are assigned "-", and all outputs are assigned "+".
b. Data were calculated and adjusted based on 1 kg dry AD feed.
c. Input iron from electrodes during EC was proportionally calculated from [7].
d. Mass balance for fungal fermentation was calculated based on 50 ml flask data.
e. It is the amount of water in the animal wastes.
f. The portion of the liquid digestate was treated by EC to produce the EC water for fungal fermentation.
g. It is the amount of water in the solid digestate.
h. The amount of the fermentation effluent was recycled to dilute the liquid digestate to make the suitable TS for the EC treatment.
i. The amount of EC water was applied for the processing of biorefinery.
j. It is the amount of liquid digestate from the AD.
k. The EC water was split into two portion, one went back to dilute the liquid digestate, the other was used as the water for fungal fermentation.
l. It was the amount of liquid fermentation effluent that could be partially used as the supplement water for EC treatment.
m. The energy input for the AD includes both heat and electricity.
n. The energy input for the EC unit is 446.65 kJ/L liquid digestate.
o. It is the energy input for the fermentation. The energy demand for pretreatment, enzymatic hydrolysis, fungal fermentation and post-processing is 1.25 MJ/L fermentation broth (unpublished data).
p. The energy output of the AD is the methane energy. Low heating value of methane is 50 kJ/g methane.

## 4.5 Conclusion

The biorefinery system can produce 17 g fungal biomass with 12% chitin/chitosan from 1 kg dry animal wastes. The mass and energy balance analysis concludes that the biorefinery is an energy neutral and fresh-water free biorefining system with a net energy and water outputs of 1.69 MJ per kg dry animal wastes and 8.5 kg per kg dry animal wastes, respectively, Correspondingly, the self-sustaining concept that synergistically integrates AD, EC, and fungal fermentation to convert agricultural wastes into value-added product is concluded. The concept provides a win-win solution for agricultural waste management and biorefining of value-added chemical production.

# CHAPTER 5 EXPLORING EUKARYOTE FORMATE UTILIZATION TO IMPROVE ENERGY AND CARBON METABOLISM OF LIPID ACCUMULATION

## 5.1 Abstract

It is well accepted that eukaryotes could utilize formate as an auxiliary energy source to enhance their growth. While its potential role as carbon source in eukaryotes is not well investigated. Our study on an oleaginous fungus, *Umbelopsis isabellina*, elucidates its ability to use formate as both energy and carbon sources to not only support growth but also shift metabolic fluxes to enhance accumulation of target metabolites. In the case of *U. isabellina*, formate supplement significantly enhanced the accumulation of biomass and lipids, and also influenced the profile of fatty acids. With addition of formate, fungal biomass and lipids were increased by 13% and 33%, respectively, and a significant shift in the fatty acids profile from long chain length to short chain length was also observed.

Key words: formate oxidation and assimilation in eukaryotic system, auxiliary energy source, co-consumption of formate and glucose, lipid synthesis

## 5.2 Introduction

Microbial one-carbon (C1) metabolism plays a critical role in global carbon cycles [161]. Due to its solubility and reducing power, formate, a stable intermediate from $CO_2$ reduction [64], has attracted increasing attention to be used as carbon or energy sources to support microbial growth. Microbial formate utilization has been intensively studied in methylotrophs and lithoautotrophs [72, 162, 163] as energy, electron and carbon source. There are two interdependent processes naturally existed to achieve formate metabolism: formate oxidation and formate assimilation [164-166]. The formate oxidation relies on

NAD(P)H-dependent formate dehydrogenase (FDH) that transfers electrons from formate to NAD(P)H, and facilitate ATP synthesis to support cell growth [167-169]. For example, *Ralstonia eutropha* uses the formate oxidation to gain ATP and NAD(P)H, and to support the Calvin Cycle to fix $CO_2$ [161]. In contrast, the formate assimilation directly incorporates formate as carbon source to support cell growth. The serine pathway in some methylotrophs is an example of such a route [161] where formate is assimilated through tetrahydrofolate (THF) fixation to form methylene-THF. $N^5$, $N^{10}$ methylene THF can go through serine pathway through oxidation and or be reduced to $N^5$ methyl-THF and go through vitamin B12 and methionine related one carbon metabolic pathway. [170].

Some eukaryotes, particularly methylotrophic and non-methylotrophic yeasts, possess formate oxidation pathway to use formate as an energy source to support their growth [171-173]. It has also been reported that formate as an auxiliary energy source enhances carbon utilization efficiency of eukaryote fermentation [174]. With addition of formate, Penicillin G production of *Penicillium chrysogenum* fermentation was significantly improved [73], and yeast growth and lipid accumulation were largely increased [175]. However, it has not been reported to date that eukaryotes owns both formate oxidation and assimilation pathways. Our study discovered that an oleaginous fungus, *Umbelopsis isabellina*, is able to use formate as an auxiliary energy and carbon source to enhance fungal growth and lipid accumulation. The objectives of this paper were to: 1) elucidate the formate oxidation and assimilation pathways in U. isabellina, and 2) delineate the effects of formate on fungal growth and fatty acid accumulation.

## 5.3 Methods and Materials

### 5.3.1 Strain and seed culture

*Umbelopsis Isabellina* ATCC 42613 was obtained from the American Type Culture Collection (Manassas, VA). Spores were washed by sterile deionized water and collected after cultivation on potato dextrose agar (PDA) medium (Sigma-Aldrich, St. Louis, MO, US) at 30 °C for two weeks. Seed was cultured in 24 g $L^{-1}$ potato dextrose broth (PDB) medium (Sigma-Aldrich, St. Louis, MO, US) with 8 g $L^{-1}$ yeast extract (Neogen, Lansing, MI, US), at room temperature (~25°C) shaking speed of 180 rpm for 36 hrs. Inoculation size was 5% (v/v) if not specified.

### 5.3.2 Fermentation condition

Submerged batch fermentation was conducted at two scales of shaking flask and fermenter. For the shaking flask culture, 2 L Erlenmeyer flasks were filled with 0.7 L medium, the flasks were placed on a New Brunswick Shaker at 180 rpm and cultured at room temperature. For fermenter culture, 7.5 L fermenters (New Brunswick – Eppendorf, Bioflo 115, Hauppauge, NY, US) were filled with 3 L medium, airflow rate was 1 vvm, and the agitation speed was 200 rpm. The trace element salt solution for the culture was prepared according to the reference [141]. Sodium formate, dextrose (Sigma-Aldrich, St. Louis, MO, US) and yeast extract (Neogen, Lansing, MI, US) were the main carbon, energy and nitrogen sources for the cultures. The flask culture with formate as sole carbon source contained 0.5 g $L^{-1}$ yeast extract (Y.E) and 2 g $L^{-1}$ $^{13}$C-labeled formate. The duration of flask culture was 72 hrs. The flask culture with glucose and formate as carbon source contained 0.5 g $L^{-1}$ yeast extract (Y.E), 2 g $L^{-1}$ $^{13}$C-labeled formate, and 10 g $L^{-1}$ glucose. The medium for the fermenter with formate and as carbon source contained 1 g

$L^{-1}$ yeast extract (Y.E), 4 g $L^{-1}$ $^{13}C$-labeled formate, and 10 g $L^{-1}$ glucose. The medium for the control fermenter just includes 1 g $L^{-1}$ yeast extract (Y.E), and 10 g $L^{-1}$ glucose. The duration of fermenter culture was 48 hrs. The pH of the flask cultivation was maintained at 6.0 by manually adding 1 M sterile sulfuric acid or 1 M sodium hydroxide every 6 hrs in first 12 hrs and every 12 hrs afterwards. The pH of the fermenter cultivation was maintained at 6.0 by automatically pumping in 1 M sterilized sulfuric acid or 1 M sterilized sodium hydroxide at real-time. Samples were taken periodically for biomass and metabolite measurement.

### 5.3.3 Analytical methods

Fungal biomass with the known volume of fermentation broth was collected by vacuum filtration and washed three times by deionized water before dried at 105 °C overnight to measure the total dry mass. Formate, glucose and acetate were monitored by a HPLC method [141]. Lipid extraction of the fungal biomass was conducted using the Bligh and Dyer method [176], and the lipid content was determined gravimetrically. The extracted lipid was then subjected to methanolysis to turn fatty acids in the lipids into methyl esters [177]. The resulting methylated esters were further analyzed by gas chromatographer-mass spectrometry (GC-MS) to obtain the fatty acid profile [141]. F.A.M.E. Mix (C4-C24, Sigma-Aldrich, St. Louis, MO, US) with serial dilutions (100, 50, 25, 12.5, 6.25, 3.125, 1.5625, 0.78125 μg $ml^{-1}$) and chloroform (Sigma-Aldrich, St. Louis, MO, US) was applied as external standard. Samples were diluted ten times prior to analysis to reach reasonable detection levels. All samples, standards and blanks were spiked with 50 μg $ml^{-1}$ methyl nonadecanoate (C19:0) (Sigma-Aldrich, St. Louis, MO, US) as internal standard.

One ml broth was centrifuged at 4000 rpm for 1 min and the precipitated biomass was washed by cold phosphate buffered saline (PBS) before the nicotinamide adenine dinucleotide (NADH) measurement. The NADH was measured by the NAD+/NADH Quantification Colorimetric Kit (BioVision, San Francisco, CA, US). Standard solutions were prepared and measured on daily basis.

### 5.3.4 Carbon Isotopomer Analysis

Dried biomass samples were hydrolyzed with 6N HCl at 100°C overnight. The hydrolysate was derivatized with *N*-*tert*-butyldimethylsilyl-*N*-methyltrifluoroacetamide for gas chromatography-mass spectrometry (GC-MS) analysis [178]. The fragments [M-57] or [M-15] were used to demonstrate the incorporation of the $^{13}$C-labeled substrate – $^{13}$C-formate. These fragments contained the entire carbon backbone of the amino acids. Results are described using the notation of m+*n,* in which n represent the additional mass charge as a result of the $^{13}$C isotope (i.e., m+0 is the fractional distribution of the amino acid with no incorporation of $^{13}$C).

### 5.3.5 Genetic model analysis

The genome-scale yeast model, iMM904 (bigg.ucsd.edu) was used to simulate the metabolism of *U. isabellina* due to great similarity. The experimentally uptake and growth rates were used to provide weak constraints for the model. Glucose uptake rates were varied between 0.1 and 0.9 mmol/gDCW/h and formate uptake rates between 0 and 3 mmol/gDWC/h. The impact of glucose and formate uptake on biomass and lipid production was simulated. The flux of fatty acid and lipid syntheses were delineated. The total flux through certain fatty acid and lipid metabolites as well as energy metabolites

was calculated, and the average flux through phospholipid and glycerolipid biosynthesis pathways were concluded.

## 5.4 Results and Discussion

### 5.4.1 Formate oxidation and assimilation of *U. isabellina*

#### 5.4.1.1 $^{13}C$ -fingerprinting to elucidate fungal formate assimilation pathway

Several organisms have been found to use formate as an additional source of energy to improve overall biomass yields [73, 171, 173] through the formate oxidation pathways that the formate is oxidated into $CO_2$ to release energy for NADH generation [171, 173, 179]. It provides a separate source of NADH independent to the main carbon metabolism, which increases the capability of the strains to produce more NADH-required products. Meanwhile, it has been reported that formate has also been found to be a carbon source in the C1 metabolism in plants and other distinct organisms for the biosynthesis of serine and methionine [180]. To investigate the existance of such formate assimilation pathway in eukaryotes, $^{13}C$ labeled formate was used to unveil formate assimilation pathway(s) for *U. isabellina*.

The 15 total amino acids that can be accessed by the isotopomer analysis [181] provided the labeling information of critical precursor metabolites during formate assimilation such as pyruvate, acetyl-CoA, methylene-THF, formly-THF, glycine, and serine [161]. As shown in Figure 5.1, eight amino acids (alanine, aspartate, glutamate, glycine, leucine, methionine, phenylalanine and serine) were detected with significant labeling extent, which indicates that formate potentially flow into multiple metabolic pathways. Among them, methionine and serine are the two major amino acids with the highest $^{13}C$ labeling level. Similar labeling distributions were observed in both formate-only and

formate+glucose media. The $^{13}$C-fingerprinting measurement provided reliable isotopomer data that formate contributes to biomass accumulation through C1 pathway and anaplerotic pathway, though the amount of biomass from formate is relatively small (Fig. 5.1).

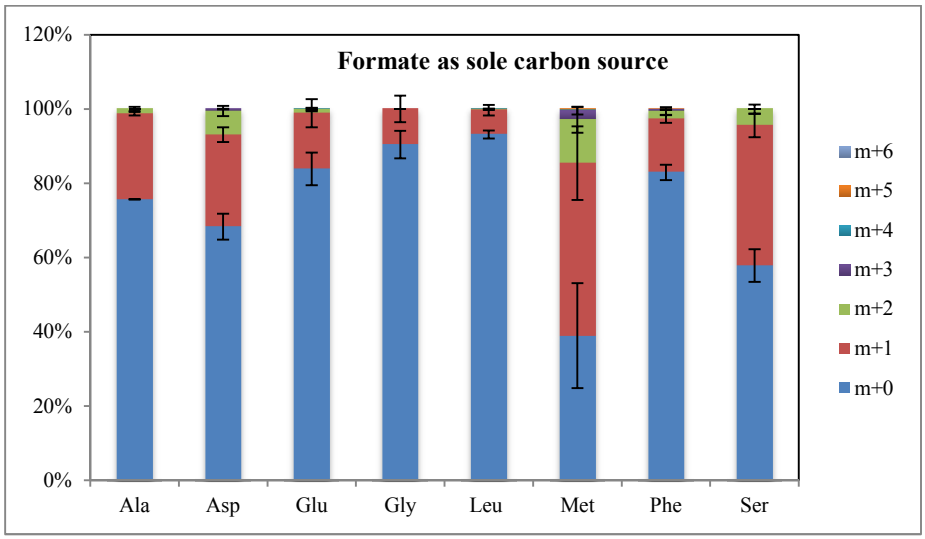


(a)

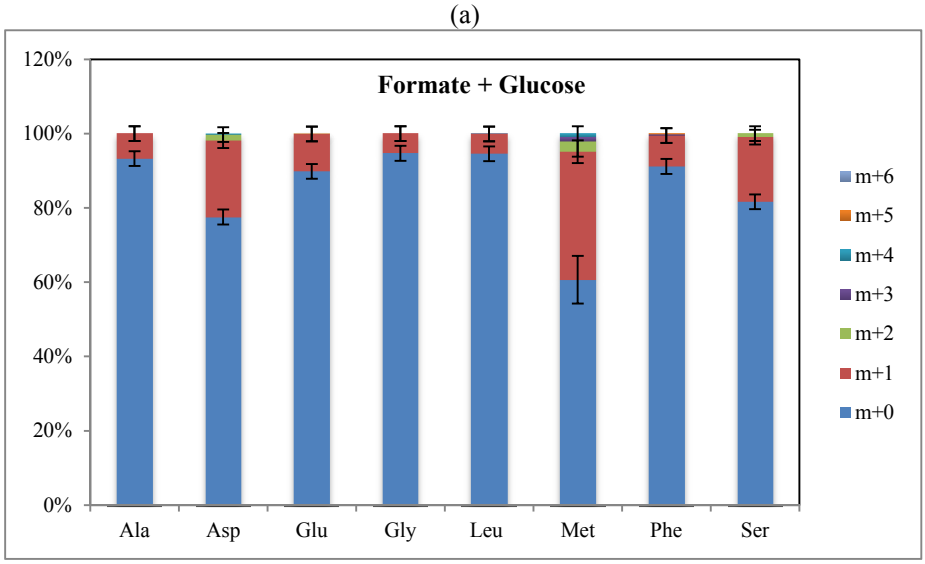


(b)

Figure 5.1 Contribution of formate carbon to amino acids in proteinic biomass of Umbelopsis Isabellina with different carbon sources [i, ii]

(a) Formate as sole carbon source. (b) Formate + Glucose.

i. Only amino acids with significant labeling pattern are displayed. Data are average of two replicates.
ii. 'm+0' means portion of specific amino acid with no carbon detected labeled; 'm+1' means portion of specific amino acid with the first carbon detected labeled; so long so forth.

#### 5.4.1.2 Formate metabolism in *U. isabellina* and its influence on fermentation performance

Fermentation kinetics of *U. isabellina* on glucose media with/without formate was also conducted (Fig. 5.2). Formate significantly improved the microbial growth after 12 hours of the culture (Fig. 5.2(a)). At the end of the culture (48 hrs), the cultivations with and without formate reached 4.3 and 3.8 g/L fungal biomass, respectively. The data also demonstrates that the formate was simultaneously consumed with glucose, which indicates that there is no catabolic repression between these glucose and formate. NADH changes were very different between cultivations with/without formate (Fig. 5.2(b)). NADH in the culture with formate peaked at 352 pmol/mg dry biomass at 24 hours and decreased to 111 pmol/mg dry biomass at the end of the culture, however, the control culture without formate had a much lower peak NADH (218 pmol/mg dry biomass at 12 hours) and approximately maintained at this level till the end of the culture. This phenomenon not only confirms that formate is an auxiliary energy source for micorbes [73, 171, 173], but also specifies that formate promotes energy generation in the initial phase of its consumption. It has been reported that formate oxidation can replace a certain amount of glucose dissimilatory flow [73], which reduces energy burden on glucose and enables metabolic flux of glucose assimilation towards other biosynthetic activities, such as accumulating more biomass. In fact, adding formate to relieve energy burden is becoming a favorable technique in synthetic biology to improve microbial carbon utilization efficiency [182].

As aforementioned, formate is evidently a carbon source for *U. isabellina.* The kinetic analysis of isotope carbon in the fungal proteins demonstrates that isotope carbon in

serine and methionine kept increasing with the increase of culture duration (Fig. 5.3). Fractions of labeled serine and methionine reached to 20% and 30%, respectively, by the end of the culture. This result aligns well with the THF mediated formate assimilation pathway that is closely related with the serine cycle [161] and methionine metabolism. Both of them facilitate the transmethylation reactions [183]. In addition, the experimental data also indicate that relatively high percentages of m+1 were incorporated into aspartate and methionine (oxaloacetate-dreived amino acids) (Fig. 5.4). The result concludes that labeled $CO_2$ was produced from the labeled formate, and then anaplerically entered into the main metabolism.

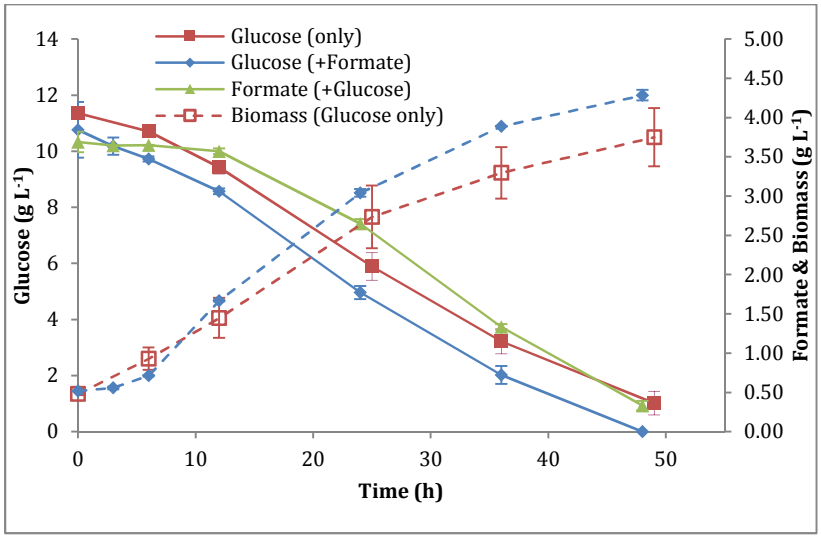


(a)

Figure 5.2 Kinetics using $^{13}$C-formate with glucose at 3 L fermenter

a.. growth and substrate consumption kinetics; b. NADH level kinetics

Figure 5.2 (cont'd)

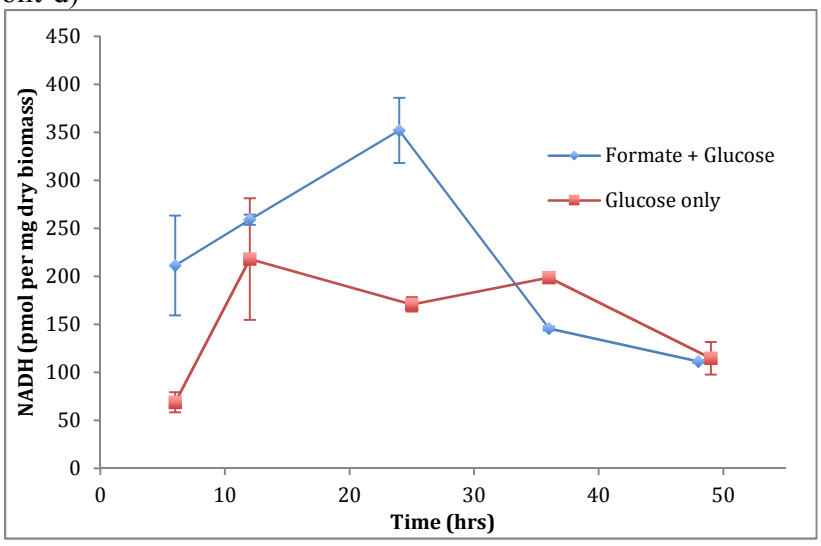


(b)

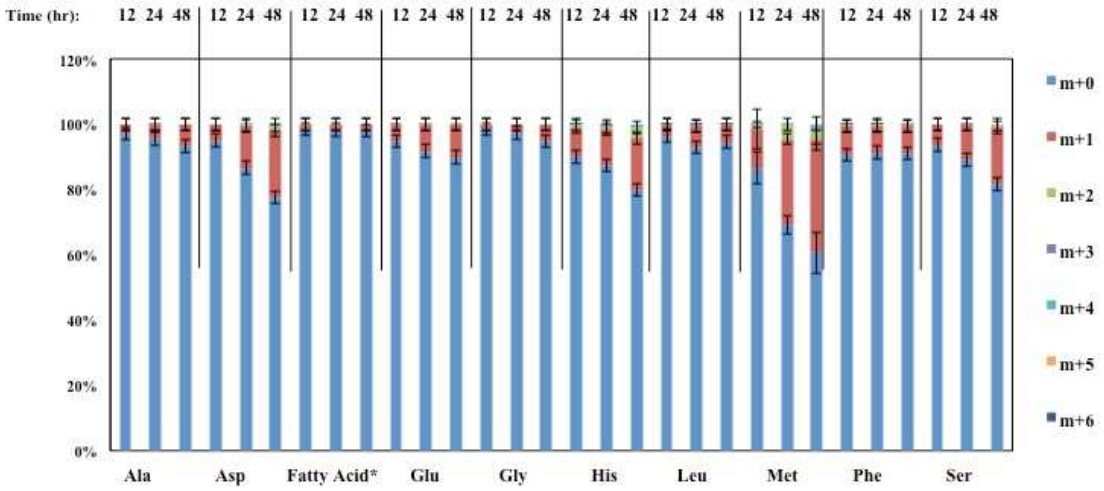


Figure 5.3 Mass isotopomer distribution of proteinogenic amino acids

Ala, Asp, Fatty Acid*, Gly, Glu, Leu, Met, Phe and Ser, for biomass collected at 12, 24, and 48 hours. Other abbreviations used: alanine, Ala; alpha-ketoglutamate, AKG; citrate, CIT; glycine, Gly; histidine, His; phenylalanine, Phe; and succinate, SUC.

*Fatty acid labeling estimated based on labeling of acetyl-CoA, which was determined from the first two carbons of leucine and the last two carbons of alanine.

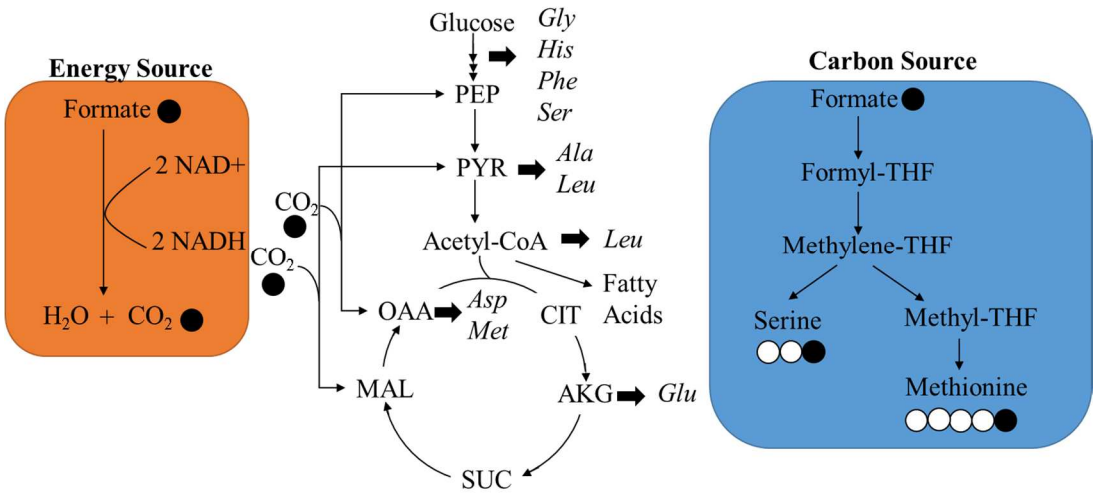


Figure 5.4 Simplified pathway of formate metabolism.

Using $^{13}$C-labeled formate, the incorporation of formate as an energy source and as an carbon source can be easily deciphered through the labeling pattern in subsequent amino acids: Aspartate(Asp), Glutamate(Glu), Leucine(Leu), Methionine (Met) and Serine (Ser). The breakdown of formate through the C1 metabolism results in a labeled carbon present in serine and methionine, while the use of formate as a provider of NADH releases a labeled $^{13}CO_2$, this labeled carbon dioxide can then be incorporated back into biomass via the cataplerotic reactions, which convert phosphoenolpyruvate (PEP) and pyruvate (PYR) into TCA metabolites, oxaloacetate (OAA) and malate (MAL). These reactions require the incorporation of $CO_2$ to convert the three-carbon intermediates into the four carbon intermediates of the TCA cycle.

A BLAST was also conducted to search for the potential key enzymes in formate metabolic pathways of *Umbelopsis isabellina*. Since some annotations are not available, we blasted key enzymes in formate metabolic pathways using a stand-alone BLAST database built from genomic sequence of *U. isabellina* and the tBLASTn search engine. The results present that possibilities of key enzymes involving in formate energy generation and assimilation pathways are very high (all e-values $<10^{-40}$), which indicates that *U. isabellina* is able to utilize formate as both energy and carbon sources for fungal metabolism. The enzymes and their functions are listed in Table 5.

| Name | Reaction |
|---|---|
| NAD-dependent formate dehydrogenase (FDH, EC 1.2.1.1) | Formate + $NAD^+ \leftrightarrow CO_2$ + NADH + $H^+$ |
| Formate tetrahydrofolate ligase (EC6.3.4.3) | ATP + formate + tetrahydrofolate ↔ ADP + phosphate + 10-formyltetrahydrofolate |
| Methenyltetrahydrofolate cyclohydrolase/dehydrogenase (EC3.5.4.9 and 1.5.1.5/15) | 5,10-methenyltetrahydrofolate + $H_2O \leftrightarrow$ 10-formyltetrahydrofolate |
| Glycine dehydrogenase (EC1.4.1.10) | glycine + $H_2O$ + NAD+ ↔ glyoxylate + $NH_3$ + NADH + $H^+$ |
| Aminomethyltransferase (EC2.1.2.10) | glycine + tetrahydrofolate + $NAD^+ \leftrightarrow$ 5,10-methylene-tetrahydrofolate + ammonium + $CO_2$ + NADH |
| Dihydrolipoyl dehydrogenase (EC1.8.1.4) | protein N6-(dihydrolipoyl)lysine + $NAD^+$ ↔ protein N6-(lipoyl)lysine + NADH + $H^+$ |
| Serine hydroxymethyltransferase (EC2.1.2.1) | 5,10-methylenetetrahydrofolate + glycine + $H_2O \leftrightarrow$ tetrahydrofolate + L-serine |
| Serine deaminase (EC4.3.1.17) | L-serine ↔ pyruvate + $NH_3$ |

Table 5.1 Key enzymes in formate metabolic pathways identified by blasting the *U. isabellina* genome

### 5.4.2 Effects of formate on lipid synthesis

#### 5.4.2.1 Lipid synthesis kinetics and fatty acids profile

Kinetics of lipid content in biomass, biomass and lipid yield from glucose ( g biomass/lipid per gram glucose consumed) and productivity (g biomass/lipid per liter per hour) were also monitored (Figs. 5.5-5.7). The lipid contents in the fungal biomass at the end of cultivation reached 43 and 38 g lipid per 100 g dry fungal biomass for the media with and without formate, respectively. Compared to the control culture, the culture on the medium with formate significantly increased biomass yield (up to 13%), biomass productivity (up to 20%), lipid yield (up to 30%), and lipid productivity (up to 70%) (Fig. 5.6). As discussed in section 5.4.1.2, the extra energy contribution from formate oxidation in the early stage of the fermentation alleviates the dissmilation burden on glucose metabolism, and subsequently allows more glucose carbon flow into assimilation pathways, which in turn promotes biomass accumulation and lipid synthesis.

Interestingly, adding formate also changed the fatty acids profile (Fig. 5.7). Short chain fatty acids (C6:0 to C16:0) were all upregulated while most of long chain fatty acids (C17:0 to C22:1) were downregulated with the addition of formate. The fatty acid biosynthesis includes six recuring reactions until the sixteen carbon palmitic acid (C16:0) is produced [184], and requires a large amount of energy to support these reactions. The extra energy from formate oxidation certainly facilitate fatty acid synthesis. Elongation of fatty acids, however, was depressed due to the fact that at the late stage of the fermentation the medium with formate had limited energy (Fig. 5.2 (b)) and less carbon source (Fig. 5.2(a)).

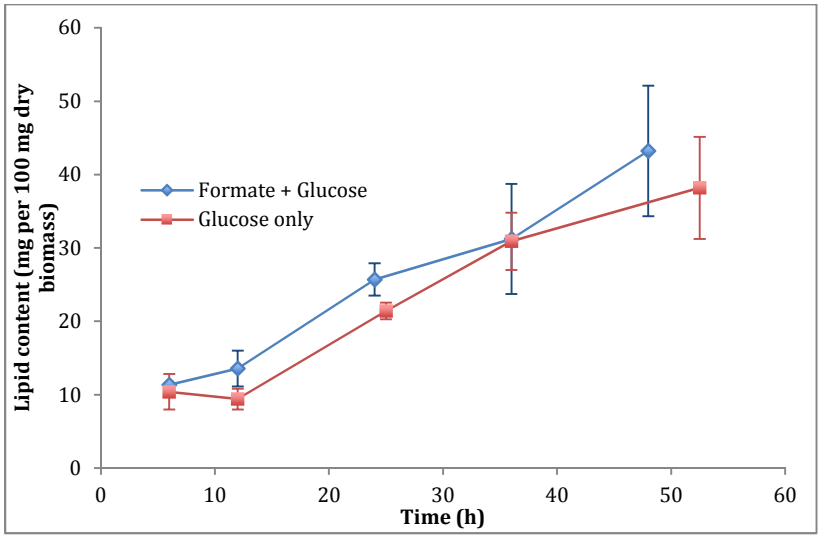


Figure 5.5 Kinetics of lipid content in *U. isabellina* during fermentation with glucose-only and with co-consumption of formate with glucose

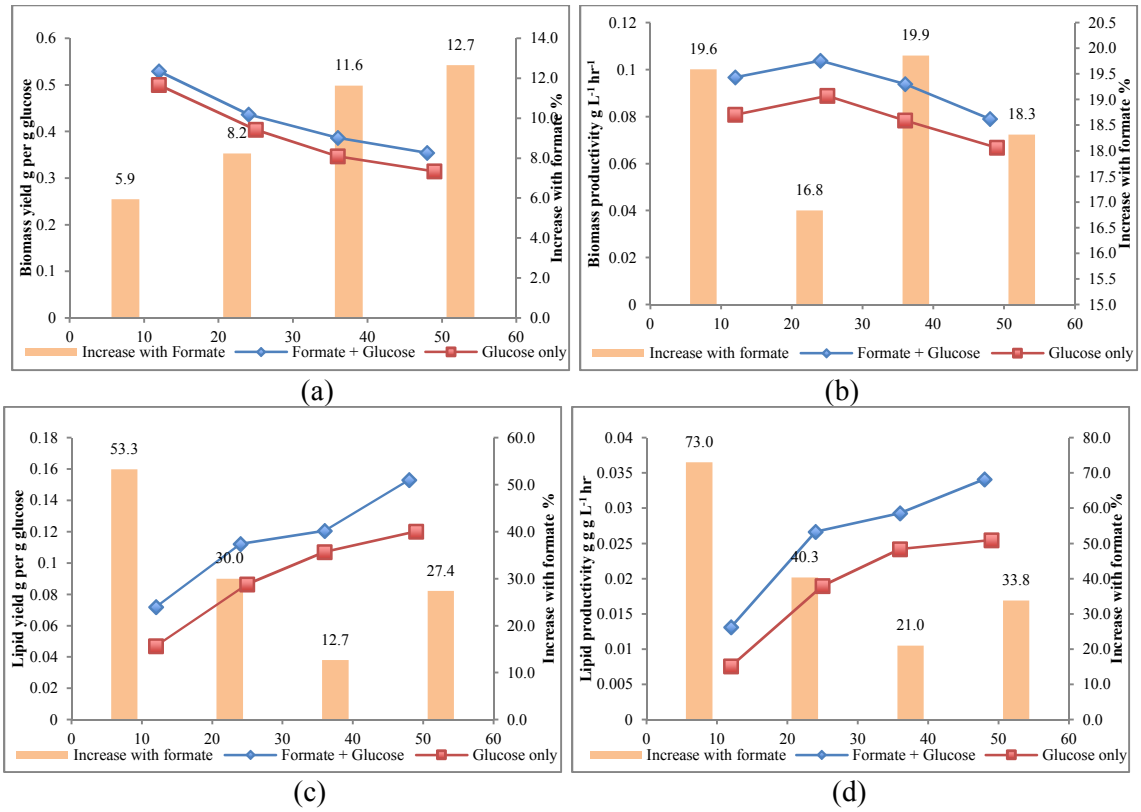


Figure 5.6 Enhancement of biomass and lipid accumulation by co-consumption of formate

(a) Biomass yield kinetics. (b) Biomass productivity kinetics. (c) Lipid yield kinetics. (d) Lipid productivity kinetics.

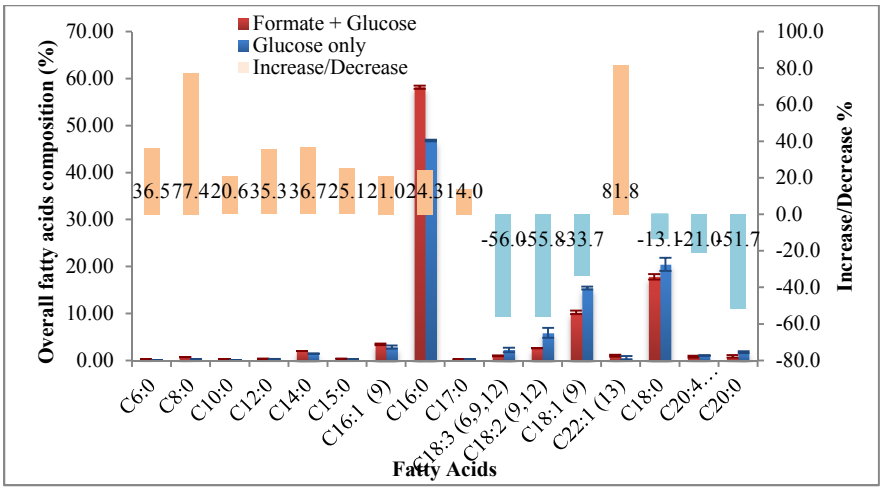


(a)

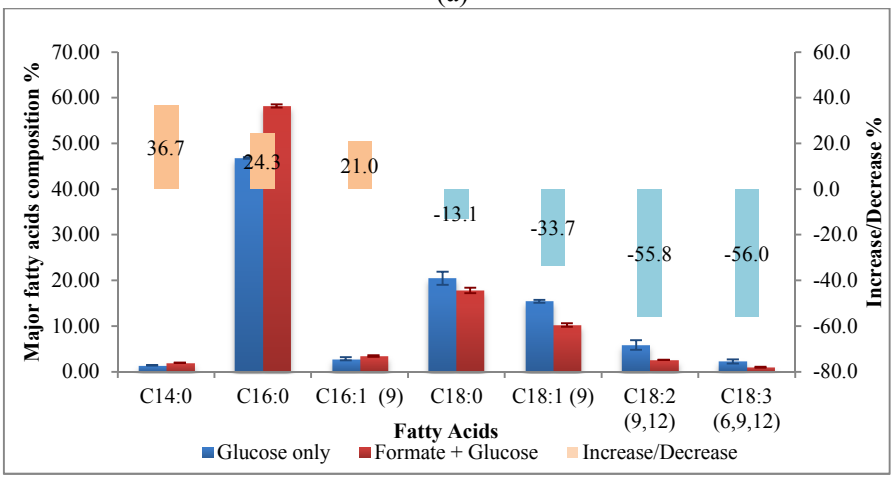


(b)

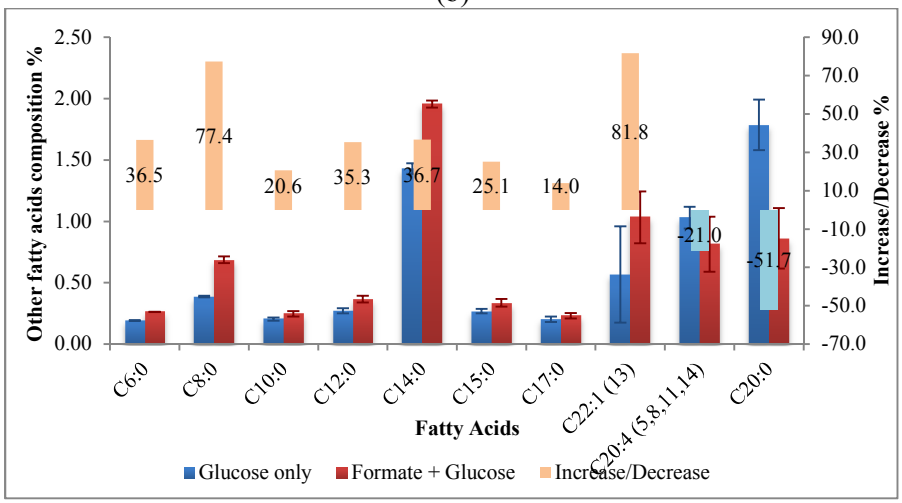


(c)

Figure 5.7 Fatty acid composition profile shift with formate

(a) Overall fatty acids shift in carbon chain length. (b) Major fatty acids shift in carbon chain length (with fatty aicd content > 2%). (c) Minor fatty acids shift in carbon chain length (with fatty aicd content < 2%)

#### 5.4.2.2 Flux balance analysis (FBA) to investigate the effects of formate on lipid synthesis

FBA was developed to understand the genetic and physiological fundamentals of fungal formate metabolism using the genome-scale yeast model, iMM904 (bigg.ucsd.edu) and kinetic data. The experimentally uptake and growth rates were used to provide weak constraints for the model (Table A7). Glucose uptake rates were varied between 0.1 and 0.9 mmol/gDCW/h and formate uptake rates between 0 and 3 mmol/gDWC/h. The impact of glucose and formate uptake on biomass and lipid production was simulated. The flux through about 119 reactions (Table A8) involved in fatty acid and lipid synthesis were noted. The total flux through certain fatty acid and lipid metabolites as well as energy metabolites – atp, nadh, nadph (Table A9) was computed. Moreover, the average flux through phospholipid and glycerolipid biosynthesis pathways were computed.

For glucose consumption rates around 0.5mmol/gDCW/h, uptake of formate increases biomass growth as well as the fluxes in the lipid biosynthesis pathways (Fig. 5.8). Interestingly, this corresponds to the point where total flux of ATP in the mitochondria is between 4.6 to 4.9 mmol/gDCW/h. This appears to be an energy threshold point beyond which no increase in growth rate is observed. At very high glucose consumption rates (around 0.8mmol/gDCW/h), the uptake of formate doesn't improve biomass growth. Moreover, the magnitude of fluxes in lipid biosynthesis pathways are unchanged (figure not shown). At glucose consumption of 0.5mmol/gDCW/h, activity shift in different lipid biosynthesis pathways indicates that different uptake rates may correspond to formation of different kinds of lipids. This shift was not observed at higher glucose uptake rates.

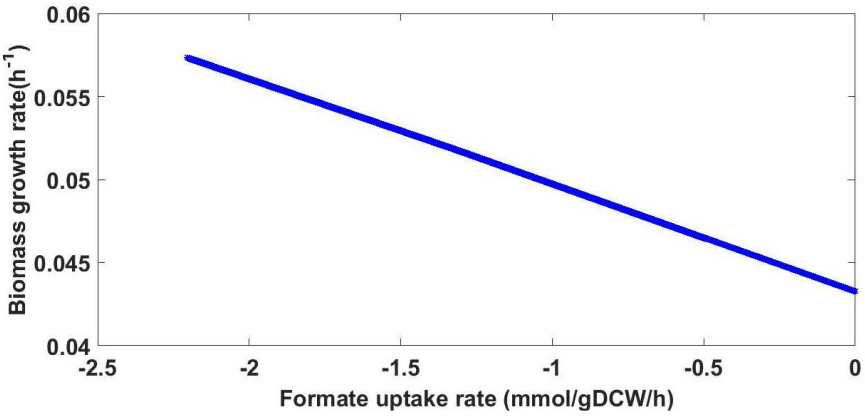


(a)

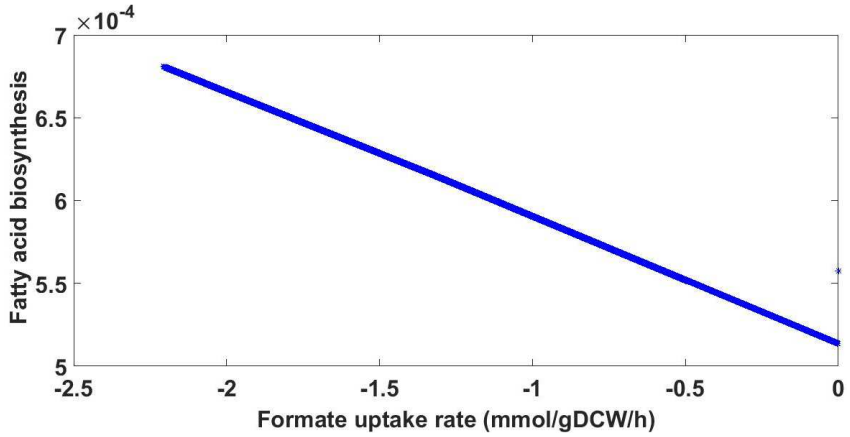


(b)

Figure 5.8 Influence of glucose and formate uptake rates on the biomass growth and different lipid metabolic flux.

(a). Influence of formate uptake rate on biomass growth under 0.5 mmol/gDCW/h of glucose uptake rate

(b). Influence of formate uptake rate on fatty acid pathway flux under 0.5 mmol/gDCW/h of glucose uptake rate

## 5.5 Conclusions

The results concluded that formate and glucose could be utilized simultaneously without catabolic repression. Formate was identified as both carbon and energy sources in the culture of *U. isabellina* based on $^{13}$C-fingerprinting analysis and kinetic study. Both THF based C1 assimilation pathway and anaplerotic pathway were most likely counted for incorporation of formate as a carbon source. Extra NADH-dependent energy generated

from formate oxidation led to enhanced biomass accumulation and elevated fatty acid synthesis as well as a significant shift in carbon chain length of the lipid profile. Future studies should further decipher major pathways for fungal formate assimilation and formate-based lipid synthesis in *U. isabellina* to develop genetic engineering and fermentation strategies to utilize formate, and move these pathways into other microbial platforms for different environmental and energy applications.

# CHAPTER 6 CONCLUSIONS AND FUTURE WORK

## 6.1 Conclusions

This study presents an integrated organic waste utilization concept to address issues that animal waste management practices encounter: odor problem, greenhouse gas emission, and ground/surface water contamination. The integrated concept includes anaerobic digestion, electrocoagulation, algal cultivation, and fungal cultivation of fine chemical production and $CO_2$ utilization. Animal manure was first treated by an anaerobic digester to produce energy from biogas to support other unit operations in the system. Raw biogas, liquid digestate and solid digestate are three outputs from the digestion operation that need further treatments.

Electrocoagulation was adopted to treat the nutrient-rich liquid digestate. 90% and 99% of COD and TP removal from liquid digestate were achieved from an optimized electrocoagulation process. Raw biogas was also pumped through the electrocoagulation treated liquid digestate to further enhance the performance of nutrient removal from liquid digestate and at the same time remove $H_2S$ from raw biogas. High $H_2S$ removal efficiency (>99%) and less energy consumption (36% of energy reduction) were achieved by the biogas-facilitated electrocoagulation. However, electrocoagulation treatment has difficulty in removing the highly soluble ammonia nitrogen. Therefore, algal cultivation was applied to absorb remained total nitrogen (88% removal) and to accumulate an algal biomass rich in lipids (35%) and proteins (53%). It was also discovered that the dissolved $Fe^{3+}$in the electrocoagulation treated water significantly enhanced the algal growth and lipid accumulation. Integration of electrocoagulation with biogas clean-up ($H_2S$ removal)

and algal cultivation provides a multi-functional path of reclaiming the water, purifying biogas and fixing $CO_2$ for value-added algal biomass production.

Solid digestate was investigated as a potential lignocellulosic feedstock to produce chitin/chitosan using a fungal fermentation. Electrocoagulation treated liquid digestate was used as the processing water to maximize sustainability. The fungal fermentation was able to convert 1 kg of dry solid digestate into 17 g of fungal biomass containing 12 % of chitin (10% of glucosamine). In addition, since biogas energy was used to power the process, the solid digestate utilization was self-sustained. The results clearly demonstrate that integration of fungal fermentation of solid digestate with anaerobic digestion and electrocoagulation leads to an energy neutral and fresh-water free biorefinery concept to convert animal wastes into value-added chemicals.

Moreover, the integrated concept also includes a $CO_2$ utilization process to further reduce footprint of animal waste utilization. $CO_2$ in raw biogas can be electrochemically converted to formate. Formate as an organic acid can be utilized by microbes to facilitate fermentation processes. A novel fungal formate utilization concept has been developed by this study. Unlike previous conclusion that formate only contributed to additional energy generation, the studied fungus, *Umbelopsis Isabellina*, demonstrates an unique capability to utilize formate as both energy and carbon sources. $^{13}C$ metabolic tracing and NADH dynamics analyses verified the dual role of formate, which is the first time that such observation has been reported in fungal fermentation. The groundbreaking investigation over the fungal formate utilization could lead to discovery of new pathways for carbon fixation to sequester $CO_2$ from a variety of sources including biogas.

## 6.2 Future work

This study successfully presented an integrated animal waste utilization concept to turn an environmental liability to usable resources. In order to transform the concept into real applications and benefit animal agriculture, the following research topics should be further studied.

1. Optimization and modeling of electrocoagulation on raw liquid digestate,
2. Scale-up of biogas-facilitated electrocoagulation process,
3. Exploration of other value-added chemicals from solid digestate such as unsaturated fatty acids and organic acids (adipic acid and muconic acid),
4. Fermentation strategies and genetic modification to enhance eukaryotic formate utilization, and
5. Techno-economic analysis and life cycle analysis of the integrated animal waste utilization concept.

# APPENDIX

| Gas composition | | At the beginning of biogas pumping | At the end of biogas pumping |
|---|---|---|---|
| CH4 (%, v/v) | Gas-in | 44.45 | 44.45 |
| | Gas-out | 44.16 | 46.35 |
| CO2 (%, v/v) | Gas-in | 45.95 | 45.95 |
| | Gas-out | 29.62 | 47.9 |
| H2S (ppm) | Gas-in | 378.55 | 378.55 |
| | Gas-out | ND ** | 34.95 |
| NH3 (%, v/v) | Gas-in | ND | ND |
| | Gas-out | ND | ND |

Table A.1 Change of biogas composition during the biogas pumping process *

*: Data are the average of two replicates.
**: ND represents not detectable.

| Student t-test (TN removal efficiency) | | | |
|---|---|---|---|
| Comparison | t | one-tail 95% t-critical value | Significant? |
| 5% vs. 0.04% | 6.57064 | 6.31375 | Yes |
| 5% vs. 10% | 9.73057 | 2.91999 | Yes |
| 0.04% vs. 10% | 4.65886 | 6.31375 | No |

Table A.2 Statistical analysis of TN removal efficiency between three $CO_2$ levels

*Data were analyzed with n=2.

| Student t-test (TP removal efficiency) | | | |
|---|---|---|---|
| Comparison | t | one-tail 95% t-critical | Significant? |
| 5% vs. 0.04% | 4.42781 | 2.91999 | Yes |
| 5% vs. 10% | 0.762 | 6.31375 | No |
| 0.04% vs. 10% | 8.42407 | 2.91999 | Yes |

Table A.3 Statistical analysis of TP removal efficiency between three $CO_2$ levels

*Data were analyzed with n=2.

| Student t-test (Biomass yield) | | | |
|---|---|---|---|
| Comparison | t | one-tail 95% t-critical | Significant? |
| 5% vs. 0.04% | 53.89054 | 6.31375 | Yes |
| 5% vs. 10% | 12.59866 | 6.31375 | Yes |
| 0.04% vs. 10% | 25.09999 | 2.91999 | Yes |

Table A.4 Statistical analysis of algal biomass yield between three $CO_2$ levels

*Data were analyzed with n=2.

| Student t-test ($\mu_h$) | | | |
|---|---|---|---|
| Comparison | t | one-tail 95% t-critical | Significant? |
| 5% vs. 0.04% | 27.06806 | 6.31375 | Yes |
| 5% vs. 10% | 4.95629 | 2.91999 | Yes |
| 0.04% vs. 10% | 14.08008 | 6.31375 | Yes |

Table A.5 Statistical analysis of highest specific growth rate between three $CO_2$ levels

*Data were analyzed with n=2.

| Student t-test ($P_h$) | | | |
|---|---|---|---|
| Comparison | t | one-tail 95% t-critical | Significant? |
| 5% vs. 0.04% | 18.83115 | 6.31375 | Yes |
| 5% vs. 10% | 2.24908 | 2.91999 | No |
| 0.04% vs. 10% | 11.03483 | 6.31375 | Yes |

Table A.6 Statistical analysis of highest biomass productivity between three $CO_2$ levels

*Data were analyzed with n=2.

| | Glucose (mmol/gDCW/h) | | Formate (mmol/gDCW/h) | | Biomass (mmol/gDCW/h) | |
|---|---|---|---|---|---|---|
| Fermentation condition | Formate+ Glucose | Glucose only | Formate+ Glucose | Glucose only | Formate+ Glucose | Glucose only |
| 3L fermenter | -0.609 | -0.576 | -0.499 | - | 0.054 | 0.031 |
| 3 L fermenter | -0.505 | -0.577 | -0.816 | - | 0.027 | 0.037 |
| 0.7L flask | -0.484 | -0.397 | -0.345 | - | 0.012 | 0.010 |
| 0.7L flask | -0.026 | - | -0.117 | - | 0.017 | - |

Table A.7 Average uptake rates and biomass growth rates

| Reaction | Subsystem |
|---|---|
| Acyldihydroxyacetonephosphate reductase | S_Phospholipid_Biosynthesis |
| 1 Acyl glycerol 3 phosphate acyltransferase | S_Phospholipid_Biosynthesis |
| CDP diacylglycerol serine O phosphatidyltransferae mitochondrial | S_Phospholipid_Biosynthesis |
| Choline phosphate cytididyltransferase | S_Phospholipid_Biosynthesis |
| Choline kinase | S_Phospholipid_Biosynthesis |
| Cardiolipin synthase mitochondrial | S_Phospholipid_Biosynthesis |
| Diacylglycerol cholinephosphotransferase | S_Phospholipid_Biosynthesis |
| Diacylglycerol pyrophosphate phosphatase | S_Phospholipid_Biosynthesis |
| CDP Diacylglycerol synthetase | S_Phospholipid_Biosynthesis |
| CDP Diacylglycerol synthetase mitochondrial | S_Phospholipid_Biosynthesis |
| Ethanolamine kinase | S_Phospholipid_Biosynthesis |
| Ethanolaminephosphotransferase | S_Phospholipid_Biosynthesis |
| Glycerol 3 phosphate acyltransferase glycerol 3 phosphate | S_Phospholipid_Biosynthesis |
| Glycerol 3 phosphate acyltransferase glycerone phosphate | S_Phospholipid_Biosynthesis |
| Lyso phosphatidylcholine acyltransferase acyltransferase | S_Phospholipid_Biosynthesis |
| Lipid phosphate phosphatase | S_Phospholipid_Biosynthesis |
| Methylene fatty acyl phospholipid synthase | S_Phospholipid_Biosynthesis |
| Inositol 1 3 4 5 6 pentakisphosphate 2 kinase nuclear | S_Phospholipid_Biosynthesis |
| Inositol 1 3 4 5 triphosphate 6 kinase nucleus | S_Phospholipid_Biosynthesis |
| Inositol 1 4 5 6 tetrakisphosphate 3 kinase nucleus | S_Phospholipid_Biosynthesis |
| Inositol 1 4 5 triphosphate 6 kinase nucleus | S_Phospholipid_Biosynthesis |
| Inositol 1 4 5 trisphosphate 3 kinase nucleus | S_Phospholipid_Biosynthesis |
| Myo-inositol 1-phosphatase | S_Phospholipid_Biosynthesis |
| Myo Inositol 1 phosphate synthase | S_Phospholipid_Biosynthesis |
| Phosphatidate kinase | S_Phospholipid_Biosynthesis |
| Phosphoethanolamine cytidyltransferase | S_Phospholipid_Biosynthesis |
| Phosphatidylethanolamine N methyltransferase | S_Phospholipid_Biosynthesis |
| Phosphatidylglycerol phosphate phosphatase A mitochondrial | S_Phospholipid_Biosynthesis |
| 1 phosphatidylinositol 3 5 bisphosphate 5 phosphatase | S_Phospholipid_Biosynthesis |
| Phosphatidylinositol 3 phosphate 4 kinase | S_Phospholipid_Biosynthesis |
| Phosphatidylinositol 3 phosphate 5 kinase yeast specfic | S_Phospholipid_Biosynthesis |
| 1 phosphatidylinositol 4 5 bisphosphate 5 phosphatase | S_Phospholipid_Biosynthesis |
| 1 phosphatidylinositol 4 5 bisphosphate phosphodiesterase | S_Phospholipid_Biosynthesis |
| Phosphatidylinositol 4 phosphate 5 kinase yeast specfic | S_Phospholipid_Biosynthesis |
| 1 phosphatidylinositol 3 kinase | S_Phospholipid_Biosynthesis |
| Phosphatidylinositol 4 kinase | S_Phospholipid_Biosynthesis |
| Phosphatidylinositol 4 kinase nuclear yeast specifc | S_Phospholipid_Biosynthesis |

Table A.8 Specific reactions in lipid biosynthesis pathways for fatty acid flux analysis

Table A.8 (cont'd)

| | |
|---|---|
| Phosphatidylinositol synthase | S_Phospholipid_Biosynthesis |
| Phosphatidyl N methylethanolamine N methyltransferase | S_Phospholipid_Biosynthesis |
| Phosphatidylserine decarboxylase Golgi | S_Phospholipid_Biosynthesis |
| Phosphatidylserine decarboxylase mitochondrial | S_Phospholipid_Biosynthesis |
| Phosphatidylserine decarboxylase vacuolar | S_Phospholipid_Biosynthesis |
| Phosphatidylserine synthase | S_Phospholipid_Biosynthesis |
| Phosphatidylserine synthase mitochondrial | S_Phospholipid_Biosynthesis |
| Acetyl-CoA C-acetyltransferase | S_Fatty_Acid__Biosynthesis |
| Acetyl CoA C acetyltransferase mitochondrial | S_Fatty_Acid__Biosynthesis |
| Acetyl-CoA carboxylase | S_Fatty_Acid__Biosynthesis |
| Acetyl Coa carboxylase mitochondrial | S_Fatty_Acid__Biosynthesis |
| Acetyl-CoA ACP transacylase | S_Fatty_Acid__Biosynthesis |
| Acetyl CoA ACP transacylase | S_Fatty_Acid__Biosynthesis |
| Myristicoyl CoA desaturase n C140CoA n C141CoA | S_Fatty_Acid__Biosynthesis |
| Palmitoyl CoA desaturase n C160CoA n C161CoA | S_Fatty_Acid__Biosynthesis |
| Stearoyl CoA desaturase n C180CoA n C181CoA | S_Fatty_Acid__Biosynthesis |
| Oleoyl CoA desaturase n C181CoA n C182CoA | S_Fatty_Acid__Biosynthesis |
| Fatty-acyl-ACP hydrolase | S_Fatty_Acid__Biosynthesis |
| Fatty-acyl-ACP hydrolase | S_Fatty_Acid__Biosynthesis |
| Fatty-acyl-ACP hydrolase | S_Fatty_Acid__Biosynthesis |
| Fatty-acyl-ACP hydrolase | S_Fatty_Acid__Biosynthesis |
| Fatty-acyl-ACP hydrolase | S_Fatty_Acid__Biosynthesis |
| Fatty acyl ACP hydrolase | S_Fatty_Acid__Biosynthesis |
| Fatty acyl ACP hydrolase | S_Fatty_Acid__Biosynthesis |
| Fatty acyl ACP hydrolase | S_Fatty_Acid__Biosynthesis |
| Fatty acid CoA ligase decanoate peroxisomal | S_Fatty_Acid__Biosynthesis |
| Fatty acid CoA ligase dodecanoate peroxisomal | S_Fatty_Acid__Biosynthesis |
| Fatty acid CoA ligase tetradecanoate | S_Fatty_Acid__Biosynthesis |
| Fatty acid CoA ligase tetradecanoate peroxisomal | S_Fatty_Acid__Biosynthesis |
| Fatty acid CoA ligase tetradecenoate | S_Fatty_Acid__Biosynthesis |
| Fatty acid CoA ligase tetradecenoate peroxisomal | S_Fatty_Acid__Biosynthesis |
| Fatty acid CoA ligase hexadecanoate | S_Fatty_Acid__Biosynthesis |
| Fatty acid CoA ligase hexadecanoate peroxisomal | S_Fatty_Acid__Biosynthesis |
| Fatty acid CoA ligase hexadecenoate | S_Fatty_Acid__Biosynthesis |
| Fatty acid CoA ligase hexadecenoate peroxisomal | S_Fatty_Acid__Biosynthesis |

Table A.8 (cont'd)

| | |
|---|---|
| Fatty acid CoA ligase octadecanoate | S_Fatty_Acid__Biosynthesis |
| Fatty acid CoA ligase octadecenoate | S_Fatty_Acid__Biosynthesis |
| Fatty acid CoA ligase octadecynoate | S_Fatty_Acid__Biosynthesis |
| Fatty acid CoA ligase n C240 peroxisomal | S_Fatty_Acid__Biosynthesis |
| Fatty acid CoA ligase n C260 peroxisomal | S_Fatty_Acid__Biosynthesis |
| Fatty acid CoA ligase octanoate peroxisomal | S_Fatty_Acid__Biosynthesis |
| Fatty acid synthase n C100 | S_Fatty_Acid__Biosynthesis |
| Fatty acyl ACP synthase n C100ACP mitochondrial | S_Fatty_Acid__Biosynthesis |
| Fatty acyl CoA synthase n C100CoA | S_Fatty_Acid__Biosynthesis |
| Fatty acid synthase n C120 | S_Fatty_Acid__Biosynthesis |
| Fatty acyl ACP synthase n C120ACP mitochondrial | S_Fatty_Acid__Biosynthesis |
| Fatty acyl CoA synthase n C120CoA | S_Fatty_Acid__Biosynthesis |
| Fatty acid synthase n C140 | S_Fatty_Acid__Biosynthesis |
| Fatty acyl ACP synthase n C140ACP mitochondrial | S_Fatty_Acid__Biosynthesis |
| Fatty acyl CoA synthase n C140CoA | S_Fatty_Acid__Biosynthesis |
| Fatty acid synthase n C141 | S_Fatty_Acid__Biosynthesis |
| Fatty acyl ACP synthase n C141ACP mitochondrial | S_Fatty_Acid__Biosynthesis |
| Fatty acid synthase n C160 | S_Fatty_Acid__Biosynthesis |
| Fatty acyl ACP synthase n C160ACP mitochondrial | S_Fatty_Acid__Biosynthesis |
| Fatty acyl CoA synthase n C160CoA | S_Fatty_Acid__Biosynthesis |
| Fatty acid synthase n C161 | S_Fatty_Acid__Biosynthesis |
| Fatty acyl ACP synthase n C161ACP mitochondrial | S_Fatty_Acid__Biosynthesis |
| Fatty acid synthase n C180 | S_Fatty_Acid__Biosynthesis |
| Fatty acyl ACP synthase n C180ACP mitochondrial | S_Fatty_Acid__Biosynthesis |
| Fatty acyl CoA synthase n C180CoA | S_Fatty_Acid__Biosynthesis |
| Fatty acid synthase n C181 | S_Fatty_Acid__Biosynthesis |
| Fatty acyl ACP synthase n C181ACP mitochondrial | S_Fatty_Acid__Biosynthesis |
| Fatty acyl ACP synthase n C182ACP mitochondrial | S_Fatty_Acid__Biosynthesis |
| Fatty acid synthase n C240 lumped reaction | S_Fatty_Acid__Biosynthesis |
| Fatty acid synthase n C260 | S_Fatty_Acid__Biosynthesis |
| Fatty acyl ACP synthase n C80ACP mitochondrial lumped reaction | S_Fatty_Acid__Biosynthesis |
| Fatty acyl CoA synthase n C80CoA lumped reaction | S_Fatty_Acid__Biosynthesis |
| Fatty acid synthase n C80 lumped reaction | S_Fatty_Acid__Biosynthesis |

Table A.8 (cont'd)

| | |
|---|---|
| Malonyl-CoA-ACP transacylase | S_Fatty_Acid__Biosynthesis |
| Malonyl CoA ACP transacylase mitochondrial | S_Fatty_Acid__Biosynthesis |
| Alcohol dehydrogenase glycerol NADP | S_Glycerolipid_Metabolism |
| Dihydroxyacetone kinase | S_Glycerolipid_Metabolism |
| Glycerol 3 phosphate dehydrogenase NAD | S_Glycerolipid_Metabolism |
| Glycerol 3 phosphate dehydrogenase NAD mitochondrial | S_Glycerolipid_Metabolism |
| Glycerol 3 phosphate dehydrogenase FAD mitochondrial | S_Glycerolipid_Metabolism |
| Glycerol-3-phosphatase | S_Glycerolipid_Metabolism |
| Glycerol dehydrogenase NADP dependent | S_Glycerolipid_Metabolism |
| Glycerol kinase | S_Glycerolipid_Metabolism |
| Glycerophosphodiester phosphodiesterase (Glycerophosphocholine) | S_Glycerolipid_Metabolism |
| Phosphatidylcholine diacylglycerol acyltransferase | S_Glycerolipid_Metabolism |
| Triacylglycerol lipase | S_Glycerolipid_Metabolism |
| Triglycerol synthesis | S_Glycerolipid_Metabolism |

| Metabolite | Formula |
|---|---|
| Decanoyl-ACP (n-C10:0ACP) | C21H39N2O8PRS |
| Decanoate (n-C10:0) | C10H19O2 |
| Decanoate (n-C10:0) | C10H19O2 |
| Decanoate (n-C10:0) | C10H19O2 |
| Decanoyl-CoA (n-C10:0CoA) | C31H50N7O17P3S |
| Decanoyl-CoA (n-C10:0CoA) | C31H50N7O17P3S |
| Dodecanoyl-ACP (n-C12:0ACP) | C23H43N2O8PRS |
| Dodecanoyl-ACP (n-C12:0ACP) | C23H43N2O8PRS |
| Dodecanoate (n-C12:0) | C12H23O2 |
| Dodecanoate (n-C12:0) | C12H23O2 |
| Dodecanoate (n-C12:0) | C12H23O2 |
| Dodecanoyl-CoA (n-C12:0CoA) | C33H54N7O17P3S |
| Dodecanoyl-CoA (n-C12:0CoA) | C33H54N7O17P3S |
| Hexadecanoate (n-C16:0) | C16H31O2 |
| Hexadecanoate (n-C16:0) | C16H31O2 |
| Hexadecanoate (n-C16:0) | C16H31O2 |
| Hexadecenoate (n-C16:1) | C16H29O2 |
| Hexadecenoate (n-C16:1) | C16H29O2 |
| Hexadecenoate (n-C16:1) | C16H29O2 |
| Hexadecenoyl-CoA (n-C16:1CoA) | C37H60N7O17P3S |
| Hexadecenoyl-CoA (n-C16:1CoA) | C37H60N7O17P3S |
| Cis-hexadec-9-enoyl-[acyl-carrier protein] (n-C16:1) | C27H49N2O8PRS |
| Cis-hexadec-9-enoyl-[acyl-carrier protein] (n-C16:1) | C27H49N2O8PRS |
| Myristoyl-ACP (n-C14:0ACP) | C25H47N2O8PRS |
| Myristoyl-ACP (n-C14:0ACP) | C25H47N2O8PRS |
| Octanoyl-ACP (n-C8:0ACP) | C19H35N2O8PRS |
| Octanoyl-CoA (n-C8:0CoA) | C29H46N7O17P3S |
| Octanoyl-CoA (n-C8:0CoA) | C29H46N7O17P3S |
| Octadecanoyl-ACP (n-C18:0ACP) | C29H55N2O8PRS |
| Octadecanoyl-ACP (n-C18:0ACP) | C29H55N2O8PRS |
| Octadecanoate (n-C18:0) | C18H35O2 |
| Octadecanoate (n-C18:0) | C18H35O2 |
| Octadecanoate (n-C18:0) | C18H35O2 |
| Octadecenoate (n-C18:1) | C18H33O2 |
| Octadecenoate (n-C18:1) | C18H33O2 |
| Octanoate (n-C8:0) | C8H15O2 |

Table A.9 Important metabolites in lipid biosynthesis

Table A.9 (cont'd)

| | |
|---|---|
| Octanoate (n-C8:0) | C8H15O2 |
| Cis-octadec-11-enoyl-[acyl-carrier protein] (n-C18:1) | C29H53N2O8PRS |
| Cis-octadec-11-enoyl-[acyl-carrier protein] (n-C18:1) | C29H53N2O8PRS |
| Octadecenoyl-CoA (n-C18:1CoA) | C39H64N7O17P3S |
| Octadecenoyl-CoA (n-C18:1CoA) | C39H64N7O17P3S |
| Palmitoyl-ACP (n-C16:0ACP) | C27H51N2O8PRS |
| Palmitoyl-ACP (n-C16:0ACP) | C27H51N2O8PRS |
| Palmitoyl-CoA (n-C16:0CoA) | C37H62N7O17P3S |
| Palmitoyl-CoA (n-C16:0CoA) | C37H62N7O17P3S |
| Stearoyl-CoA (n-C18:0CoA) | C39H66N7O17P3S |
| Stearoyl-CoA (n-C18:0CoA) | C39H66N7O17P3S |
| Tetradecanoyl-CoA (n-C14:0CoA) | C35H58N7O17P3S |
| Tetradecanoyl-CoA (n-C14:0CoA) | C35H58N7O17P3S |
| Cis-tetradec-7-enoyl-[acyl-carrier protein] (n-C14:1) | C25H45N2O8PRS |
| Cis-tetradec-7-enoyl-[acyl-carrier protein] (n-C14:1) | C25H45N2O8PRS |
| Tetradecenoyl-CoA (n-C14:1CoA) | C35H56N7O17P3S |
| Tetradecenoyl-CoA (n-C14:1CoA) | C35H56N7O17P3S |
| Tetradecanoate (n-C14:0) | C14H27O2 |
| Tetradecanoate (n-C14:0) | C14H27O2 |
| Tetradecanoate (n-C14:0) | C14H27O2 |
| Tetradecenoate (n-C14:1) | C14H25O2 |
| Tetradecenoate (n-C14:1) | C14H25O2 |

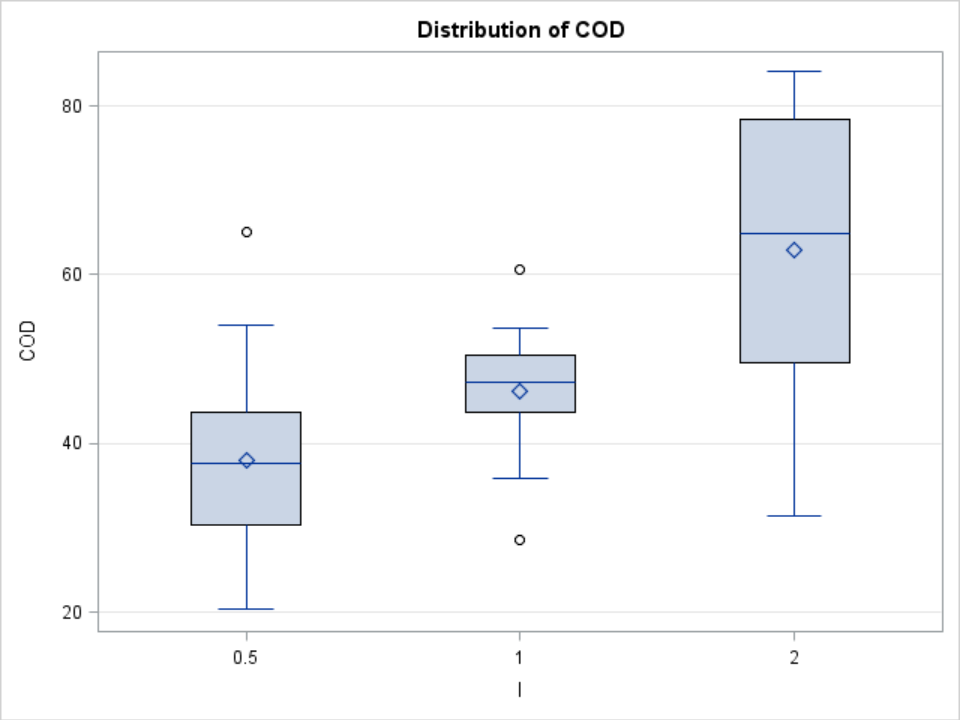


(a)

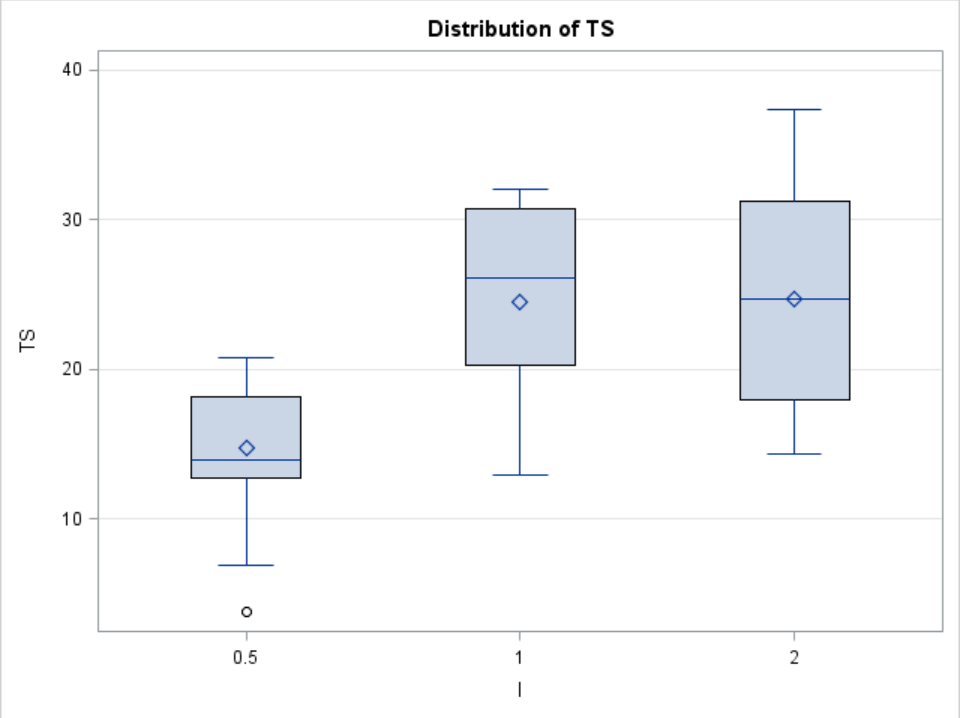


(b)

Figure A.1 Boxplots for COD removal (a) and TS removal (b) with different current levels in 1st EC

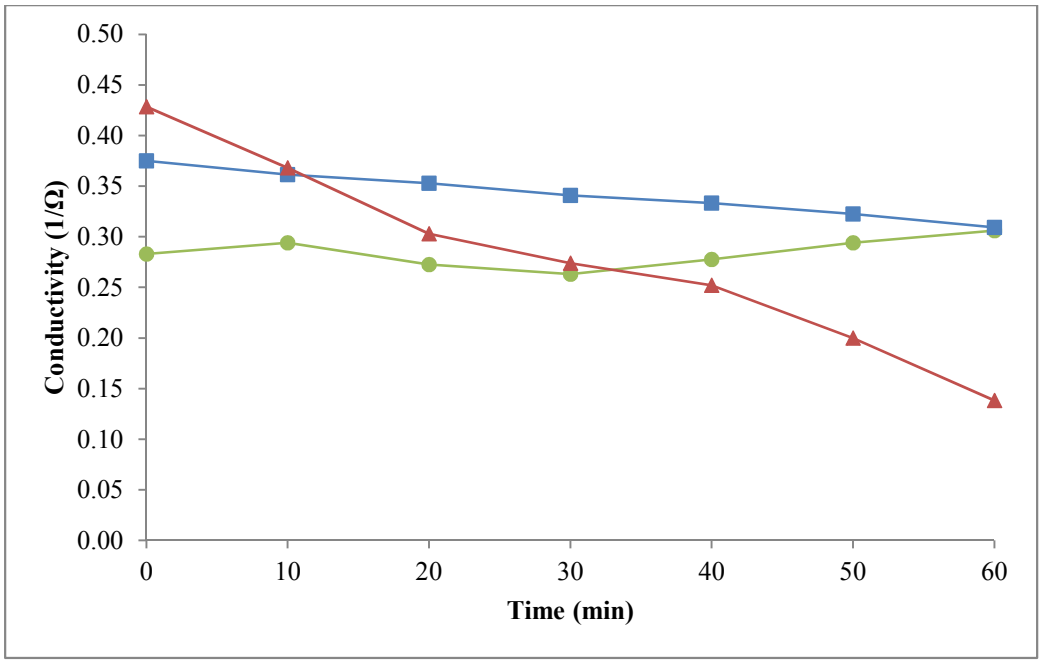


Figure A.2 Comparison of dynamic changes of conductivity within different current strengths for the 1st stage EC

Diamond green stands for 0.5A, 60 min, and electrode of type A;
Square blue stands for 1A, 60 min, and electrodes of type A;
Triangle red stands for 2A, 60 min, and electrode of type A.
*: Data represent the average of two replicates.

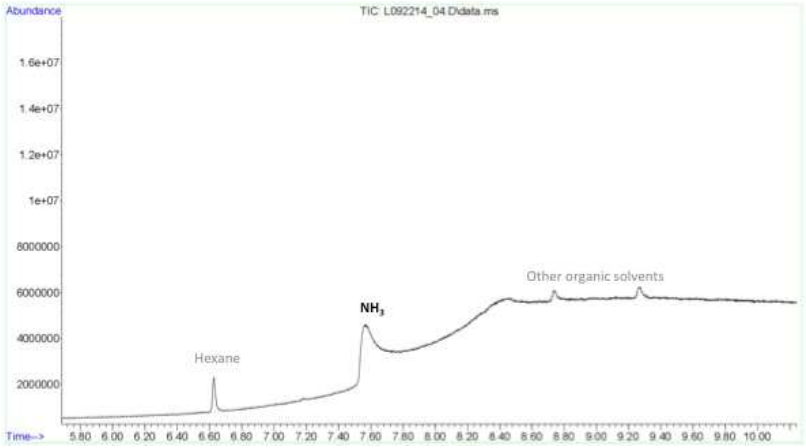


(a)

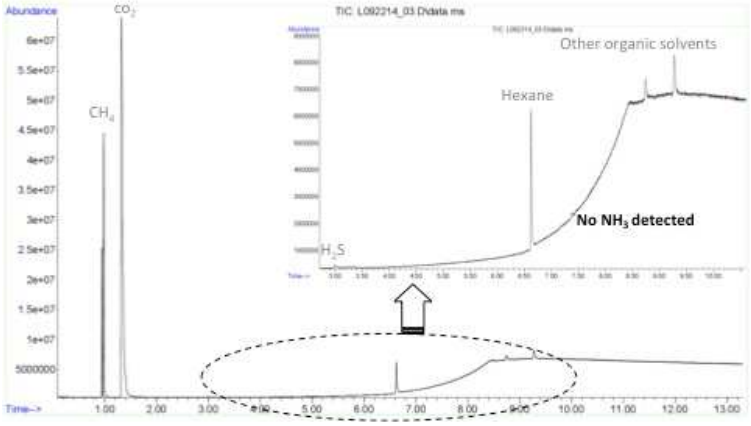


(b)

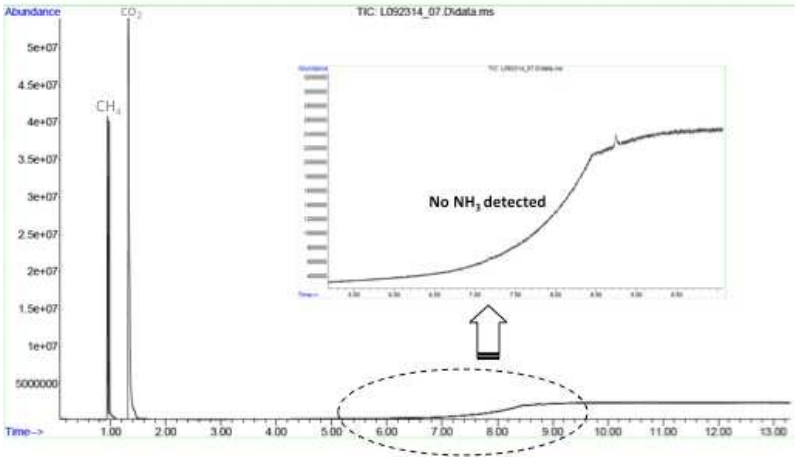


(c)

Figure A.3 $NH_3$ in biogas during the biogas pumping by GC-MS analysis

(a). GC profile of headspace gas sample from saturated ammonia hydrous solution.
(b). GC profile of inlet gas sample at the beginning phase of biogas pumping process.
(c). GC profile of outlet gas sample at the beginning phase of biogas pumping process.
(d). GC profile of inlet gas sample at the ending phase of biogas pumping process.
(e). GC profile of outlet gas sample at the ending phase of biogas pumping process.

Figure A.3 (cont'd)

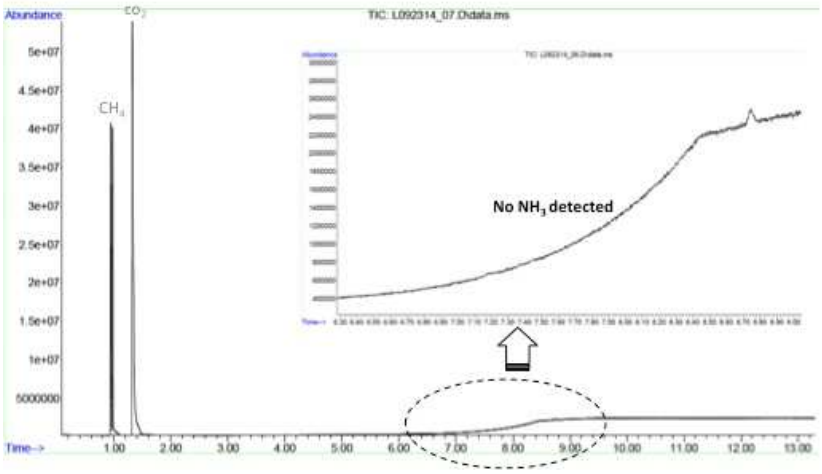


(d)

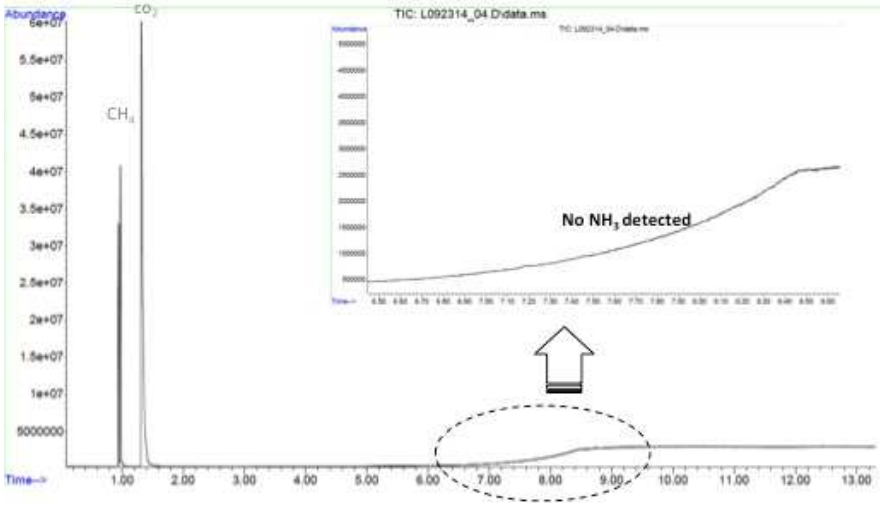


(e)

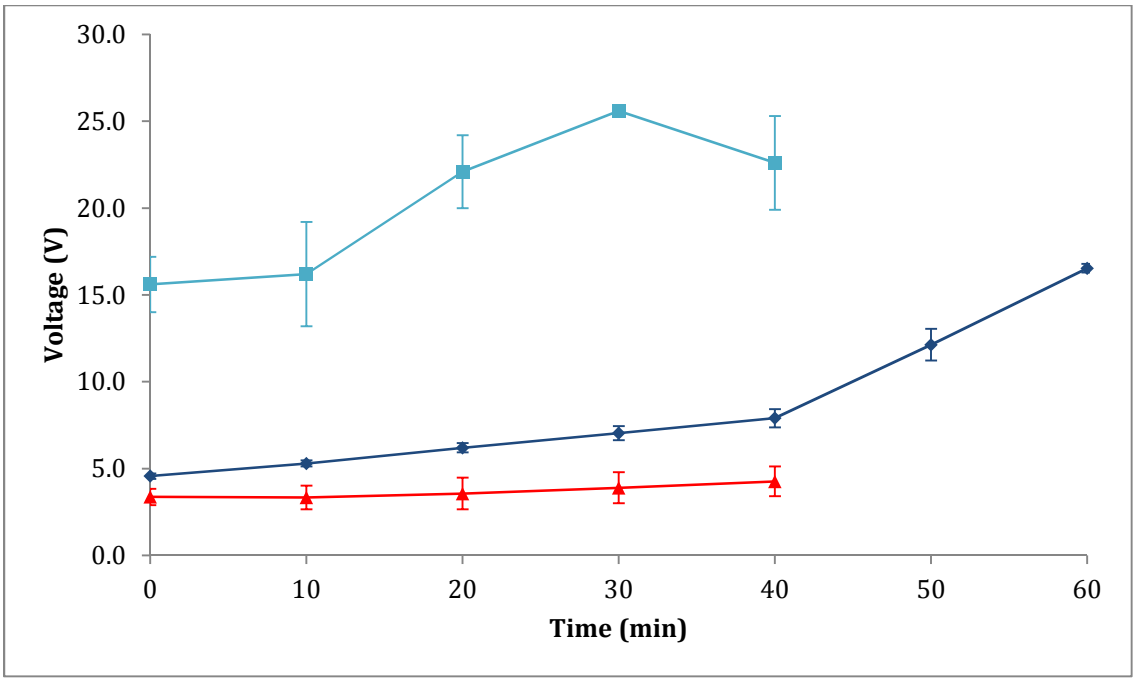


Figure A.4 Voltage change between the 1st EC treatment, 2nd no-biogas-pumped (NBP) treatment, and 2nd biogas pumped (BP) treatment

Triangle red stands for the 2nd EC treatment on BP solution;
Square light blue stands for the 2nd EC treatment on NBP solution;
Diamond dark blue stands for the 1st EC treatment.

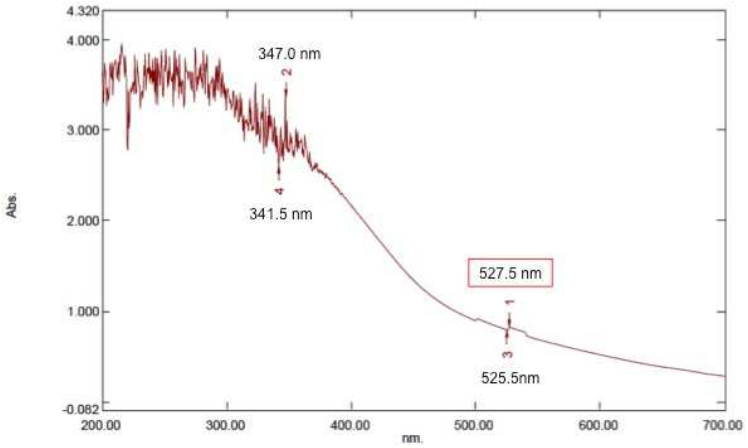


(a)

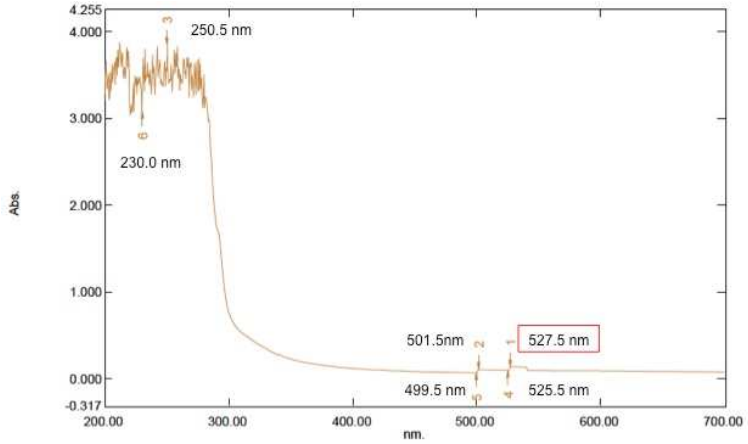


(b)

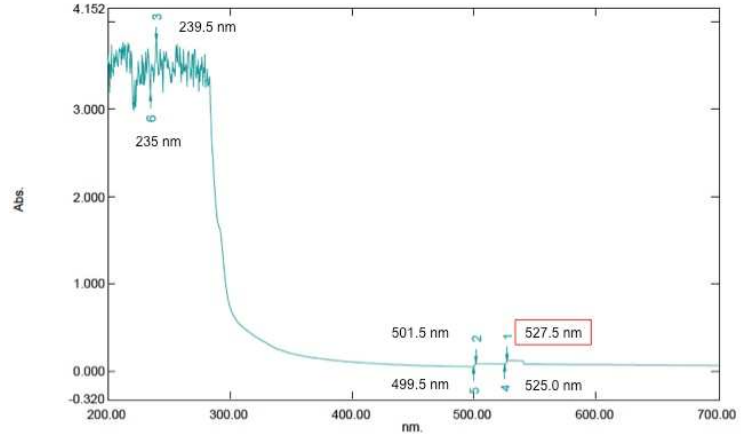


(c)

Figure A.5 Light absorbance profiles of the solutions in the wavelength rage of 200-700 nm

(a). Absorbance profile for AD effluent pre EC treatment.
(b). Absorbance profile for effluent water post EC treatment with BP.
(c). Absorbance profile for effluent water post EC treatment with NBP.

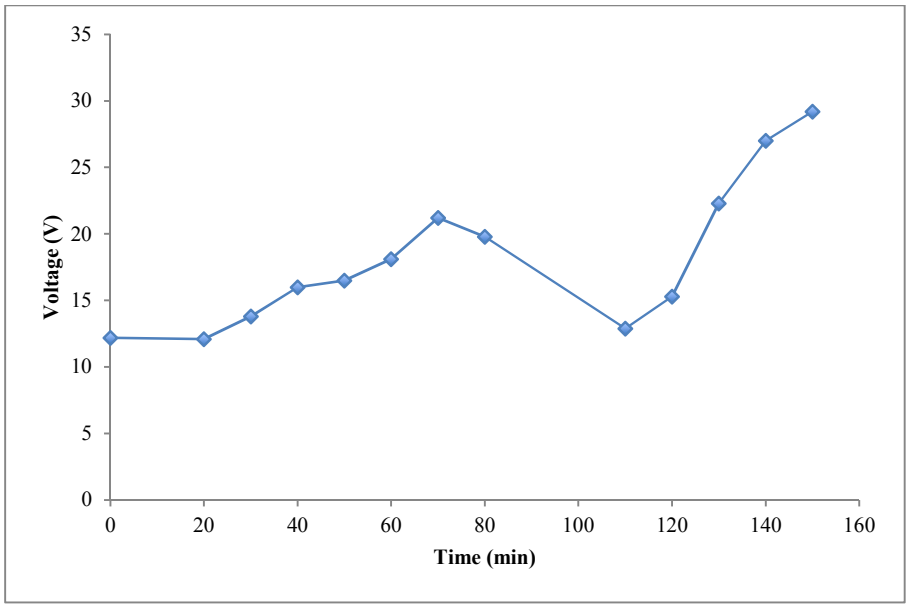


Figure A.6 Voltage change during EC treatment on high loading AD effluent

*EC condition: current level=10A, volume=3.5L

# BIBLIOGRAPHY

## BIBLIOGRAPHY


1. Copeland, C., Animal waste and water quality: EPA regulation of concentrated animal feeding operations (CAFOs). 2008, CRS Report to Congress.

2. Energy Information Administration, *Greenhouse Gas Emissions in the United States*. 2007.

3. Mata-Alvarez, J., S. Mace, and P. Llabres, Anaerobic digestion of organic solid wastes. An overview of research achievements and perspectives. Bioresource technology, 2000. **74**(1): p. 3-16.

4. Liu, Z., et al., Integration of sewage sludge digestion with advanced biofuel synthesis. Bioresour Technol, 2013. **132**: p. 166-70.

5. Service, U.E.R., Confined Animal and Manure Nutrient Data System. 1997.

6. USDA, D., EPA Biogas Opportunities Roadmap. 2014.

7. Liu, Z., et al., A new multiple-stage electrocoagulation process on anaerobic digestion effluent to simultaneously reclaim water and clean up biogas. J Hazard Mater, 2015. **285**: p. 483-90.

8. Rodriguez, J., et al., Removal of non-biodegradable organic matter from landfill leachates by adsorption. Water Res, 2004. **38**(14-15): p. 3297-303.

9. Al-Malah, K., M.O.J. Azzam, and N.I. Abu-Lail, *Olive mills effluent (OME) wastewater post-treatment using activated clay.* Separation and Purification Technology, 2000. **20**(2–3): p. 225-234.

10. Tyagi, V.K., et al., Enhancement of Coagulation Flocculation Process Using Anionic Polymer for the Post Treatment of UASB Reactor Effluent. Separation Science and Technology, 2010. **45**(5): p. 626-634.

11. Chernicharo, C.A.L., *Post-Treatment Options for the Anaerobic Treatment of Domestic Wastewater.* Reviews in Environmental Science and Bio/Technology, 2006. **5**(1): p. 73-92.

12. Penetra, R.G., et al., Post-treatment of effluents from anaerobic reactor treating domestic sewage by dissolved-air flotation. Water Science and Technology, 1999. **40**(8): p. 137-143.

13. Apollo, S., M.S. Onyango, and A. Ochieng, An integrated anaerobic digestion and UV photocatalytic treatment of distillery wastewater. J Hazard Mater, 2013. **261**: p. 435-42.

14. Battimelli, A., et al., Anaerobic digestion of waste activated sludge combined with ozone post-treatment and recycling. Water Sci Technol, 2003. **48**(4): p. 61-8.

15. Mollah, M.Y., et al., *Electrocoagulation (EC)--science and applications.* J Hazard Mater, 2001. **84**(1): p. 29-41.

16. Mollah, M.Y., et al., *Fundamentals, present and future perspectives of electrocoagulation.* J Hazard Mater, 2004. **114**(1-3): p. 199-210.

17. Howe, K.J., et al., *Principles of water treatment*. 2012: Wiley.

18. Bellebia, S., et al., Experimental investigation of chemical oxygen demand and turbidity removal from cardboard paper mill effluents using combined electrocoagulation and adsorption processes. Environmental Progress & Sustainable Energy, 2012. **31**(3): p. 361-370.

19. Parga, J.R., et al., Cyanide Detoxification of Mining Wastewaters with TiO2 Nanoparticles and Its Recovery by Electrocoagulation. Chemical Engineering & Technology, 2009. **32**(12): p. 1901-1908.

20. Sengil, I.A. and M. Ozacar, Treatment of dairy wastewaters by electrocoagulation using mild steel electrodes. J Hazard Mater, 2006. **137**(2): p. 1197-205.

21. Lei, X. and T. Maekawa, Electrochemical treatment of anaerobic digestion effluent using a Ti/Pt–IrO2 electrode. Bioresource Technology, 2007. **98**(18): p. 3521-3525.

22. Yetilmezsoy, K., et al., Decolorization and COD reduction of UASB pretreated poultry manure wastewater by electrocoagulation process: a post-treatment study. J Hazard Mater, 2009. **162**(1): p. 120-32.

23. Jiang, A., Ammonia recovery from digested dairy manure as nitrogen fertilizer. 2009, Washington State University.

24. Mulder, A., *The quest for sustainable nitrogen removal technologies.* Water Sci Technol, 2003. **48**(1): p. 67-75.

25. Wang, L., et al., Anaerobic digested dairy manure as a nutrient supplement for cultivation of oil-rich green microalgae Chlorella sp. Bioresource technology, 2010. **101**(8): p. 2623-2628.

26. Tambone, F., et al., Assessing amendment properties of digestate by studying the organic matter composition and the degree of biological stability during the anaerobic digestion of the organic fraction of MSW. Bioresour Technol, 2009. **100**(12): p. 3140-2.

27. Manure, F.D., Dairy Waste Anaerobic Digestion Handbook. 2001.

28. Tambone, F., et al., Assessing amendment and fertilizing properties of digestates from anaerobic digestion through a comparative study with digested sludge and compost. Chemosphere, 2010. **81**(5): p. 577-583.

29. Liao, W., et al., Leaching-bed reactor for producing stabilised plant growing media from dairy manure. Biosystems engineering, 2010. **106**(3): p. 278-285.

30. Inyang, M., et al., *Biochar from anaerobically digested sugarcane bagasse.* Bioresour Technol, 2010. **101**(22): p. 8868-72.

31. Yao, Y., et al., Biochar derived from anaerobically digested sugar beet tailings: characterization and phosphate removal potential. Bioresour Technol, 2011. **102**(10): p. 6273-8.

32. Sun, L., S. Wan, and W. Luo, Biochars prepared from anaerobic digestion residue, palm bark, and eucalyptus for adsorption of cationic methylene blue dye: characterization, equilibrium, and kinetic studies. Bioresour Technol, 2013. **140**: p. 406-13.

33. Yue, Z., et al., Development of a new bioethanol feedstock–anaerobically digested fiber from confined dairy operations using different digestion configurations. biomass and bioenergy, 2011. **35**(5): p. 1946-1953.

34. Teater, C., et al., Assessing solid digestate from anaerobic digestion as feedstock for ethanol production. Bioresource technology, 2011. **102**(2): p. 1856-1862.

35. Yue, Z., et al., A sustainable pathway of cellulosic ethanol production integrating *anaerobic digestion with biorefining.* Biotechnol Bioeng, 2010. **105**(6): p. 1031-9.

36. Bramono, S.E., et al., A mesophilic Clostridium species that produces butanol from monosaccharides and hydrogen from polysaccharides. Bioresource technology, 2011. **102**(20): p. 9558-9563.

37. Zhong, Y., et al., A self-sustaining advanced lignocellulosic biofuel production by integration of anaerobic digestion and aerobic fungal fermentation. Bioresour Technol, 2015. **179**: p. 173-9.

38. Zhang, Y.H., Reviving the carbohydrate economy via multi-product lignocellulose biorefineries. J Ind Microbiol Biotechnol, 2008. **35**(5): p. 367-75.

39. FitzPatrick, M., et al., A biorefinery processing perspective: treatment of lignocellulosic materials for the production of value-added products. Bioresour Technol, 2010. **101**(23): p. 8915-22.

40. Werpy, T., et al., Top value added chemicals from biomass. Volume 1-Results of screening for potential candidates from sugars and synthesis gas. 2004, DTIC Document.

41. Lucia, L.A., et al., *Chemicals and energy from biomass.* Canadian journal of chemistry, 2006. **84**(7): p. 960-970.

42. Liu, Y., W. Liao, and S. Chen, Co-production of lactic acid and chitin using a pelletized filamentous fungus Rhizopus oryzae cultured on cull potatoes and glucose. Journal of applied microbiology, 2008. **105**(5): p. 1521-1528.

43. Xiaobo, X., L. Jianping, and C. Peilin, *Advances in the research and development of acrylic acid production from biomass.* Chinese Journal of Chemical Engineering, 2006. **14**(4): p. 419-427.

44. Danner, H. and R. Braun, *Biotechnology for the production of commodity chemicals from biomass.* Chem. Soc. Rev., 1999. **28**(6): p. 395-405.

45. Liu, Y., W. Liao, and S. Chen, Co-production of lactic acid and chitin using a pelletized filamentous fungus Rhizopus oryzae cultured on cull potatoes and glucose. Journal of Applied Microbiology, 2008. **105**(5): p. 1521-1528.

46. Teng, W.L., et al., *Concurrent production of chitin from shrimp shells and fungi.* Carbohydr Res, 2001. **332**(3): p. 305-16.

47. Wu, T., et al., Physicochemical properties and bioactivity of fungal chitin and chitosan. J Agric Food Chem, 2005. **53**(10): p. 3888-94.

48. Hermosa, R., et al., *Plant-beneficial effects of Trichoderma and of its genes.* Microbiology, 2012. **158**(1): p. 17-25.

49. Ryckebosch, E., M. Drouillon, and H. Vervaeren, *Techniques for transformation of biogas to biomethane.* Biomass and bioenergy, 2011. **35**(5): p. 1633-1645.

50. Abatzoglou, N. and S. Boivin, *A review of biogas purification processes.* Biofuels, Bioproducts and Biorefining, 2009. **3**(1): p. 42-71.

51. Grierson, J. and M. Allen, Process and apparatus for removal of H2S from gaseous streams using membrane purification of recycle solution, Assignee: The Dow Chemical Company, PCT Patent, WO 92/17401. International Publication date: October, 1992. **15**.

52. Adib, F., A. Bagreev, and T.J. Bandosz, Analysis of the relationship between H2S removal capacity and surface properties of unimpregnated activated carbons. Environmental science & technology, 2000. **34**(4): p. 686-692.

53. Syed, M., et al., REMOVAL OF HYDROGEN SULFIDE FROM GAS STREAMS USING BIOLOGICAL PROCESSES• A REVIEW. Canadian Biosystems Engineering, 2006. **48**: p. 2.

54. Broekhuis, R.R., D.J. Koch, and S. Lynn, A medium-temperature process for removal of hydrogen sulfide from sour gas streams with aqueous metal sulfate solutions. Industrial & engineering chemistry research, 1992. **31**(12): p. 2635-2642.

55. Persson, M., Evaluation of upgrading techniques for biogas. Report SGC, 2003. **142**.

56. Hagen, M., Adding gas from biomass to the gas grid. 2001: SGC.

57. Rutledge, B., California biogas industry assessment white paper. Available on, 2005.

58. Kim, T.J., B. Li, and M.B. Hägg, *Novel fixed-site–carrier polyvinylamine membrane for carbon dioxide capture.* Journal of Polymer Science Part B: Polymer Physics, 2004. **42**(23): p. 4326-4336.

59. Esteves, I. and J.P.B. Mota, Simulation of a new hybrid membrane/pressure swing adsorption process for gas separation. Desalination, 2002. **148**(1): p. 275-280.

60. Hu, X., et al., CO2 Fixation, Lipid Production, and Power Generation by a Novel Air-Lift-Type Microbial Carbon Capture Cell System. Environ Sci Technol, 2015. **49**(17): p. 10710-7.

61. Christenson, L. and R. Sims, Production and harvesting of microalgae for wastewater treatment, biofuels, and bioproducts. Biotechnol Adv, 2011. **29**(6): p. 686-702.

62. Chen, R., et al., Freshwater algal cultivation with animal waste for nutrient removal and biomass production. Biomass and Bioenergy, 2012. **39**: p. 128-138.

63. Tang, D., et al., CO2 biofixation and fatty acid composition of Scenedesmus obliquus and Chlorella pyrenoidosa in response to different CO2 levels. Bioresour Technol, 2011. **102**(3): p. 3071-6.

64. Jones, J.P., G.K. Prakash, and G.A. Olah, *Electrochemical CO2 reduction: recent advances and current trends.* Israel Journal of Chemistry, 2014. **54**(10): p. 1451-1466.

65. Hori, Y., Electrochemical CO2 reduction on metal electrodes, in Modern aspects of electrochemistry. 2008, Springer. p. 89-189.

66. Mahmood, M.N., D. Masheder, and C.J. Harty, Use of gas-diffusion electrodes for high-rate electrochemical reduction of carbon dioxide. I. Reduction at lead, indium- and tin-impregnated electrodes. Journal of applied electrochemistry, 1987. **17**(6): p. 1159-1170.

67. Hori, Y., et al., Electrocatalytic process of CO selectivity in electrochemical reduction of CO 2 at metal electrodes in aqueous media. Electrochimica Acta, 1994. **39**(11): p. 1833-1839.

68. Schuchmann, K. and V. Muller, Direct and reversible hydrogenation of CO2 to formate by a bacterial carbon dioxide reductase. Science, 2013. **342**(6164): p. 1382-5.

69. Reda, T., et al., Reversible interconversion of carbon dioxide and formate by an electroactive enzyme. Proc Natl Acad Sci U S A, 2008. **105**(31): p. 10654-8.

70. Schauer, N.L. and J.G. Ferry, *Metabolism of formate in Methanobacterium formicicum.* J Bacteriol, 1980. **142**(3): p. 800-7.

71. Igamberdiev, A.U., N.V. Bykova, and L.A. Kleczkowski, *Origins and metabolism of formate in higher plants.* Plant Physiology and Biochemistry, 1999. **37**(7): p. 503-513.

72. Li, H., et al., Integrated electromicrobial conversion of CO2 to higher alcohols. Science, 2012. **335**(6076): p. 1596.

73. Harris, D.M., et al., Formate as an auxiliary substrate for glucose-limited cultivation of Penicillium chrysogenum: impact on penicillin G production and biomass yield. Applied and environmental microbiology, 2007. **73**(15): p. 5020-5025.

74. Zeng, J., et al., Lignocellulosic biomass as a carbohydrate source for lipid production by Mortierella isabellina. Bioresource technology, 2013. **128**: p. 385-391.

75. Maclellan, J., et al., Anaerobic treatment of lignocellulosic material to co-produce methane and digested fiber for ethanol biorefining. Bioresour Technol, 2013. **130**: p. 418-23.

76. Dean, R.B., *PROCESSES FOR WATER RECLAMATION.* Waste Management & Research, 1991. **9**(5): p. 425-430.

77. Mollah, M.Y.A., et al., *Electrocoagulation (EC) - science and applications.* Journal of Hazardous Materials, 2001. **84**(1): p. 29-41.

78. Chen, G.H., *Electrochemical technologies in wastewater treatment.* Separation and Purification Technology, 2004. **38**(1): p. 11-41.

79. Butler, E., et al., *Electrocoagulation in Wastewater Treatment.* Water, 2011. **3**: p. 495-525.

80. Mollah, M.Y.A., et al., *Fundamentals, present and future perspectives of electrocoagulation.* Journal of Hazardous Materials, 2004. **114**(1-3): p. 199-210.

81. Hector A. Moreno-Casillas, D.L.C., Jewel A.G. Gomes, and J.R.P. Paul Morkovsky, Eric Peterson, *Electrocoagulation mechanism for COD removal.* Separation and Purification Technology, 2007. **56**(2): p. 7.

82. Nazih K. Shammas, M.-F.P., and Alain Grasmick, *Wastewater Treatment by Electrocoagulation–Flotation.* Flotation Technology, 2010. **12**: p. 21.

83. Kobya, M., E. Senturk, and M. Bayramoglu, *Treatment of poultry slaughterhouse wastewaters by electrocoagulation.* J Hazard Mater, 2006. **133**(1-3): p. 172-6.

84. Nicolas Abatzoglou, S.B., *A review of biogas purifi cation processes.* Biofuel Bioproducts & Biorefining, 2009. **3**(1): p. 29.

85. M, G.J.a.A., Process and apparatus for removal of H2S from gaseous streams using membrane purifi cation of recycle solution. 1992, The Dow Chemical Company: USA.

86. Dabrowski, A., et al., Adsorption of phenolic compounds by activated carbon--a critical review. Chemosphere, 2005. **58**(8): p. 1049-70.

87. Bagreev, A. and T.J. Bandosz, A Role of Sodium Hydroxide in the Process of Hydrogen Sulfide Adsorption/Oxidation on Caustic-Impregnated Activated Carbons. Industrial & Engineering Chemistry Research, 2002. **41**(4): p. 672-679.

88. Schweigkofler, M. and R. Niessner, *Removal of siloxanes in biogases.* J Hazard Mater, 2001. **83**(3): p. 183-96.

89. Jin, Y., M.C. Veiga, and C. Kennes, Effects of pH, CO2, and flow pattern on the autotrophic degradation of hydrogen sulfide in a biotrickling filter. Biotechnol Bioeng, 2005. **92**(4): p. 462-71.

90. Conde, J.L., et al., *Biogas purification process using intensive microalgae cultures.* Biotechnology Letters, 1993. **15**(3): p. 317-320.

91. M. Syed, G.S., P. Falletta and M. Béland, *Removal of hydrogen sulfide from gas streams using biological processes - a review.* Canadian Biosystems Engineering, 2006. **48**: p. 14.

92. Jirka, A.M.C., M.J.,, *Analytical Chemistry*. Vol. 47(8). 1975.

93. Agency, E.P., Turbidity methods & measurement. 1999.

94. Zuo, Q., et al., Combined electrocoagulation and electroflotation for removal of fluoride from drinking water. J Hazard Mater, 2008. **159**(2-3): p. 452-7.

95. Adhoum, N., et al., Treatment of electroplating wastewater containing Cu2+, Zn2+ and Cr(VI) by electrocoagulation. J Hazard Mater, 2004. **112**(3): p. 207-13.

96. Holt, P.K., et al., *A quantitative comparison between chemical dosing and electrocoagulation.* Colloids and Surfaces A: Physicochemical and Engineering Aspects, 2002. **211**(2–3): p. 233-248.

97. Avsar, Y., U. Kurt, and T. Gonullu, Comparison of classical chemical and electrochemical processes for treating rose processing wastewater. J Hazard Mater, 2007. **148**(1-2): p. 340-5.

98. Adhoum, N. and L. Monser, *Decolourization and removal of phenolic compounds from olive mill wastewater by electrocoagulation.* Chemical Engineering and Processing: Process Intensification, 2004. **43**(10): p. 1281-1287.

99. Lei, X. and T. Maekawa, Electrochemical treatment of anaerobic digestion effluent using a Ti/Pt-IrO2 electrode. Bioresour Technol, 2007. **98**(18): p. 3521-5.

100. Yetilmezsoy, K., et al., Decolorization and COD reduction of UASB pretreated poultry manure wastewater by electrocoagulation process: A post-treatment study. Journal of Hazardous Materials, 2009. **162**(1): p. 120-132.

101. Avsar, Y., U. Kurt, and T. Gonullu, Comparison of classical chemical and electrochemical processes for treating rose processing wastewater. Journal of Hazardous Materials, 2007. **148**(1-2): p. 340-345.

102. Shoesmith, D.W., et al., The formation of ferrous monosulfide polymorphs during the corrosion of iron by aqueous hydrogen-sulfide at 21-degrees-c. Journal of the Electrochemical Society, 1980. **127**(5): p. 1007-1015.

103. Golan, E., *The U.S. Food Waste Challenge*. 2013, U.S. Department of Agriculture.

104. Liu, Z., et al., A new multiple-stage electrocoagulation process on anaerobic digestion effluent to simultaneously reclaim water and clean up biogas. J Hazard Mater, 2014. **285C**: p. 483-490.

105. Kong, Q.X., et al., Culture of Microalgae Chlamydomonas reinhardtii in Wastewater for Biomass Feedstock Production. Applied Biochemistry and Biotechnology, 2010. **160**(1): p. 9-18.

106. Khan, M. and N. Yoshida, Effect of L-glutamic acid on the growth and ammonium removal from ammonium solution and natural wastewater by Chlorella vulgaris NTM06. Bioresource Technology, 2008. **99**(3): p. 575-582.

107. Martinez, M.E., et al., Nitrogen and phosphorus removal from urban wastewater by the microalga Scenedesmus obliquus. Bioresource Technology, 2000. **73**(3): p. 263-272.

108. Gonzalez, L.E., R.O. Canizares, and S. Baena, Efficiency of ammonia and phosphorus removal from a Colombian agroindustrial wastewater by the microalgae Chlorella vulgaris and Scenedesmus dimorphus. Bioresource Technology, 1997. **60**(3): p. 259-262.

109. Jimenez-Perez, M.V., et al., Growth and nutrient removal in free and immobilized planktonic green algae isolated from pig manure. Enzyme and Microbial Technology, 2004. **34**(5): p. 392-398.

110. Nrc, Nutrient requirements of dairy cattle. 7th rev. ed, 2001: p. 381.

111. Hoober, J.K., The Chlamydomonas Sourcebook. A Comprehensive Guide to Biology and Laboratory Use. Elizabeth H. Harris. Academic Press, San Diego, CA, 1989. xiv, 780 pp., illus. $145. 1989, American Association for the Advancement of Science.

112. Hutner, S.H., et al., *Some approaches to the study of the role of metals in the metabolism of microorganisms.* Proceedings of the American Philosophical Society, 1950: p. 152-170.

113. American Public Health, A., et al., *Standard methods for the examination of water and wastewater*. Vol. 2. 1915: American Public Health Association.

114. Jirka, A.M. and M.J. Carter, Micro semiautomated analysis of surface and waste waters for chemical oxygen demand. Analytical chemistry, 1975. **47**(8): p. 1397-1402.

115. Van Wychen, S. and L.M.L. Laurens, *Determination of Total Carbohydrates in Algal Biomass.* Contract, 2013. **303**: p. 275-3000.

116. Bligh, E.G. and W.J. Dyer, A Rapid Method of Total Lipid Extraction and *Purification.* Canadian Journal of Biochemistry and Physiology, 1959. **37**(8): p. 911-917.

117. Holt, P., G. Barton, and C. Mitchell, *Electrocoagulation as a wastewater treatment.* The Third Annual Australian Environmental Engineering Research Event, 1999. **1000**: p. 41-46.

118. de-Bashan, L.E., et al., Removal of ammonium and phosphorus ions from synthetic wastewater by the microalgae Chlorella vulgaris coimmobilized in alginate

beads with the microalgae growth-promoting bacterium Azospirillum brasilense. Water Res, 2002. **36**(12): p. 2941-8.

119. Yun, Y.S., et al., *Carbon dioxide fixation by algal cultivation using wastewater nutrients.* Journal of Chemical Technology and Biotechnology, 1997. **69**(4): p. 451-455.

120. Tam, N.F.Y. and Y.S. Wong, Effect of ammonia concentrations on growth of Chlorella vulgaris and nitrogen removal from media. Bioresource technology, 1996. **57**(1): p. 45-50.

121. Chiu, S.Y., et al., Reduction of CO2 by a high-density culture of Chlorella sp. in a semicontinuous photobioreactor. Bioresour Technol, 2008. **99**(9): p. 3389-96.

122. Agustí, S., Light environment within dense algal populations: cell size influences on self-shading. Journal of plankton research, 1991. **13**(4): p. 863-871.

123. Juneja, A., R.M. Ceballos, and G.S. Murthy, Effects of environmental factors and nutrient availability on the biochemical composition of algae for biofuels production: a review. Energies, 2013. **6**(9): p. 4607-4638.

124. Kavanova, M., et al., Phosphorus deficiency decreases cell division and elongation in grass leaves. Plant Physiol, 2006. **141**(2): p. 766-75.

125. Ng, W.H.A. and H.B. Liu, Diel Variation of the Cellular Carbon to Nitrogen Ratio of Chlorella Autotrophica (Chlorophyta) Growing in Phosphorus- and Nitrogen-Limited Continuous Cultures. Journal of Phycology, 2015. **51**(1): p. 82-92.

126. Park, C., et al., Evaluation of the extracellular proteins in full-scale activated sludges. Water Res, 2008. **42**(14): p. 3879-89.

127. Wang, M., et al., Kinetics of nutrient removal and expression of extracellular polymeric substances of the microalgae, Chlorella sp. and Micractinium sp., in wastewater treatment. Bioresour Technol, 2014. **154**: p. 131-7.

128. Becker, E.W., *Micro-algae as a source of protein.* Biotechnology advances, 2007. **25**(2): p. 207-210.

129. Liu, Z.Y., G.C. Wang, and B.C. Zhou, *Effect of iron on growth and lipid accumulation in Chlorella vulgaris.* Bioresour Technol, 2008. **99**(11): p. 4717-22.

130. USDA National Agricultural Statistics Service, *Farms, land in farms, and livestock operations*. 2009.

131. Nallathambi Gunaseelan, V., *Anaerobic digestion of biomass for methane production: A review.* Biomass and Bioenergy, 1997. **13**(1–2): p. 83-114.

132. Yue, Z.B., et al., A Sustainable Pathway of Cellulosic Ethanol Production Integrating Anaerobic Digestion With Biorefining. Biotechnology and Bioengineering, 2010. **105**(6): p. 1031-1039.

133. Liao, W., Y. Liu, and D. Hodge, *Integrated Farm-Based Biorefinery.* Biorefineries: Integrated Biochemical Processes for Liquid Biofuels, 2014: p. 255-270.

134. Liu, Z., et al., A new multiple-stage electrocoagulation process on anaerobic digestion effluent to simultaneously reclaim water and clean up biogas. Journal of Hazardous Materials, 2015. **285**: p. 483-490.

135. Sanyal, O., et al., Development of polyelectrolyte multilayer membranes to reduce the COD level of electrocoagulation treated high-strength wastewater. Journal of Membrane Science, 2015. **496**: p. 259-266.

136. Yue, Z., et al., Development of a new bioethanol feedstock – Anaerobically digested fiber from confined dairy operations using different digestion configurations. Biomass and Bioenergy, 2011. **35**(5): p. 1946-1953.

137. Yusof, N.L.B.M., L.Y. Lim, and E. Khor, *Preparation and characterization of chitin beads as a wound dressing precursor.* Journal of biomedical materials research, 2001. **54**(1): p. 59-68.

138. Ravi Kumar, M.N.V., *A review of chitin and chitosan applications.* Reactive and Functional Polymers, 2000. **46**(1): p. 1-27.

139. Nutrition, S.o.D.C., C.o.A. Nutrition, and N.R. Council, *Nutrient Requirements of Dairy Cattle: Seventh Revised Edition, 2001*. 2001: The National Academies Press.

140. Liu, Z. and Y. Liu, Synergistic integration of electrocoagulation and algal cultivation to treat liquid anaerobic digestion effluent and accumulate algal biomass. Process Biochemistry, 2016. **51**(1): p. 89-94.

141. Ruan, Z., et al., Evaluation of lipid accumulation from lignocellulosic sugars by Mortierella isabellina for biodiesel production. Bioresour Technol, 2012. **110**: p. 198-205.

142. Sluiter, A., et al., *Determination of extractives in biomass.* Laboratory Analytical Procedure (LAP), 2005. **1617**.

143. Peniston, Q.P. and E.L. Johnson, Method of recovering chitosan and other by-products from shellfish waste and the like. 1975, Google Patents.

144. Dhillon, G.S., et al., *Green synthesis approach: extraction of chitosan from fungus mycelia.* Crit Rev Biotechnol, 2013. **33**(4): p. 379-403.

145. Chysirichote, T., et al., Quantification of the glucosamine content in the filamentous fungus Monascus ruber cultured on solid surfaces. J Basic Microbiol, 2014. **54**(5): p. 350-7.

146. Teater, C., et al., Assessing solid digestate from anaerobic digestion as feedstock for ethanol production. Bioresource Technology, 2011. **102**(2): p. 1856-1862.

147. Liao, W., et al., Co-production of fumaric acid and chitin from a nitrogen-rich lignocellulosic material – dairy manure – using a pelletized filamentous fungus Rhizopus oryzae ATCC 20344. Bioresource Technology, 2008. **99**(13): p. 5859-5866.

148. Arcidiacono, S. and D.L. Kaplan, Molecular weight distribution of chitosan isolated from Mucor rouxii under different culture and processing conditions. Biotechnol Bioeng, 1992. **39**(3): p. 281-6.

149. Saito, K., Y. Hasa, and H. Abe, *Production of lactic acid from xylose and wheat straw by Rhizopus oryzae.* J Biosci Bioeng, 2012. **114**(2): p. 166-9.

150. Chatterjee, S., et al., Enhancement of growth and chitosan production by Rhizopus oryzae in whey medium by plant growth hormones. Int J Biol Macromol, 2008. **42**(2): p. 120-6.

151. Hang, Y.D., *Chitosan production fromRhizopus oryzae mycelia.* Biotechnology letters, 1990. **12**(12): p. 911-912.

152. Tan, S.C., et al., *The chitosan yield of zygomycetes at their optimum harvesting time.* Carbohydrate Polymers, 1996. **30**(4): p. 239-242.

153. Pochanavanich, P. and W. Suntornsuk, *Fungal chitosan production and its characterization.* Lett Appl Microbiol, 2002. **35**(1): p. 17-21.

154. Yoshihara, K., et al., Chitosan productivity enhancement in Rhizopus oryzae YPF-61A by D-psicose. J Biosci Bioeng, 2003. **95**(3): p. 293-7.

155. Wu, M., et al., *Consumptive water use in the production of bioethanol and petroleum gasoline.* Center for Transportation Research, Energy Systems Division, Argonne National Laboratory, Chicago, USA, 2008.

156. Subhadra, B.G. and M. Edwards, Coproduct market analysis and water footprint of simulated commercial algal biorefineries. Applied Energy, 2011. **88**(10): p. 3515-3523.

157. Fingerman, K.R., et al., *Accounting for the water impacts of ethanol production.* Environmental Research Letters, 2010. **5**(1): p. 014020.

158. Martín, M., E. Ahmetovic, and I.E. Grossmann, *Optimization of water consumption in second generation bioethanol plants.* Industrial & Engineering Chemistry Research, 2010. **50**(7): p. 3705-3721.

159. Queiroz, M.I., et al., *Fish processing wastewater as a platform of the microalgal biorefineries.* Biosystems engineering, 2013. **115**(2): p. 195-202.

160. Fava, F., et al., Biowaste biorefinery in Europe: opportunities and research & development needs. New biotechnology, 2015. **32**(1): p. 100-108.

161. Bar-Even, A., et al., Design and analysis of metabolic pathways supporting formatotrophic growth for electricity-dependent cultivation of microbes. Biochim Biophys Acta, 2013. **1827**(8-9): p. 1039-47.

162. Torella, J.P., et al., *Efficient solar-to-fuels production from a hybrid microbial-water-splitting catalyst system.* Proceedings of the National Academy of Sciences of the United States of America, 2015. **112**(8): p. 2337-2342.

163. Tremblay, P.L. and T. Zhang, *Electrifying microbes for the production of chemicals.* Frontiers in Microbiology, 2015. **6**: p. 10.

164. Bar-Even, A., et al., Design and analysis of metabolic pathways supporting formatotrophic growth for electricity-dependent cultivation of microbes. Biochimica Et Biophysica Acta-Bioenergetics, 2013. **1827**(8-9): p. 1039-1047.

165. Tai, Y.S. and K.C. Zhang, *ENZYME PATHWAYS C1 metabolism redesigned.* Nature Chemical Biology, 2015. **11**(6): p. 384-386.

166. Siegel, J.B., et al., *Computational protein design enables a novel one-carbon assimilation pathway.* Proceedings of the National Academy of Sciences of the United States of America, 2015. **112**(12): p. 3704-3709.

167. Atkinson, P.W., J.A. King, and M.J. Hynes, Identification of the acia gene controlled by the amda regulatory gene in aspergillus-nidulans. Current Genetics, 1985. **10**(2): p. 133-138.

168. Babel, W., U. Brinkmann, and R.H. Muller, *The auxiliary substrate concept - an approach for overcoming limits of microbial performances.* Acta Biotechnologica, 1993. **13**(3): p. 211-242.

169. Chow, C.M. and U.L. Rajbhandary, *Developmental regulation of the gene for formate dehydrogenase in neurospora-crassa.* Journal of Bacteriology, 1993. **175**(12): p. 3703-3709.

170. Peyraud, R., et al., *Demonstration of the ethylmalonyl-CoA pathway by using 13C metabolomics.* Proceedings of the National Academy of Sciences, 2009. **106**(12): p. 4846-4851.

171. Bruinenberg, P.M., et al., Utilization of formate as an additional energy-source by glucose-limited chemostat cultures of candida-utilis CBS-621 and Saccharomyces-cerevisiae CBS-8066 - evidence for the absence of transhydrogenase activity in yeasts. Archives of Microbiology, 1985. **142**(3): p. 302-306.

172. Hazeu, W. and R.A. Donker, A continuous culture study of methanol and formate utilization by the yeast pichia-pastoris. Biotechnology Letters, 1983. **5**(6): p. 399-404.

173. Babel, W., R.H. Muller, and K.D. Markuske, *Improvement of growth-yield of yeast on glucose to the maximum by using an additional energy-source.* Archives of Microbiology, 1983. **136**(3): p. 203-208.

174. Babel, W., The auxiliary substrate concept: from simple considerations to heuristically valuable knowledge. Engineering in Life Sciences, 2009. **9**(4): p. 285-290.

175. Lian, J., et al., Yeast fermentation of carboxylic acids obtained from pyrolytic aqueous phases for lipid production. Bioresource technology, 2012. **118**: p. 177-186.

176. Bligh, E.G. and W.J. Dyer, *A rapid method of total lipid extraction and purification.* Can J Biochem Physiol, 1959. **37**(8): p. 911-7.

177. Indarti, E., et al., *Direct FAME synthesis for rapid total lipid analysis from fish oil and cod liver oil.* Journal of Food Composition and Analysis, 2005. **18**(2): p. 161-170.

178. You, L., et al., Metabolic Pathway Confirmation and Discovery Through 13C-labeling of Proteinogenic Amino Acids. Journal of Visual Experiments, 2012(59): p. e3583.

179. Hu, Q., et al., Microalgal triacylglycerols as feedstocks for biofuel production: perspectives and advances. The Plant Journal, 2008. **54**(4): p. 621-639.

180. Li, R., M. Moore, and J. King, *Investigating the regulation of one-carbon metabolism in Arabidopsis thaliana.* Plant Cell Physiol, 2003. **44**(3): p. 233-41.

181. Dauner, M. and U. Sauer, GC-MS analysis of amino acids rapidly provides rich information for isotopomer balancing. Biotechnology Progress, 2000. **16**: p. 642-649.

182. Wu, G., et al., Metabolic Burden: Cornerstones in Synthetic Biology and Metabolic Engineering Applications. Trends Biotechnol, 2016.

183. Brosnan, M.E., et al., Division of labour: how does folate metabolism partition between one-carbon metabolism and amino acid oxidation? Biochemical Journal, 2015. **472**(2): p. 135-146.

184. Dijkstra, A.J., R.J. Hamilton, and W. Hamm, *Trans fatty acids*. 2008: John Wiley & Sons.